



University of Kentucky
UKnowledge

KWRRRI Research Reports

Kentucky Water Resources Research Institute

9-1981

Low Pressure Membrane Separation Process to Remove Heavy Metal Complexes


Digital Object Identifier: <https://doi.org/10.13023/kwrrri.rr.129>

Dibakar Bhattacharyya
University of Kentucky, db@uky.edu

Chin-Shun Cheng
University of Kentucky

[Click here to let us know how access to this document benefits you.](#)

Follow this and additional works at: https://uknowledge.uky.edu/kwrrri_reports

 Part of the [Complex Mixtures Commons](#), and the [Water Resource Management Commons](#)

Repository Citation

Bhattacharyya, Dibakar and Cheng, Chin-Shun, "Low Pressure Membrane Separation Process to Remove Heavy Metal Complexes" (1981). *KWRRRI Research Reports*. 74.
https://uknowledge.uky.edu/kwrrri_reports/74

This Report is brought to you for free and open access by the Kentucky Water Resources Research Institute at UKnowledge. It has been accepted for inclusion in KWRRRI Research Reports by an authorized administrator of UKnowledge. For more information, please contact UKnowledge@lsv.uky.edu.

LOW PRESSURE MEMBRANE SEPARATION PROCESS TO
REMOVE HEAVY METAL COMPLEXES

By

Dr. Dibakar Bhattacharyya
Principal Investigator

Ching-Shun Cheng
Graduate Assistant

Project Number: B-059-KY (Completion Report)
Agreement Number: 14-34-0001-9073 (FY 1979)
Period of Project: October 1978 - September 1981

Water Resources Research Institute
University of Kentucky
Lexington, Kentucky

The work upon which this report is based was supported in part by funds provided by the Office of Water Research and Technology, United States Department of the Interior, Washington, D.C., as authorized by the Water Research and Development Act of 1978. Public Law 95-467.

September 1981

DISCLAIMER

Contents of this report do not necessarily reflect the views and policies of the Office of Water Research and Technology, United States Department of the Interior, Washington, D.C., nor does mention of trade names or commercial products constitute their endorsement or recommendation for use by the U.S. Government.

ABSTRACT

Title: Low Pressure Membrane Separation Process
To Remove Heavy Metal Complexes

The overall objective of this investigation is to establish the rejection behavior of heavy metals in the presence of complexing agents, utilizing negatively charged ultrafiltration membranes. An extensive experimental investigation is conducted with Zn^{2+} , Cd^{2+} , Cu^{2+} , and Cu^{1+} in the presence of cyanide, ethylenediamine tetraacetic acid, and oxalates, under insignificant concentration polarization condition. The rejection dependence of the heavy metals is found to be a function of feed metal concentration, metal types, complexing agent to metal feed molar ratio, pH and ionic strength. The dependence of rejection behavior of heavy metals and complexing agents on pH and concentration is explained in terms of metal complex species distribution and Donnan Exclusion model. For EDTA and oxalate systems, the rejections of metal are independent of initial metal concentration; whereas for the cyanide system the rejections of both metal and cyanide decrease with concentration. At transmembrane pressure of $5.6 \times 10^5 \text{ N/m}^2$, metal rejections range between 77% to 96%. For all cases, the rejection of metal is highly dependent on the size and charge of the complex metal species. For example, the rejections of $Zn(CN)_4^{2-} > Zn(CN)_3^{1-}$, and $Cu(EDTA)^{2-} > Cu(CN)_3^{2-} > Cu(C_2O_4)^{2-}$ are observed.

Descriptors: Heavy Metals, Membrane Process, Waste
Water Treatment

Identifiers: Charged Membrane Ultrafiltration, Donnan
Exclusion, Rejection Model, Complex Species,
Chelating Agents

TABLE OF CONTENTS

	PAGE
ABSTRACT.....	iii
TABLE OF CONTENTS.....	iv
LIST OF TABLES.....	vii
LIST OF ILLUSTRATIONS.....	ix
 Chapter	
I. INTRODUCTION.....	1
II. LITERATURE REVIEW OF CHARGED MEMBRANE ULTRAFILTRATION.....	6
III. OBJECTIVES OF THIS INVESTIGATION.....	9
IV. MEMBRANE SEPARATION MECHANISMS.....	11
A. Solution Diffusion Model.....	12
B. Pore Model.....	14
C. Donnan Equilibrium Model.....	15
D. Nernst-Planck Model.....	17
V. COMPLEXATION REACTION MODELS.....	20
A. Dissociation of Complexing Agents.....	21
B. Metal Complexation Equilibria.....	24
1. General	
2. Metal Complexation Calculations	
3. Average Charge Calculations	
VI. EXPERIMENTAL.....	49
A. Equipment.....	49
B. Chemicals Used.....	52
C. Procedure.....	54
D. Analytical Procedures.....	57

Chapter	Page
VII. RESULTS AND DISCUSSIONS.....	60
A. Membrane Characterization.....	60
B. Rejection of Individual Complexing Agents.....	62
C. Metal-Cyanide Rejection Studies.....	69
1. Effect of CN_T/Zn_T on the Total Metal and Total Cyanide Rejection	
2. Effect of Ionic Strength on Zn-CN System	
3. Effect of Feed Concentration on Zinc Cyanide Rejection	
4. Calculation of Free Cyanide (CN^-) Rejection in the Metal-Complex Systems	
D. Metal-EDTA Rejection Studies.....	84
1. Effect of $EDTA_T/M_T$ on Rejection	
2. Calculation of Total Metal Rejection Based on Rejections of Individual Components	
E. Metal-Oxalate Rejection Studies.....	89
1. Effect of pH on the Rejection of Total Copper and Total Oxalate in Cu^{2+} -OX System	
2. Effect of OX_T/Cu_T Molar Ratio on the Total Copper and Total Oxalate Rejection	
3. Effect of Ionic Strength on the Rejection of total Copper in the presence of Oxalate	
4. Effect of Feed Concentration on Total Copper and Total Oxalate Rejection	
F. Ultrafiltration Experiments at High Water Recovery.....	101
VIII. SUMMARY AND CONCLUSIONS.....	106

NOMENCLATURE.....	115
APPENDIX.....	118
REFERENCES.....	127

LIST OF TABLES

Table	Page
1. Membrane Separation Mechanisms.....	3
2. Dependence of Rejections on Coion Charge with Negatively-charged Ultrafiltration Membranes (16).....	8
3. Dissociation Constants of Complexing Agents (32).....	23
4. Overall Formation Constants of Various Metal Complexes (33).....	31
5. Dissociation Constants of Various Cu-EDTA Complexes.....	31
6. Copper Containing Species Distribution at Various pH in Cu ²⁺ -OX Systems (C _i = 1.55 mM Cu _T , OX _T /Cu _T =4.0).....	43
7. Properties of PTAL Membranes.....	53
8. Atomic Absorption Characteristics.....	58
9. Characteristics of New Membranes.....	64
10. Rejection of NaCN at pH 10.....	65
11. Calculated Concentrations of Various Species in Zn-CN Systems (pH = 10, C _i = 1.55 mM Zn _T).....	76
12. Parameters to fit C _f = kC _i ⁿ for Zn-CN System....	82
13. Calculated Total Metal Rejection Values Based on Experimental Rejection of M ²⁺ and M(EDTA) ²⁻	90

Table	Page
14. Effect of Pressure on Cu_T Rejection in Cu^{2+} -OX System ($OX_T/Cu_T \approx 4$).....	91
15. Concentration of Uncharged Cu(OX) Species.....	96
16. Approximation Rejection Values of Various Anions Based on ${}^R_{CuCl_2} = 0.34$ at 1.55 mM, $P = 5.6 \times 10^5$ N/m ²	113

LIST OF ILLUSTRATIONS

Figure	Page
1. Distribution of Various Species of HCN in Aqueous Solutions as a Function of pH.....	25
2. Distribution of Various Species of EDTA in Aqueous Solutions as a Function of pH.....	26
3. Distribution of Various Species of Oxalic Acid in Aqueous Solutions as a Function of pH.....	27
4. Conditional Stability Constants of Various M-EDTA Complexes as a Function of pH.....	35
5. Distribution of Various Species in Zn-CN System as a Function of CN_T/Zn_T Molar Ratio.....	37
6. Distribution of Various Species in Cd-CN System as a Function of CN_T/Cd_T Molar Ratio.....	38
7. Distribution of Various Species in Cu^{1+} -CN System as a Function of CN_T/Cu_T Molar Ratio.....	40
8. Distribution of Various Species in Cu^{2+} -EDTA System as a Function of pH.....	41
9. Distribution of Various Species in Cu^{2+} -OX System as a Function of OX_T/Cu_T Molar Ratio.....	44
10. Average Charge \bar{n} in Zn-CN System as a Function of CN_T/Zn_T Molar Ratio.....	45
11. Average Charge \bar{n} in Cd-CN System as a Function of CN_T/Cd_T Molar Ratio.....	45
12. Average Charge \bar{n} in Cu^{1+} -CN System as a Function of CN_T/Cu_T Molar Ratio.....	46

Figure	Page
13. Average Charge \bar{n} in Cu^{2+} -OX System as a Function of OX_T/Cu_T Molar Ratio.....	4/
14. Schematic Diagram of Membrane Unit.....	50
15. Specification of the Ultrafiltration Cell.....	51
16. Comparison of Calculated and Experimental Water Fluxes for PTAL Membranes.....	61
17. Distilled Water Flux (Solute Free) at Various Applied Pressure for PTAL Membranes.....	63
18. Effect of pH on EDTA Rejection.....	67
19. Effect of pH on Oxalic Acid Rejection.....	68
20. Effect of Pressure on the Rejection of Zn_T in Zn-CN System.....	70
21. Rejection Behavior of Zn_T and CN_T as a Function of Feed Molar Ratio (CN_T/Zn_T) for Zn-CN System.....	71
22. Rejection Behavior of Cd_T and CN_T as a Function of Feed Molar Ratio (CN_T/Cd_T) for Cd-CN System.....	72
23. Rejection Behavior of Cu_T and CN_T as a Function of Feed Molar Ratio (CN_T/Cu_T) for Cu^{1+} -CN System.....	73
24. Effect of Ionic Strength (NaNO_3) on Zn_T Rejection for Zn-CN System.....	77
25. Effect of Feed Zn_T Concentration on Zinc Rejection.....	79
26. Effect of Feed Zn_T Concentration on Ultrafiltrate Zinc Concentration for Zn-CN System.....	80
27. Effect of Feed CN_T Concentration on Ultrafiltrate Cyanide Concentration for Zn-CN System.....	81

Figure	Page
28. Rejection Behavior of Zn_T and $EDTA_T$ as a Function of Feed Molar Ratio ($EDTA_T/Zn_T$) for Zn-EDTA System.....	85
29. Rejection Behavior of Cd_T and $EDTA_T$ as a Function of Feed Molar Ratio ($EDTA_T/Cd_T$) for Cd-EDTA System.....	86
30. Rejection Behavior of Cu_T and $EDTA_T$ as a Function of Feed Molar Ratio ($EDTA_T/Cu_T$) for Cu^{2+} -EDTA System.....	87
31. Rejection Behavior of Cu_T and OX_T as a Function of pH for Cu- OX^T System.....	93
32. Rejection Behavior of Cu_T and OX_T as a Function of Feed Molar Ratio (OX_T/Cu_T) for Cu^{2+} -OX System at pH 4.0 and 6.0.....	94
33. Effect of Ionic Strength ($NaNO_3$) Rejection for Cu^{2+} -OX System.....	97
34. Effect of Feed Cu_T Concentration of Ultrafiltrate Copper Concentration for Cu^{2+} -OX System.....	99
35. Effect of Feed OX_T Concentration on Ultrafiltrate Oxalate Concentration for Cu^{2+} -OX System.....	100
36. Fractional Removal of Zn_T as a Function of Water Recovery for Zn^T -CN System at $CN_T/Zn_T = 4.0$	103
37. Fractional Removal of Cu_T as a Function of Water Recovery for Cu^{2+} -EDTA System at $EDTA_T/Cu_T = 4.0$	103
38. Fractional Removal of Cu_T as a Function of Water Recovery for Cu^{2+} -OX System at $OX_T/Cu_T = 4.0$	104

Figure	Page
39. Calculated Fractional Removals of Zn_T as a Function of Water Recovery for Zn-CN System at $CN_T/Zn_T = 4.0$	105
40. Comparison of Metal Rejection Behavior with Average Charge \bar{n}	108
41. Dependence of Zn_T Rejection on Feed Solution Species ^T Distribution for Zn-CN System.....	110
42. Effect of Three Different Complexing Agents on Relative Metal Rejection Behavior.....	112

I. INTRODUCTION

Membrane processes provide a broadly applicable technique for the separation and concentration of various inorganic and organic compounds from aqueous systems. Since the practical cellulose acetate reverse osmosis membrane came into existence twenty years ago, considerable attempt has been made to improve the membrane capability and performance. The development of composite membranes by using in-situ interfacial polymerization technique has provided membranes with high solute separation characteristics (1). By varying the materials and physical conditions of the two layers on porous support, several types of membranes could be obtained. The composite membranes perform better than cellulose acetate membranes in almost all aspects including water flux, solute rejection, temperature effect, stability in acid and base, and pressure requirement.

Another development in reverse osmosis membrane technology is the development of high pressure charged membranes with good water flux characteristics. Hiroshi Nomura et al. (2) have investigated the properties of charged membranes prepared from the sulfonation and amination of SBR resins. The sulfonated membranes showed

relatively low salt rejection and high production rate, whereas aminated membranes showed high rejection and low production rate. The low salt rejection of sulfonated membranes was improved by amination so that a sandwiched type membrane could be obtained. Although the selectivity based on rejection was not very high, the strong exclusions of ions of higher valencies resulted in higher rejection. Despite its limited use in terms of selective removal of metal ions and metal containing species, relatively high pressure is needed in order to effect the water recovery.

The conventional ultrafiltration membrane process used to remove large organic molecules is mainly based on sieving mechanism. Ultrafiltration membranes with various pore sizes are commercially available. It is a low pressure process, and is used for macromolecules. Ultrafiltration membranes containing charged groups have also been developed with the advantage that they not only can remove certain small molecules, but also have high selectivity for various inorganic ions. Bhattacharyya et al. (3-6) and Gregor et al. (7,8) have done extensive work along this line and have applied it in industrial processing and separations. The above three membrane separation processes can be best illustrated in Table 1.

TABLE 1

Membrane Separation Mechanisms

<u>Process</u>	<u>Membrane structure</u>	<u>Pressure range (N/m²)</u>	<u>Mechanism</u>
Reverse osmosis	Membranes of tight pore structures	$4 \times 10^6 - 7 \times 10^6$	Solution-diffusion
Conventional ultrafiltration	Membranes with different pore sizes	$7 \times 10^4 - 7 \times 10^5$	Sieving mechanism and solute-membrane interaction
Charged membrane ultrafiltration	Porous membrane with charged functional groups inside the pore	$3 \times 10^5 - 7 \times 10^5$	Donnan exclusion mechanism

The basic research involving charged membrane ultrafiltration has included separation of inorganic salts (9, 10), organic compounds (4) and surfactants in the water (11). The rejections of the metal ions in the solution depended largely on the chemical state of that ion (cation form, neutral form or anion form). This finding is important in metal removal as well as metal selective recovery.

Metal finishing operations use large quantities of rinsing water. Depending on the particular operations, the wastewater streams contain heavy metals such as copper (Cu), Cadmium (Cd), Zinc (Zn) and Cyanides, which constitute undesirable effects to human health. Hydroxide precipitation of heavy metals followed by settling process is often used to treat waste water from metal plating industry. However, the presence of complexing agents such as cyanides prevents effective precipitation. In addition, the hydrosopic metal hydroxide precipitates cause leaching problems under various storage conditions.

EDTA, known as ethylenediamine tetracetate, has been added as a powerful complexing agent in heavy metal chelation process. Kamizawa (12) has shown that EDTA is an effective chelating agent for metal removal in the reverse osmosis process.

Oxalic acid has long been used as a chelating agent for metal ions. Considerable research work has been done on metal-oxalate chemistry, yet very few publications were shown in terms of membrane processing.

Although the rejection behavior of Metal-EDTA complexes with reverse osmosis membranes (12,13) has been studied before, the rejection behavior of metal cyanide and oxalate complexes have never been studied with reverse osmosis or with conventional ultrafiltration membranes. In addition, none of these studies included the separation behavior of the associated free complexing agent. The use of charged membrane ultrafiltration for the simultaneous removal of metal ions and metal ion complexes has not been reported in the literature.

II. LITERATURE REVIEW OF CHARGED MEMBRANE ULTRAFILTRATION

Low-pressure ultrafiltration with negatively-charged, anisotropic (thin skin), noncellulosic membranes is found to be a promising technique for the metal recovery and water reuse. Gregor and coworkers (7,8) have reported the use of various polystyrene sulfonic acid-polyvinylidene fluoride charged ultrafiltration membrane in wastewater treatment. They found a significant improvement in the quality of treated sewage compared to that of the conventional biological oxidation process. The bacteria was reported to be removed completely by using his charged ultrafiltration membrane. Sachs et al. (14) have developed a new group of charged noncellulosic membranes having a performance intermediate to that of the conventional reverse osmosis membranes and conventional ultrafiltration membranes. High rejection ($R = 0.70$ to 0.90) and high water fluxes at moderate pressures ($7.0 \times 10^5 \text{ N/m}^2$) were found in their studies. Lonsdale et al. (15) have shown the rejection behavior of sodium citrate and sodium chloride on negatively-charged reverse osmosis membrane. They have been able to explain the result by the extension of Donnan's original equilibrium treatment to the non-equilibrium situation occurring in reverse osmosis.

Bhattacharyya et al. have studied various single salt (3), multi-salt(9-11) and actual wastewaters (3-5) with charged ultrafiltration membranes. The extent of separation (at transmembrane pressure less than $6 \times 10^5 \text{ N/m}^2$) of several oxyanions, alkaline earth metal salts, and heavy metal salts is discussed. In single salt experiments, they observed that the rejection by charged membranes are expected to decrease with an increase in concentration of the feed solution. Results also showed that the rejection was highly dependent on the type of ions. The rejection of metal salts on negatively-charged ultrafiltration membranes was shown to be $\text{ZnCl}_2 > \text{CaCl}_2 > \text{PbCl}_2$. The rejections of coions were dependent also on charge and species types (Table 2). It could be seen that the rejection is better for highly charged species, and monovalent oxyanion rejection is better than Cl^- . This could be explained qualitatively by the Donnan Equilibrium Model.

TABLE 2

Dependence of Rejections on Coion Charge with
Negatively-charged Ultrafiltration Membranes (16)

<u>Ion</u>	<u>Rejection</u>
PO_4^{3-}	0.98
HPO_4^{2-}	0.95
SO_4^{2-}	0.94
HAsO_4^{2-}	0.95
$\text{H}_2\text{AsO}_4^{1-}$	0.88
Cl^-	0.35

III. OBJECTIVES OF THIS INVESTIGATION

The overall objective of this investigation is to establish the rejection behavior of heavy metal ions in the presence of complexing agents, utilizing low-pressure, negatively charged ultrafiltration membranes. Extensive bench scale experiment with noncellulosic membranes were conducted with several synthetic systems.

The specific objectives are:

1. To determine the relative rejection behavior of heavy metal ions in the presence of inorganic (cyanide) and organic (EDTA and oxalate) complexing agents.
2. To determine the rejection of free complexing agents in the presence of metal complexes.
3. To establish the effects of pH, transmembrane pressure, complexing agent/metal feed molar ratio, solute concentration, and ionic strength on total metal and total complexing agents rejections.
4. To establish the rejection behavior under high water recovery conditions.
5. To develop a complex species distribution model in order to understand the metal rejection be-

havior in the presence of complexing agents.

IV. MEMBRANE SEPARATION MECHANISMS

Solute rejection by membrane processes can be defined in terms of a rejection parameter R:

$$R = 1 - C_f/C_i = 1 - J_s/(J_w C_i) \quad (1)$$

where C_f = solute concentration in the permeate.

C_i = solute concentration in the feed.

J_s = solute flux.

J_w = water flux.

If rejection is defined in terms of anion concentration, then Equation 1 could be rewritten in the following form:

$$R = 1 - J_y/(J_w C_y) \quad (2)$$

where C_y = anion concentration in the feed.

J_y = anion flux.

Depending on the nature of the membrane, transport of solute through the membrane is generally described by one of the following models.

A. Solution Diffusion Model (17)
(for tight uncharged membranes)

According to this model, each component dissolves in the membrane according to a distribution law and then diffuses through the membrane as a result of concentration and pressure differences.

The flux through the membrane is described by the following expression:

$$J_j = -[D_{j(m)} C_{j(m)} / (R'T)] (\partial \mu_j / \partial C_j) \nabla C_{j(m)} + V_j \nabla P \quad (3)$$

The first term in Equation 3 describes the concentration gradient effect on the flux while the second term in the same equation describes the pressure effect on the flux.

For water transport, if the concentration difference across the membrane is small, then the above equation can be approximated as

$$J_w = -D_{j(m)} V_j (\Delta P - \Delta \pi) / (R'T \lambda) \quad (4)$$

For salt transport,

$V_j \nabla P \ll -[D_{j(m)} C_{j(m)} / (R't)] (\partial \mu_j / \partial C_j) \nabla C_{j(m)}$, thus,

$$J_s = -D_{j(m)} (\Delta C_{j(m)} / \lambda) \quad (5)$$

Defining the distribution coefficient for the solute to be $K^* = C_{j(m)}/C_j$, then J_s can be further expressed in terms of the solute concentration in the solution (C_j) rather than in the membrane.

$$J_s = -D_s K^* (\Delta C_j / \lambda) \quad (6)$$

As a summary, the transport equation for solute and solvent can be written as follows:

$$J_w = -A(\Delta P - \Delta \pi) \quad (7)$$

$$J_s = -B \Delta C_j \quad (8)$$

where $A = D_{j(m)} V_{j(m)} / (R'T\lambda)$ and $B = D_s K^* / \lambda$.

The above equations clearly predict an increase in rejection with an increase in the net pressure difference ($\Delta P - \Delta \pi$) since salt flow through the membrane is independent of water flow. Selectivity in rejection depends on solute diffusivity in the membrane and the distribution coefficient of the solute between solution and membrane phases. Qualitatively, this model does predict the experimental result for solute rejection in many tight high pressure membranes.

B. Pore Model
(porous conventional ultrafiltration membranes)

The separations with conventional ultrafiltration membranes (20 Å to 100 Å pores) occur either because solutes are too large to enter the pores or because of frictional interactions within the pores. The Poiseuille law can be used to describe the water flux through the membrane:

$$J_w = N' \pi r'^4 \Delta P / (8 \mu \lambda) = \epsilon r'^2 \Delta P / (8 \mu \lambda) \quad (9)$$

where N' = the number of pores per unit area.

r' = the pore radius.

μ = the viscosity of water.

ϵ = the porosity = $N' \pi r'^2$.

This relationship fails to account for the effect of pore tortuosity, and pore size distribution in the membrane. Several attempts have been taken to modify this oversimplified Poiseuille equation (18-19). Differences in rejection among various solutes could be qualitatively explained by size and steric effect.

The solution-diffusion model assumes no coupling of solute and water transport, while the pore model assumes viscous flow where the solute and water transport simultaneously. For conventional ultrafiltration and/or reverse

osmosis membranes, selectivity is not achieved by a sieving mechanism alone, nor do all permeating species pass through the membrane pore at same rate by viscous flow without interaction with the membrane (20).

C. Donnan Equilibrium Model (charged membranes)

When a charged membrane is immersed in a salt solution as in the case of charged membrane ultrafiltration, a dynamic equilibrium condition is maintained (21-22). The counterion concentration is higher while the coion concentration is lower in the membrane phase than in the bulk feed solution. The equilibrium Donnan potential can be expressed as the result of equal chemical potential of the components in the solution and membrane phases.

$$E = [R'T/(Z_j F)] \{ \ln(C_j \gamma_j / (C_{j(m)} \gamma_{j(m)})) \} \quad (10)$$

For a salt $M_{z_y} Y_{z_m}$ which ionizes to M^{z_m} and Y^{-z_y} , the electroneutrality condition can be described as follows:

$$\text{in the membrane phase: } \sum Z_j C_{j(m)} - C_m^* = 0 \quad (11)$$

$$\text{in the bulk feed solution: } \sum Z_j C_j = 0 \quad (12)$$

where C_m^* is the charge capacity of the membrane.

The charge capacity, C_m^* , for negatively charged ultrafiltration membranes typically ranges between 300-2000 mM; thus the salt distribution between an aqueous solution and membrane is expressed as:

$$(C_{y(m)}/C_y)^{Z_m(\gamma_m/\gamma)^{Z_y+Z_m}} = [Z_y C_y / (C_m^* + Z_y C_{y(m)})]^{Z_y} \quad (13)$$

Define the salt distribution coefficient as:

$$K^* = C_{y(m)}/C_y \quad (14)$$

Since $Z_y C_{y(m)} \ll C_m^*$, the following expression can be derived:

$$K^* = C_{y(m)}/C_y = [Z_y^{Z_y} (C_y/C_m^*)^{Z_y} (\gamma/\gamma_m)^{Z_y+Z_m}]^{1/Z_m} \quad (15)$$

Thus, as an approximation, rejection could be expressed:

$$R = 1 - K^* \quad (16)$$

This model predicts that the ultrafiltrate concentration is a function of the membrane charge capacity, the feed concentration and the charge of the coion. Experiments showed that ultrafiltrate concentration also depends on

the type of counterions as well as coions in the feed solution. The model predicts poorer rejection of the salt with increasing feed concentration, and this is proved to be true by experiments.

Although the model does not take into account the diffusion and convective fluxes which influence the salt rejection in charged membrane ultrafiltration processes, it does provide a simple qualitative picture on the solute rejection in charged membrane ultrafiltration processes.

D. Nernst-Planck Model (charged membranes)

Dresner (23) and Lakshminarayanaiah (24) used the extended Nernst-Planck equation to describe salt rejection in charged membrane ultrafiltration process. According to this model, the flux of ions through the membrane comes from convective ion flux, Donnan potential flux and diffusion ion flux:

$$J_j = \beta_j J_w C_{j(m)} + Z_j C_{j(m)} D_{j(m)} [FE/(R'T)] - D_{j(m)} (dC_{j(m)}/dx) - C_{j(m)} D_{j(m)} (d \ln \gamma_{j(m)}/dx) \quad (17)$$

In Equation 17, one can see that the first term describes the convective solute flux, the second term accounts for the flux due to the Donnan potential while the last two

terms describe the diffusional salt flux.

β_j in Equation 17 is a correction factor for the possibility that in the pure convection mode the ions may not be swept along with the velocity of the permeating water. Dresner has integrated Equation 17 involving ultrafiltration of multicomponent solutions through charged membranes for the case of good coion exclusion.

At high water flux, $(dC_{j(m)}/dx) = 0$, and the above solute transport equation can be written in the following simpler form:

$$J_j = \beta_j J_w C_{j(m)} + Z_j C_{j(m)} D_{j(m)} [FE/(R'T)] \quad (18)$$

With good coion exclusion (i.e. $C_m^* \gg C_{y(m)}$), the coion flux for single salt systems can be written as:

$$J_y = J_w C_{y(m)} [1 - \beta(Z_y D_y / (Z_m D_m))] \quad (19)$$

Evaluating $C_{y(m)}$ by Equation 15, the solute flux J_y can be computed by Equation 19. According to this equation, the flux of solute is a function of feed concentration, membrane charge density, charge of the ion and the diffusion coefficients of ions in the membrane. The effectiveness of selective metal recovery simply depends on the

magnitude of the fluxes of various solutes in the solution.

The Nernst-Planck model differs from the Donnan equilibrium model in that the Nernst-Planck model accounts for salt-solvent coupling. This model also makes allowance for the effect of convective flow, and for variation in the properties of different ions in terms of diffusion coefficients. Both the Nernst-Planck and Donnan equilibrium models show a dependence of salt rejection on the feed concentration.

In general, the relationship between solute ultrafiltrate and feed concentration can be expressed empirically in the following form:

$$C_f = kC_i^n \quad (20)$$

in which k and n are two parameters related to the nature of solute and the membrane. For simple metal salts, n has ranged between 1.0-1.5 (9-10,16).

V. COMPLEXATION REACTION MODELS

Metal complexes are compounds that contain a central metal ion surrounded by a cluster of ions or molecules. Depending on the total charges on this entity, it may be a cation, an anion or a nonionic species.

Compounds such as ethylenediamine tetracetic acid (abbreviated as EDTA), cyanide, and oxalic acid are commonly used as complexing agents. Compounds, such as EDTA, have several sites to bond the central metal ion and are called chelating agents, while molecules such as cyanide, and oxalates ($C_2O_4^{2-}$, $HC_2O_4^{1-}$) have only one site called a ligand.

Werner coordination theory is well known as the foundation of coordination chemistry. His three important postulates are (25):

1. Most elements exhibit two types of valence:
 - (a) primary valence which corresponds to oxidation state.
 - (b) secondary valence which corresponds to coordination number.
2. Every element tends to satisfy both its primary and secondary valence.
3. The secondary valence is directed toward fixed

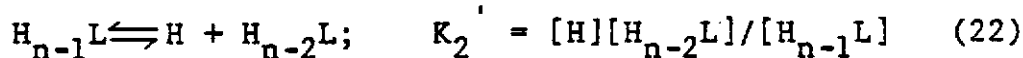
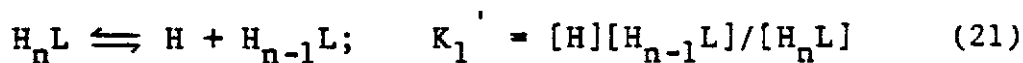
position in space.

Although the theory is able to explain many properties of complexes, he emphasized a false postulate that two kinds of valence exist for inorganic substances without any justification for their existence. Three theories are currently used to describe the nature of the bonding in metal complexes. these are:

1. valence bond theory (26).
2. the electrostatic crystal field theory (27).
3. the molecular orbital theory (28).

A. Dissociation of Complexing Agents

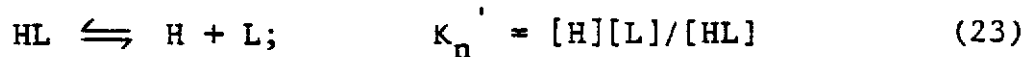
In the absence of metal ions, the complexing agent reaches equilibrium in the solution. For a polyprotic acid, the equilibria involved and the stepwise dissociation constants can be expressed as follows:



. . .

. . .

. . .



The corresponding stepwise dissociation constants for EDTA, HCN and $H_2C_2O_4$ are shown in Table 3.

Using stepwise dissociation constants, the material balance equation and charge balance relationship, a set of simultaneous equations can be solved to obtain the distribution of various species in the solution under various conditions. As an example, diprotic acid H_2L dissociate in the solution as follows:



Material balance:

$$C_L = [H_2L] + [HL] + [L^{2-}] \quad (27)$$

where C_L is the total ligand concentration.

Solving equations 24-27 simultaneously, the fraction of each species can be found as follows:

$$\alpha_0 = [H_2L]/C_L = [H^+]^2 / ([H^+]^2 + K_1[H^+] + K_1K_2) \quad (28)$$

$$\alpha_1 = [HL^-]/C_L = K_1[H^+] / ([H^+]^2 + K_1[H^+] + K_1K_2) \quad (29)$$

$$\alpha_2 = [L^{2-}]/C_L = K_1K_2 / ([H^+]^2 + K_1[H^+] + K_1K_2) \quad (30)$$

TABLE 3

Dissociation Constants of Complexing Agents (32)

<u>Complexing</u> <u>agent</u>	<u>Dissociation Constant (at 25° C)</u>			
	<u>K₁</u>	<u>K₂</u>	<u>K₃</u>	<u>K₄</u>
EDTA	1×10^{-2}	2.14×10^{-3}	6.92×10^{-7}	1×10^{-10}
HCN	6.0×10^{-10}	-	-	-
H ₂ C ₂ O ₄	6.2×10^{-2}	6.1×10^{-5}	-	-

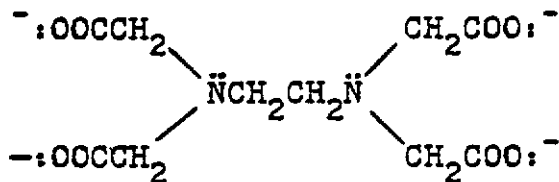
Using the above procedure, the species distributions of three different complexing agents (cyanide, EDTA, and oxalate) are computed and shown in Figures 1-3, as a function of pH.

B. Metal Complexation Equilibria

1. General

Cyanide is a well known complexing agent. It has been used in various separation processes, and in metal plating operations (29-31). It can form highly stable complexes with various metal ions in solution. Cyanide is a small charged species, (the size of CN^- is estimated to be 2 \AA). However, it forms more than one complex with metal ions. For example, both $\text{Zn}(\text{CN})_3^{1-}$ and $\text{Zn}(\text{CN})_4^{2-}$ could be found in a solution which contains zinc ion and cyanide ion. Because of the possibility of HCN gas formation, cyanide is seldom used in low pH processes.

EDTA has the structure:



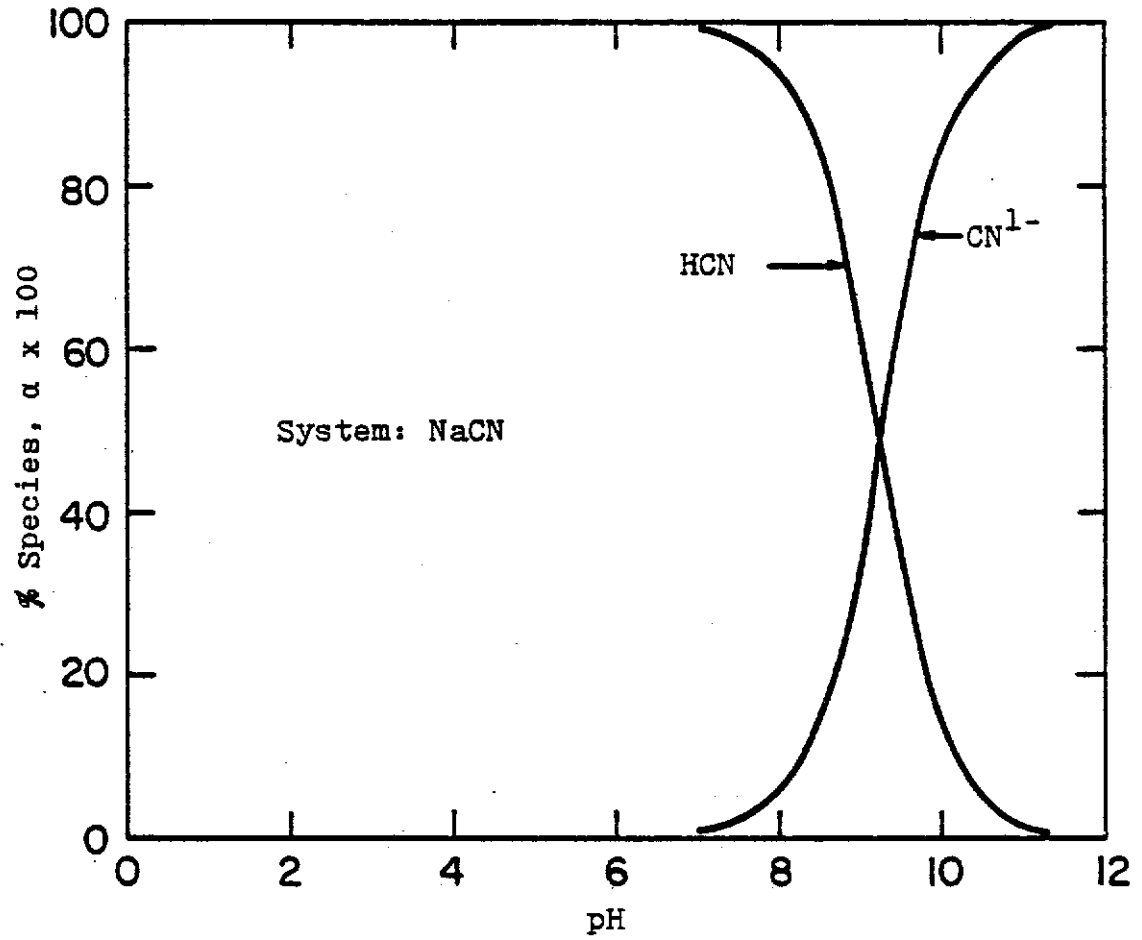


Figure 1. Distribution of Various Species of HCN in Aqueous Solutions as a Function of pH

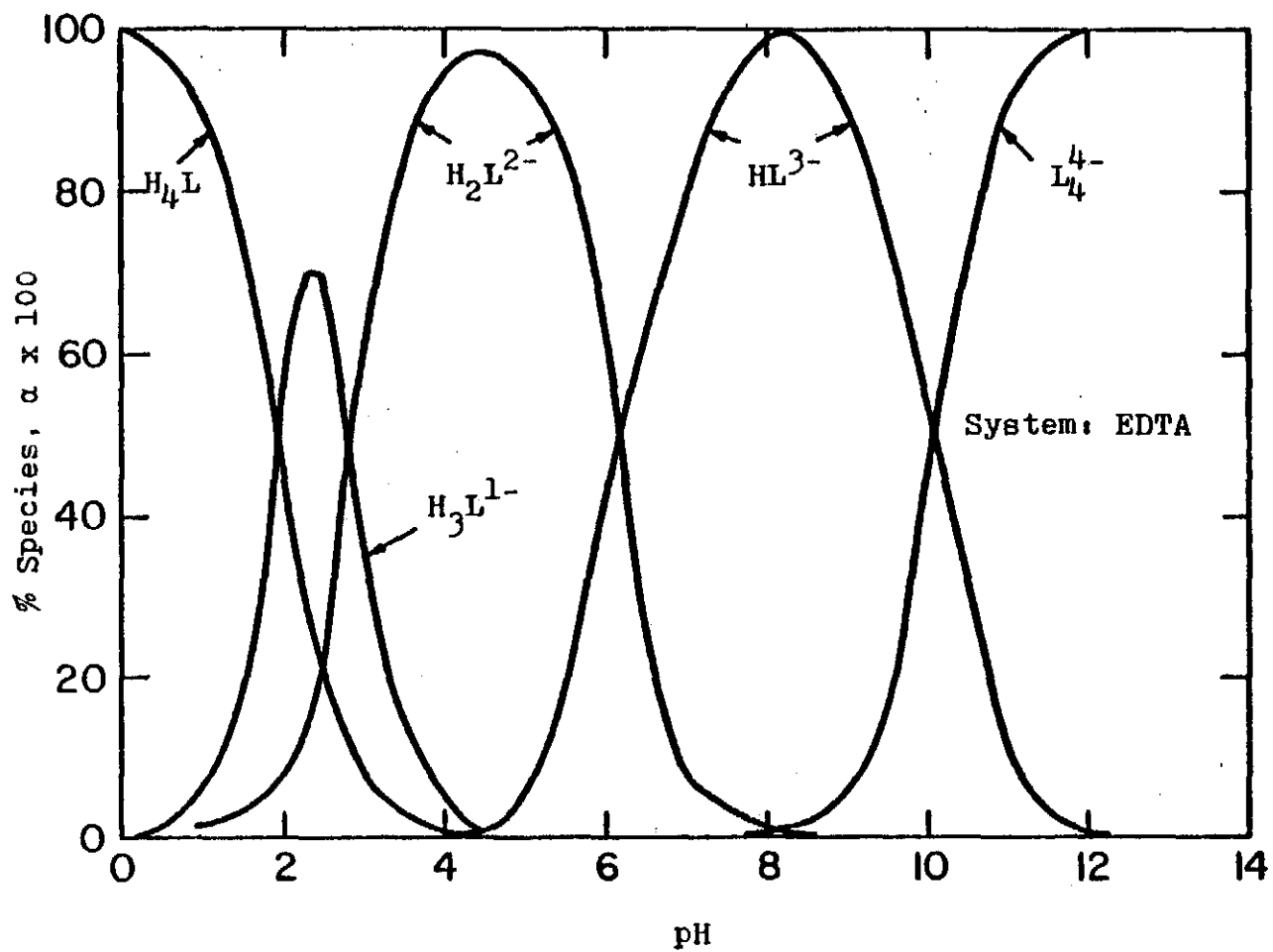


Figure 2. Distribution of Various Species of EDTA in Aqueous Solutions as a Function of pH

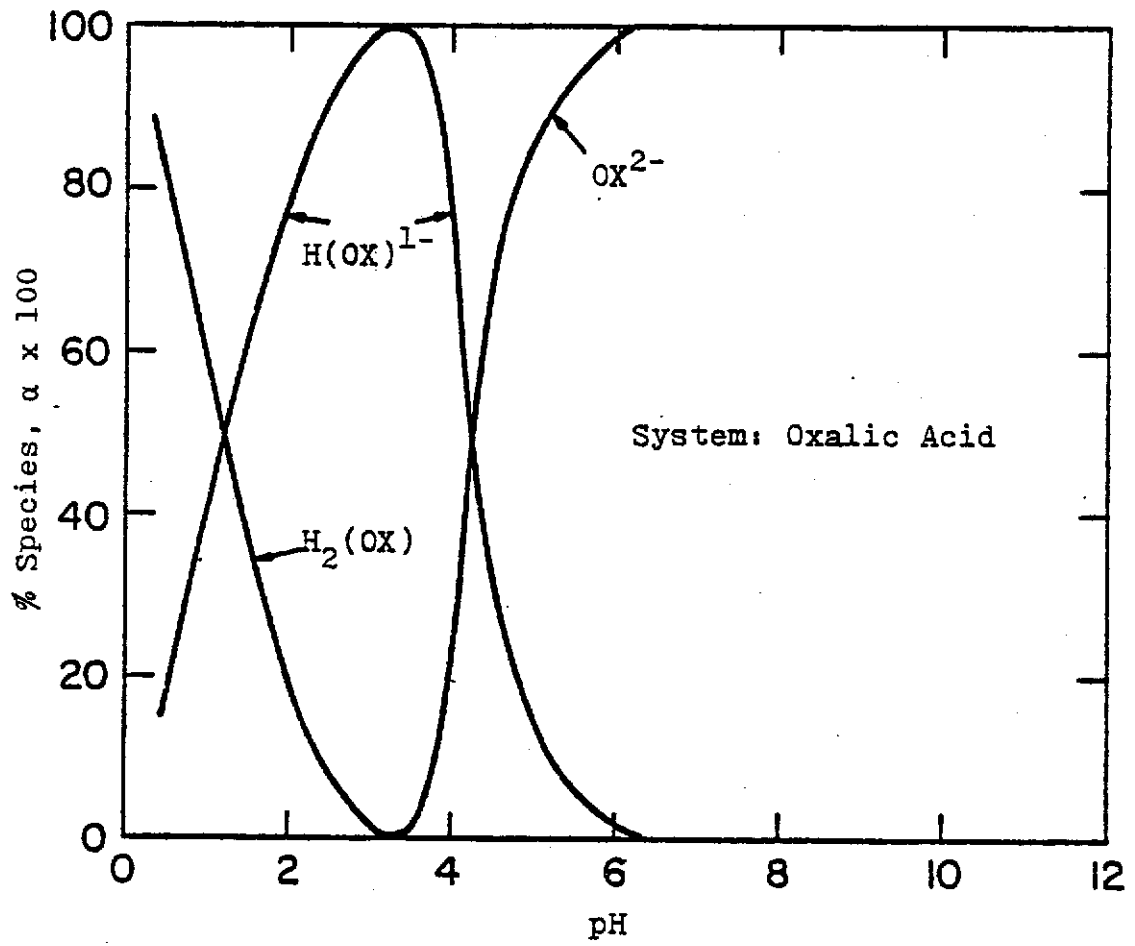
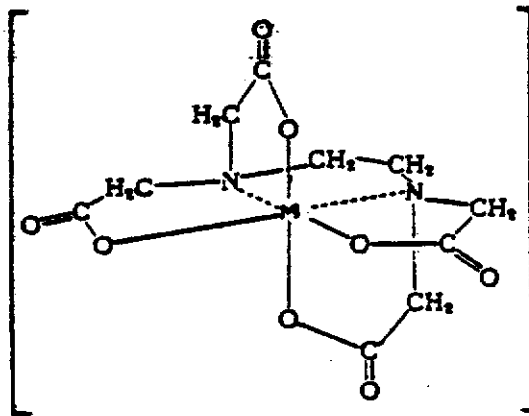


Figure 3. Distribution of Various Species of Oxalic Acid in Aqueous Solutions as a Function of pH

The size of this molecule ranges between 5 \AA - 10 \AA depending on the molecular conformation. Since the molecule has six potential sites for bonding, it is called a hexadentate ligand. One of the valuable properties of EDTA as a titrant is that it always forms 1:1 complex with the metal ions it chelates. The complex is extremely stable as can be seen from the following proposed structure:



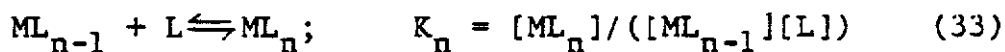
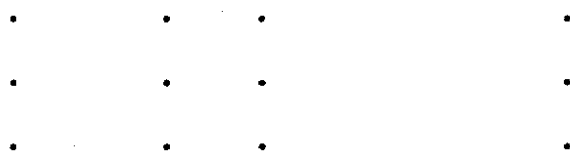
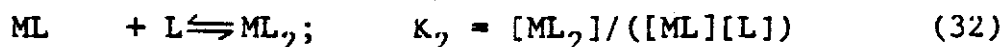
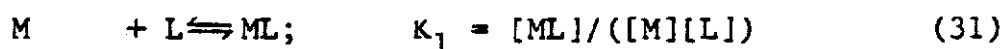
EDTA exists in various forms in aqueous solution as

shown in Figure 2.

Oxalate is another complexing agent used in this study. The size of the oxalate ion is estimated to be 5.5 \AA . Depending on the pH of the solution, the oxalic acid has two forms in water solution as shown in Figure 3. Since oxalate forms weaker complexes with heavy metals, the precipitation of metals as hydroxide may occur at high pH values.

2. Metal Complexation Calculations

In the presence of metal ions, additional equilibria have to be taken into account for complex formation. As an example, the following additional equilibria occur in the aqueous solutions:



where K_i 's are the successive stability constants characterizing the formation of the different species in

the metal complex solution.

By successive substitution, one can obtain:

$$[ML] = K_1[M][L] \quad (31a)$$

$$[ML_2] = K_1K_2[M][L]^2 \quad (32a)$$

.

.

.

$$[ML_n] = K_1K_2 \dots K_n[M][L]^n \quad (33a)$$

Denoting the products of the stepwise stability constants by β_i (overall stability constant), and the corresponding subscript, we have:

$$\beta_1 = [ML]/([M][L]) = K_1 \quad (34)$$

$$\beta_2 = [ML_2]/([M][L]^2) = K_1K_2 \quad (35)$$

.

.

.

$$\beta_n = [ML_n]/([M][L]^n) = K_1K_2 \dots K_n \quad (36)$$

The β_i values for the cases in this study are shown in Table 4. The mole fraction of the *i*th complex species in the solution, which gives the fraction of the

TABLE 4

Overall Formation Constants of Various Metal Complexes (33)

<u>System</u>	<u>logβ_1</u>	<u>logβ_2</u>	<u>logβ_3</u>	<u>logβ_4</u>
Zn ²⁺ -CN ⁻	-	-	17.31	19.18
Cd ²⁺ -CN ⁻	5.5	10.6	15.3	18.9
Cu ¹⁺ -CN ⁻	-	24	28.6	30.3
Zn ²⁺ -EDTA	16.5	-	-	-
Cd ²⁺ -EDTA	16.46	-	-	-
Cu ²⁺ -EDTA	18.80	-	-	-
Cu ²⁺ -OX	4.5	8.9	-	-

TABLE 5

Dissociation Constants of Various Cu-EDTA Complexes

<u>Complex</u>	<u>-pK</u>
Cu ²⁺ -H-L	21.8
Cu ²⁺ -OH-L	21.2

total metal ion in the complex of composition ML_i is given by:

$$\begin{aligned}\alpha_1 &= [ML_i]/C_M \\ &= \beta_1[M][L]^1 / ([M] + \beta_1[M][L] + \beta_2[M][L]^2 + \dots) \\ &= \beta_1[L]^1 / (1 + \sum_1^N \beta_1[L]^1) \quad (37)\end{aligned}$$

The mole fraction of the free metal ion is given by:

$$\alpha_0 = [M]/C_M = 1 / (1 + \beta_1[L] + \beta_2[L]^2 + \dots) \quad (38)$$

In addition to metal-ligand reactions, metal hydrolysis reactions may also be important.



Metal hydrolysis reactions have been included in all calculations presented here. In the case of copper-EDTA complexation study, species such as $CuHL^{1-}$ and $Cu(OH)L^{3-}$ exist in solution in the presence of CuL^{2-} . The dissociation constants for $CuHL^{1-}$, $Cu(OH)L^{3-}$, and CuL^{2-} are

shown in Table 5.

In the presence of other side reactions, such as the interaction of metal, ligands or metal-ligand complexes with hydrogen ions or hydroxide ions, an apparent stability constant (known as conditional stability constant) expression could be used in order to include these side reactions:

$$L_T = L' + ML + 2ML_2 + \dots \quad (43)$$

$$M_T = M' + \dots + ML + ML_2 + \dots \quad (44)$$

$$\text{where } L' = L + HL + H_2L + \dots \quad (45)$$

$$M' = M + M(OH) + M(OH)_2 + \dots \quad (46)$$

ML' can be defined in a similar way as follows:

$$ML' = ML + MHL + M(OH)L + \dots \quad (47)$$

Three new quantities (α_M' , α_L' , α_{ML}') are defined to facilitate the calculation of species distribution:

$$\alpha_M' = M/M' = M/(M + M(OH) + M(OH)_2 + \dots) \quad (48)$$

$$\alpha_L' = L/L' = L/(L + HL + H_2L + \dots) \quad (49)$$

$$\alpha_{ML}' = ML/(ML)' = ML/(ML + MHL + M(OH)L + \dots) \quad (50)$$

If the only complex formed is 1:1 type, the conditional stability constant can be defined as follows:

$$K_{ML}' = [(ML)'] / ([M'] [L']) \quad (51)$$

Combining Equation 31, and 48-51, the following expression can be obtained:

$$K_{ML}' = (K_{ML}) (\alpha_M') (\alpha_L') / \alpha_{ML}' \quad (52)$$

Figure 4 shows the relationship between conditional stability constants and pH for a number of metal-EDTA complexes, taking into account the effect of pH on $\alpha_{L^{4-}}$ for EDTA and the effect of hydroxy complexes on α_M' . The curves go through a maximum. In the lower pH range, as pH increases, the formation of complex is favored by the deprotonation of the ligand, thus the conditional stability constant is increased. At higher pH values, the formation of hydroxide complexes occurs as a competing side reaction, thus reducing the conditional stability constants. For copper, even at high pH, no significant change in conditional stability constant occurs because of high stability of the complexes.

The equilibrium concentrations of all species in

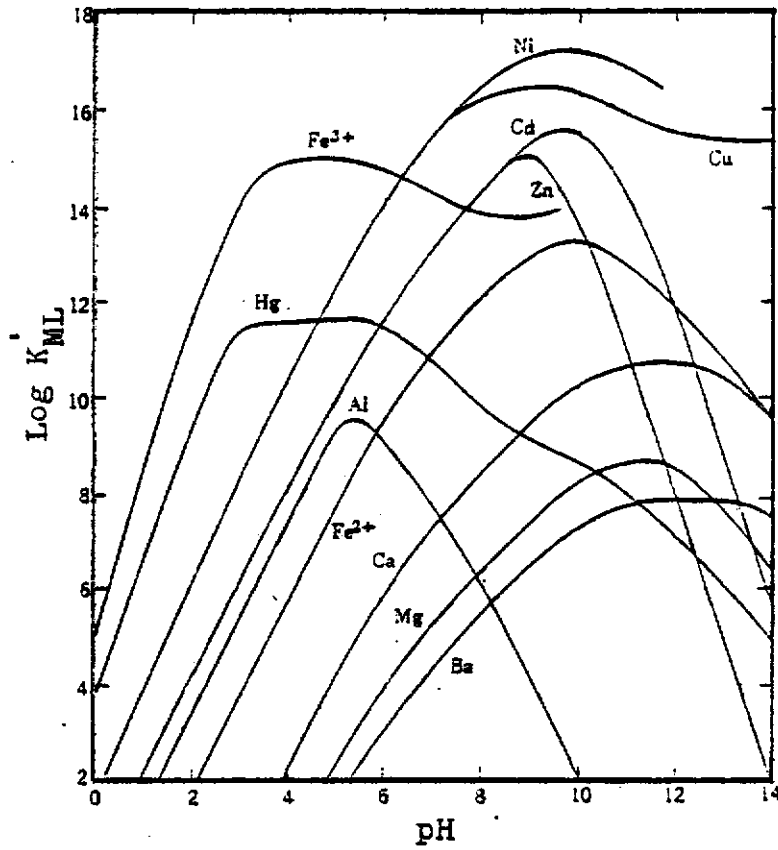


Figure 4. Conditional Stability Constants of Various M-EDTA Complexes as a Function of pH

multi-metal, multi-ligand systems can be calculated by solving a series of simultaneous equations (Equations 21-23,34-42) comprised of mass balance equations, the stability constant expressions, pH of the solution, total metal concentration, total ligand concentration, and the relevant equilibrium constants. A computer program was developed to get the solution (see Appendix 1).

Due to the formation of cyanide gas, the pH of all the metal cyanide studies was always kept above 10. The precipitation problem was encountered at the total cyanide to total metal ratio (CN_T/M_T) of less than 4. This is shown in the results and discussions section.

a. Metal-Cyanide Complexes

Species distribution in the solutions of zinc and cyanide mixtures at various CN_T/Zn_T molar ratio is shown in Figure 5. At 1.55 mM total zinc concentration, the predominant species is $Zn(CN)_3^{1-}$ at the molar ratio of 4, while $Zn(CN)_4^{2-}$ becomes predominant at the ratio of 14 or above. In the same figure, it is shown that for fixed CN_T/Zn_T , more $Zn(CN)_4^{2-}$ is formed at high total metal concentration. Similar plots for the cadmium and cyanide system are also calculated and shown in Figure 6. At ratio 4 or above, $Cd(CN)_4^{2-}$ always predominates in the solution.

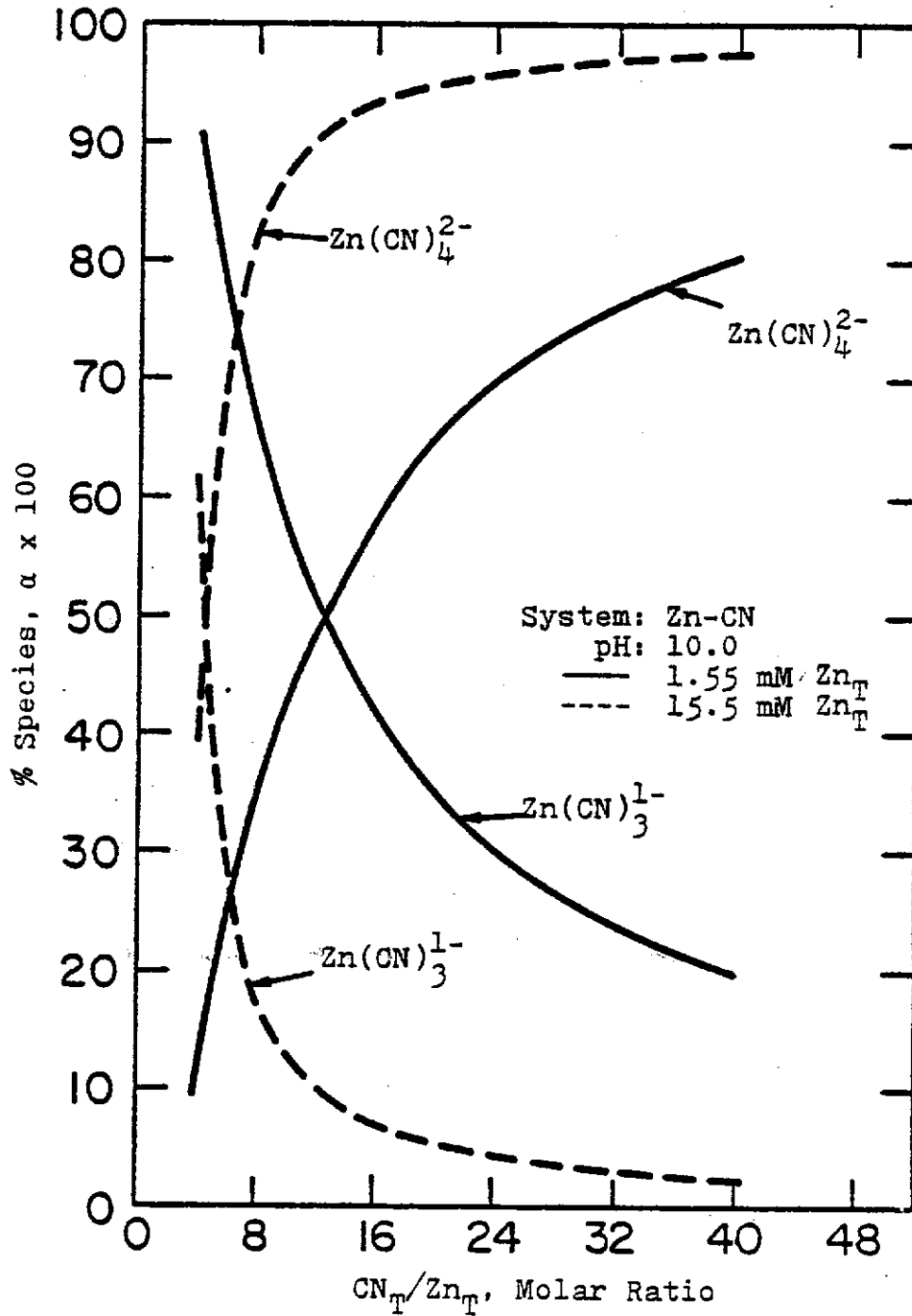


Figure 5. Distribution of Various Species in Zn-CN System as a Function of CN_T/Zn_T Molar Ratio

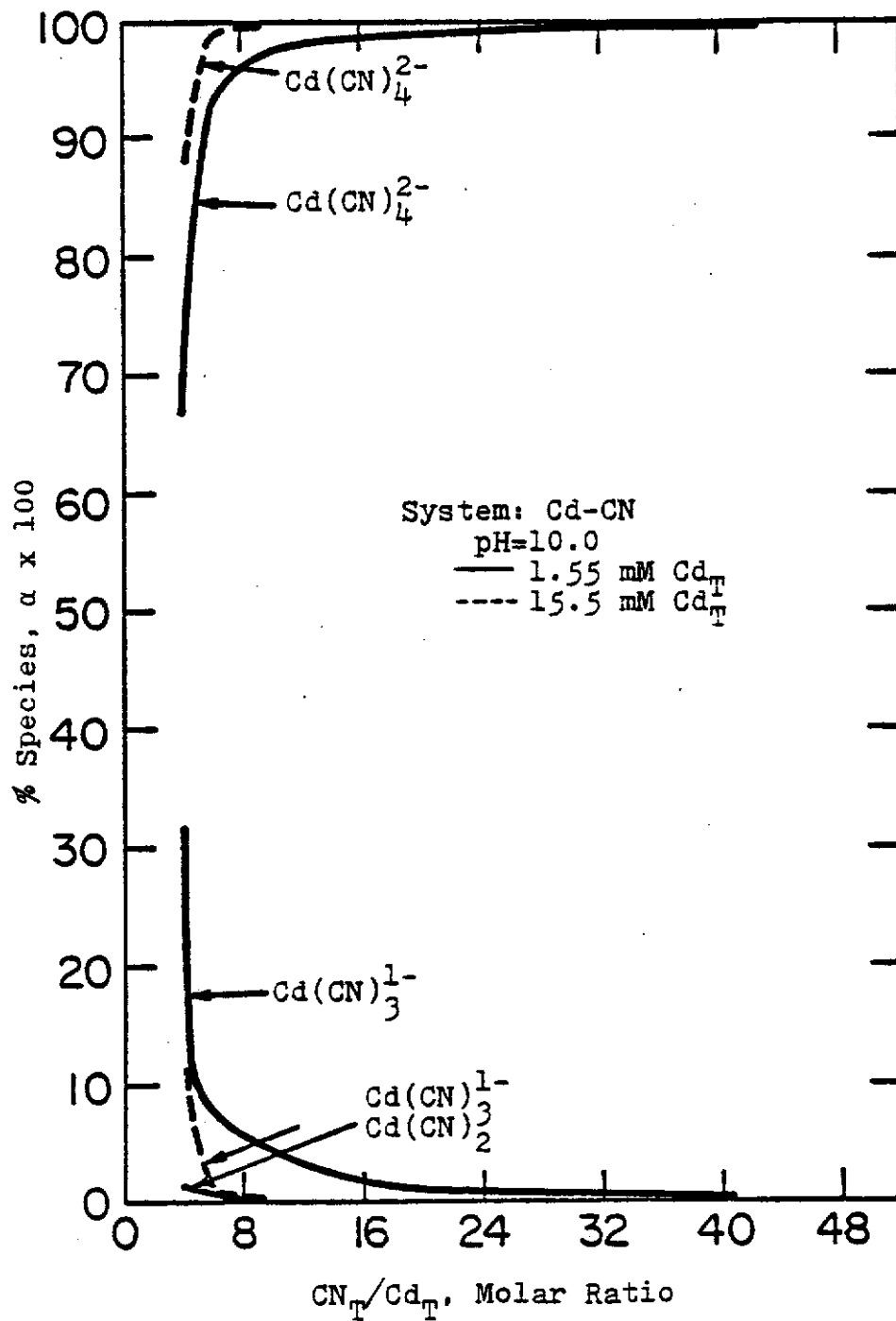


Figure 6. Distribution of Various Species in Cd-CN System as a Function of CN_T/Cd_T Molar Ratio

Species distribution in the solution of copper (Cu^{1+}) and cyanide mixtures at various CN_T/Cu_T is shown in Figure 7. At the concentration of 1.55 mM total copper concentration, $\text{Cu}(\text{CN})_3^{2-}$ predominates at a ratio 4, while $\text{Cu}(\text{CN})_4^{3-}$ predominates at a ratio 18 or above. At the higher metal concentration, $\text{Cu}(\text{CN})_4^{3-}$ predominates above CN_T/Cu_T ratio of 10.

b. Metal-EDTA Complexes

In the presence of EDTA, heavy metal could form various species (depending on pH) in solutions. The distribution of species for copper complexes at various pH is shown in Figure 8. Since the only type of complex formed is $\text{Cu}(\text{EDTA})^{2-}$ over the range of interest (pH 4-10), the species distribution is not influenced by the concentration of ligand present in the solution. It should also be noted that although complexes of different forms may exist, EDTA always forms 1:1 complex with heavy metals.

c. Metal-Oxalate Complexes

In the case of metal-oxalate complexation reactions, a precipitation problem was found for cadmium and zinc even at very high total ligand to total metal ratio in the pH range of 4-10. Copper oxalate precipitates above pH 7.

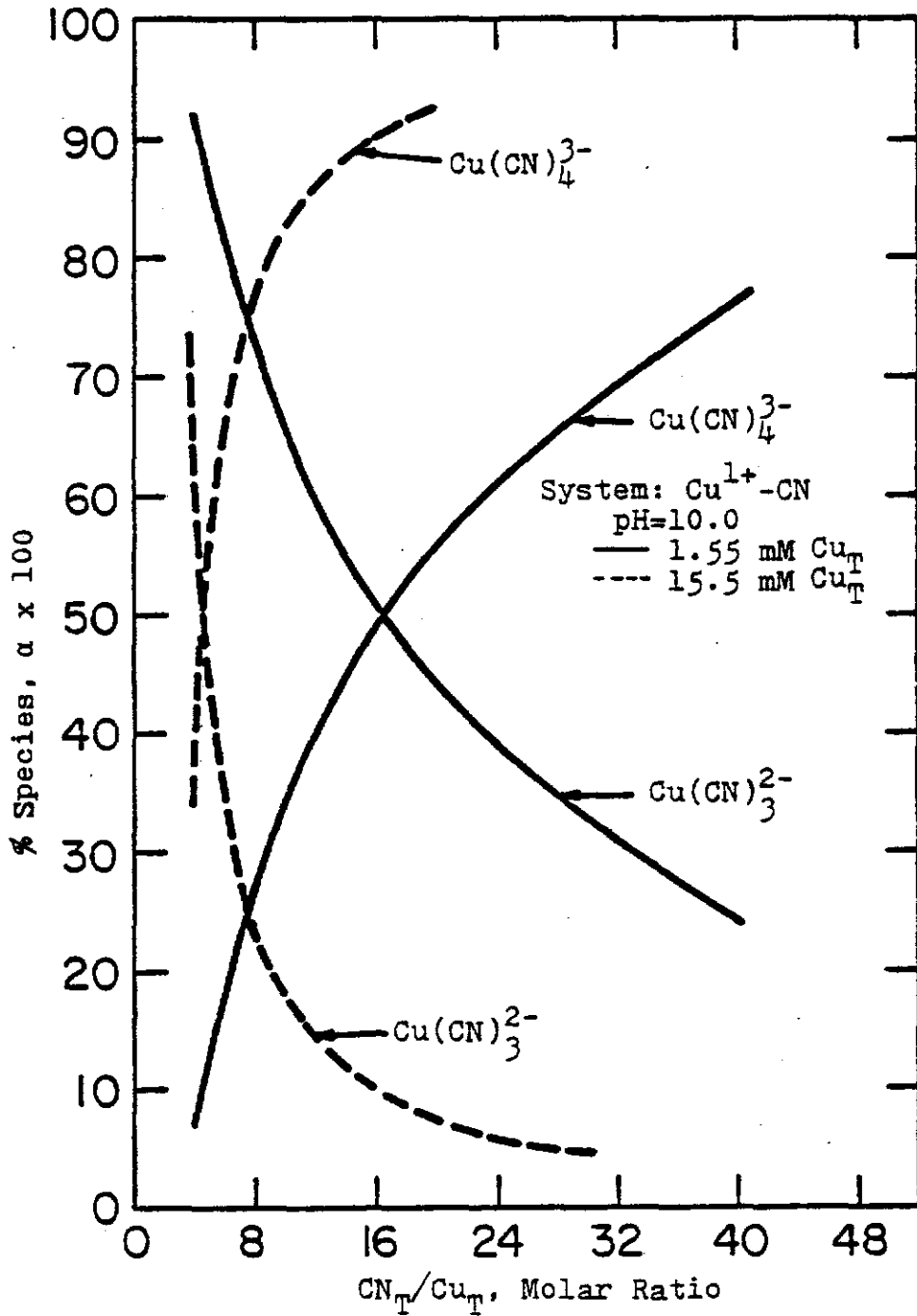


Figure 7. Distribution of Various Species in Cu^{1+} -CN System as a Function of CN_T/Cu_T Molar Ratio

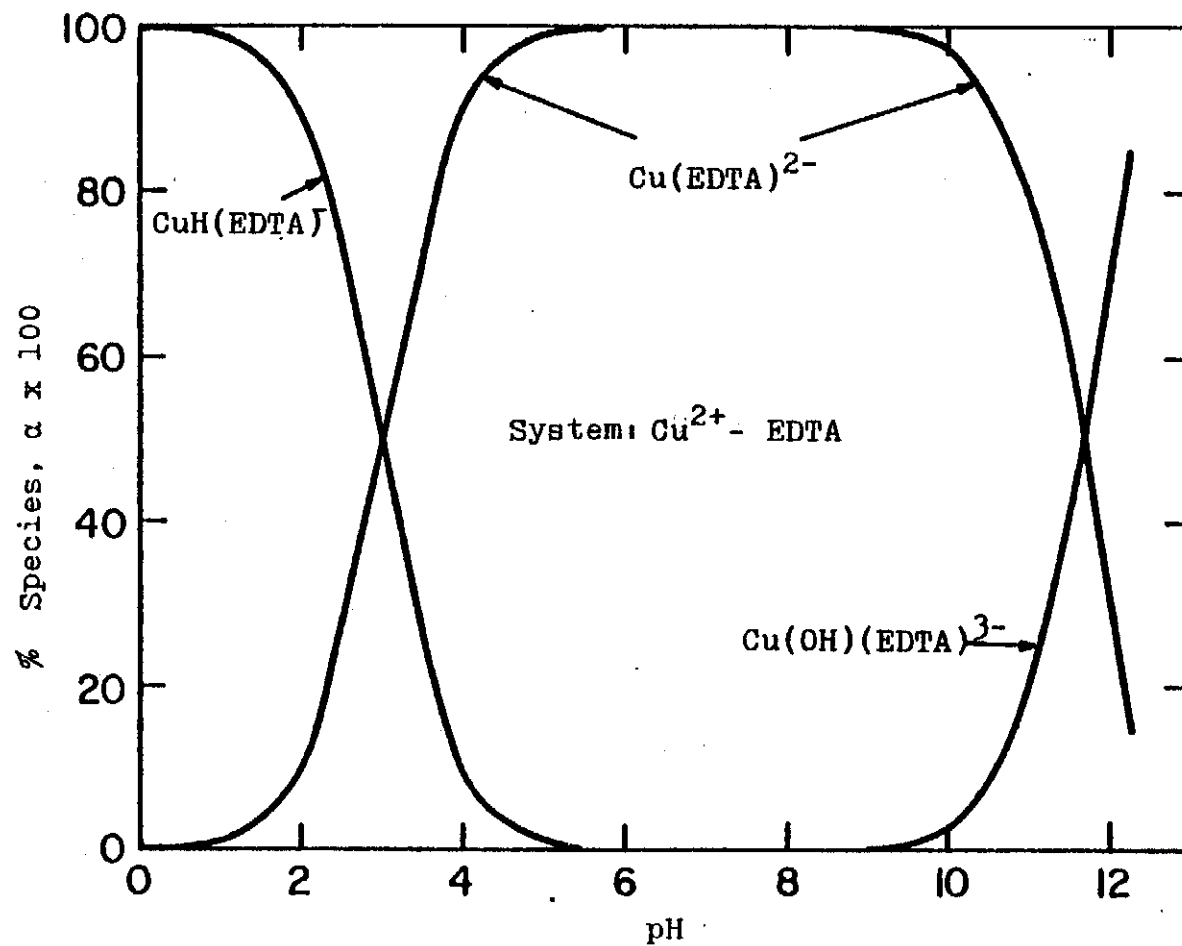


Figure 8. Distribution of Various Species in Cu^{2+} -EDTA System as a Function of pH

Experimental results confirmed this behavior. The species distribution of copper-oxalate complexes is shown in Figure 9. $\text{Cu}(\text{OX})_2^{2-}$ always predominates for $\text{OX}_T/\text{Cu}_T \geq 8$ at pH 4. The effect of pH on species distribution is shown in Table 6. At pH 6, practically all the species present in the solution is $\text{Cu}(\text{OX})_2^{2-}$. At high total metal concentration (15.5 mM), calculation shows that $\text{Cu}(\text{OX})_2^{2-}$ predominates (at both pH 4 and 6) at all OX_T/Cu_T ratios greater than 2.

3. Average Charge Calculations

The behavior of the solution which contains metal complexes could also be characterized in terms of species charge by defining a new parameter --average charge \bar{n} :

$$\bar{n} = \sum Z_i \alpha_i \quad (53)$$

where Z_i = charge of metal containing species i .

α_i = fraction of metal containing species in the solution.

Plots of \bar{n} vs. ratio of total complexing agent to total metal in various metal-cyanide, metal-oxalate systems are shown in Figure 10-13. Average charges are higher for higher total metal concentration at fixed ratio in all

TABLE 6

Copper Containing Species Distribution at Various pH
 in Cu^{2+} -OX systems ($C_i = 1.55 \text{ mM Cu}_T$, $\text{OX}_T/\text{Cu}_T = 4.0$)

<u>pH</u>	<u>Cu(OX)</u>	<u>Cu(OX)₂²⁻</u>	<u>CuH(OX)¹⁻</u>
3.5	0.071	0.924	0.001
4	0.032	0.967	-
6	0.013	0.987	-

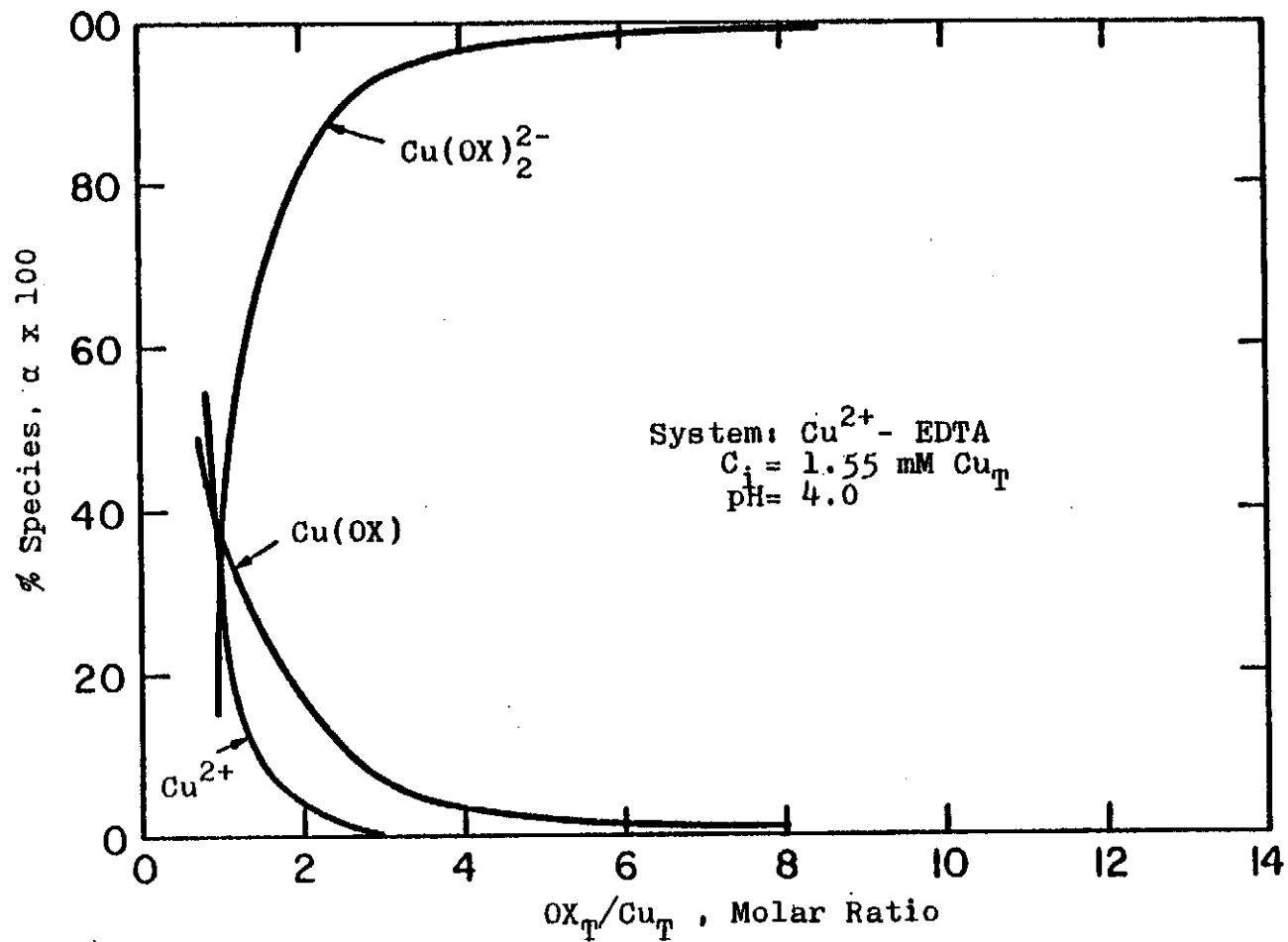


Figure 9. Distribution of Various Species in Cu^{2+} -OX System as a Function of OX_T/Cu_T Molar Ratio

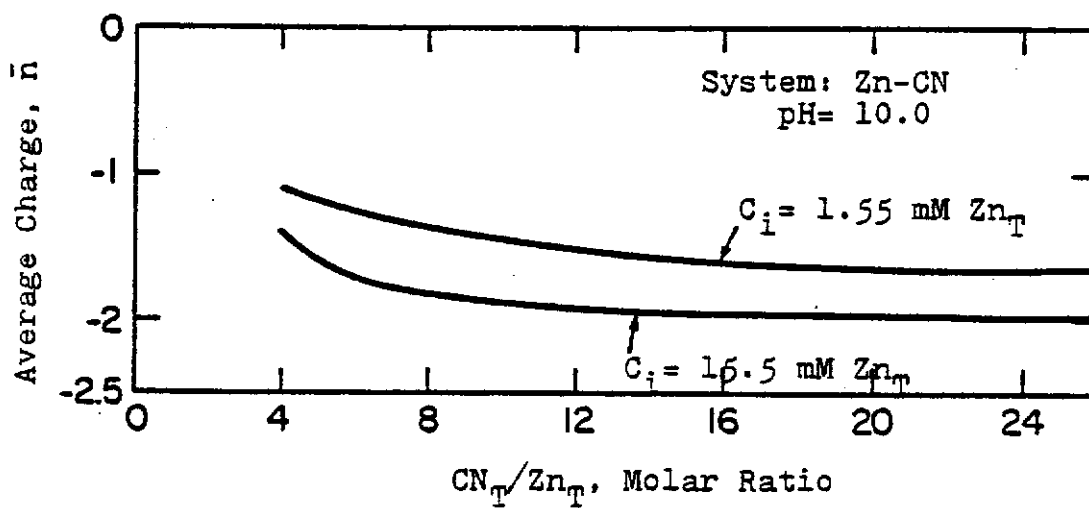


Figure 10. Average Charge \bar{n} in Zn-CN System as a Function of CN_T/Zn_T Molar Ratio

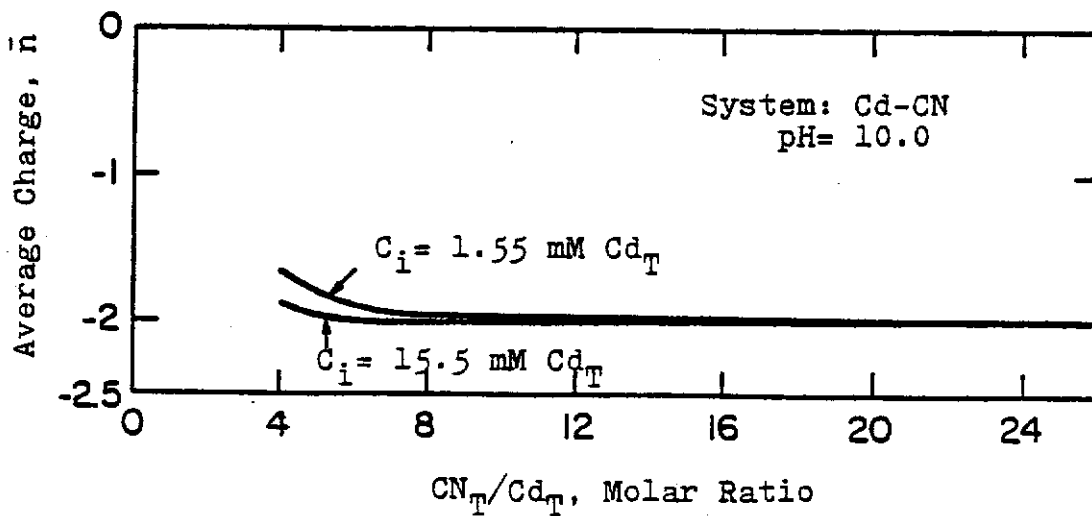


Figure 11. Average Charge \bar{n} in Cd-CN System as a Function of CN_T/Cd_T Molar Ratio

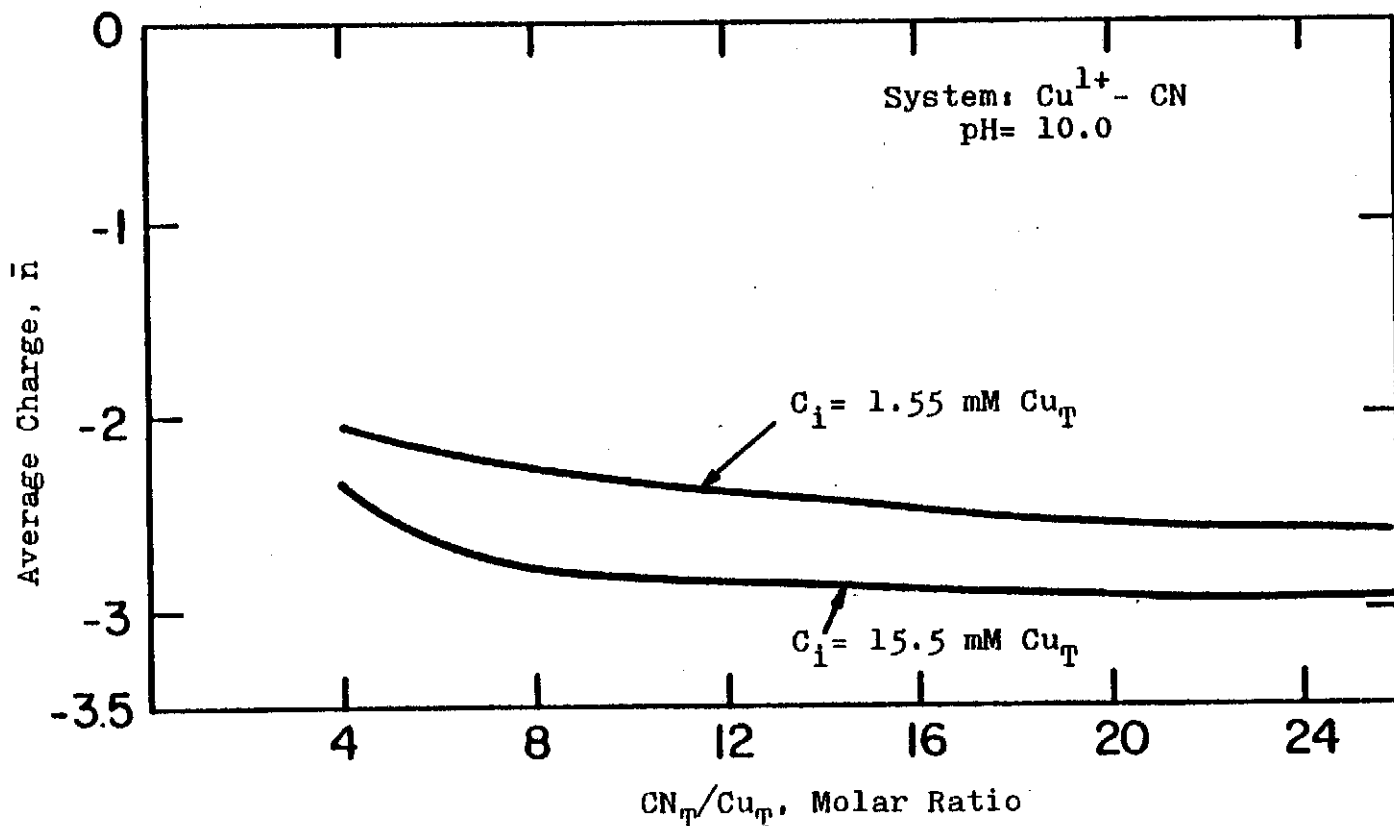


Figure 12. Average Charge \bar{n} in Cu^{1+} -CN System as a Function of CN_T/Cu_T Molar Ratio

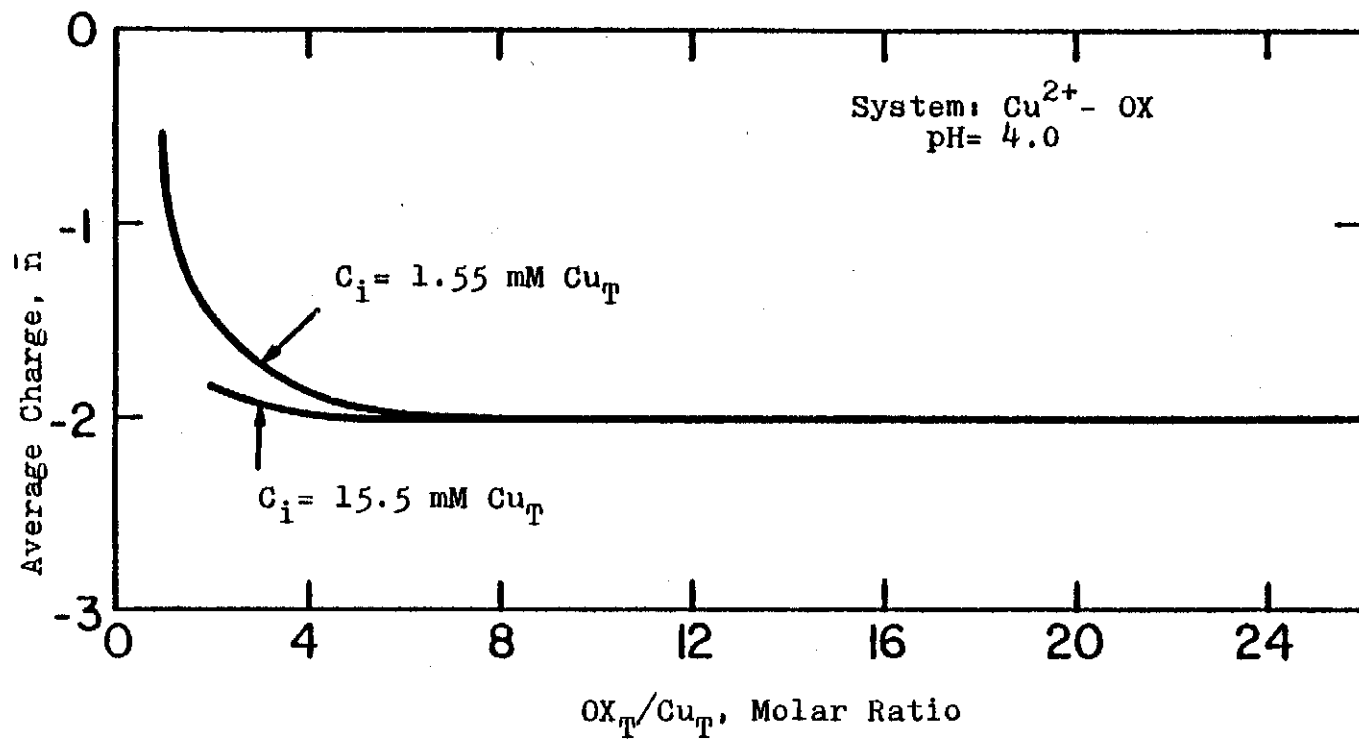


Figure 13. Average Charge \bar{n} in Cu^{2+} -OX System as a Function of OX_T/Cu_T Molar Ratio

all cases. At pH 4, the average charge for copper(II)-oxalate system is -2 at $OX_T/Cu_T \geq 6$. At pH 6 (not shown in the Figure), the average charge is -2 for $OX_T/Cu_T \geq 2$.

VI. EXPERIMENTAL

A. Equipment

The membrane ultrafiltration unit consisted of a semi-batch cell pressurized by a nitrogen tank. The ultrafiltrate samples were passed through a conductivity monitor before being collected in an erlenmeyer flask for further analysis. The schematic diagram of the ultrafiltration unit is shown in Figure 14. The specification of the ultrafiltration cell is shown in Figure 15 where the magnetic stirrer is suspended on a free rotating adjustable shaft.

A mixing speed of about 600 RPM was used for each study in order to maintain the whole solution under highly turbulent flow conditions. The Reynolds number for such a mixing system can be defined as follows (34):

$$Re = D^2 N \rho / \mu \quad (54)$$

where D = diameter of impeller or length normal to axis of rotation, cm.

N = angular velocity of agitator, revolution per second or RPS.

A Reynold number of about 40000 was used in this

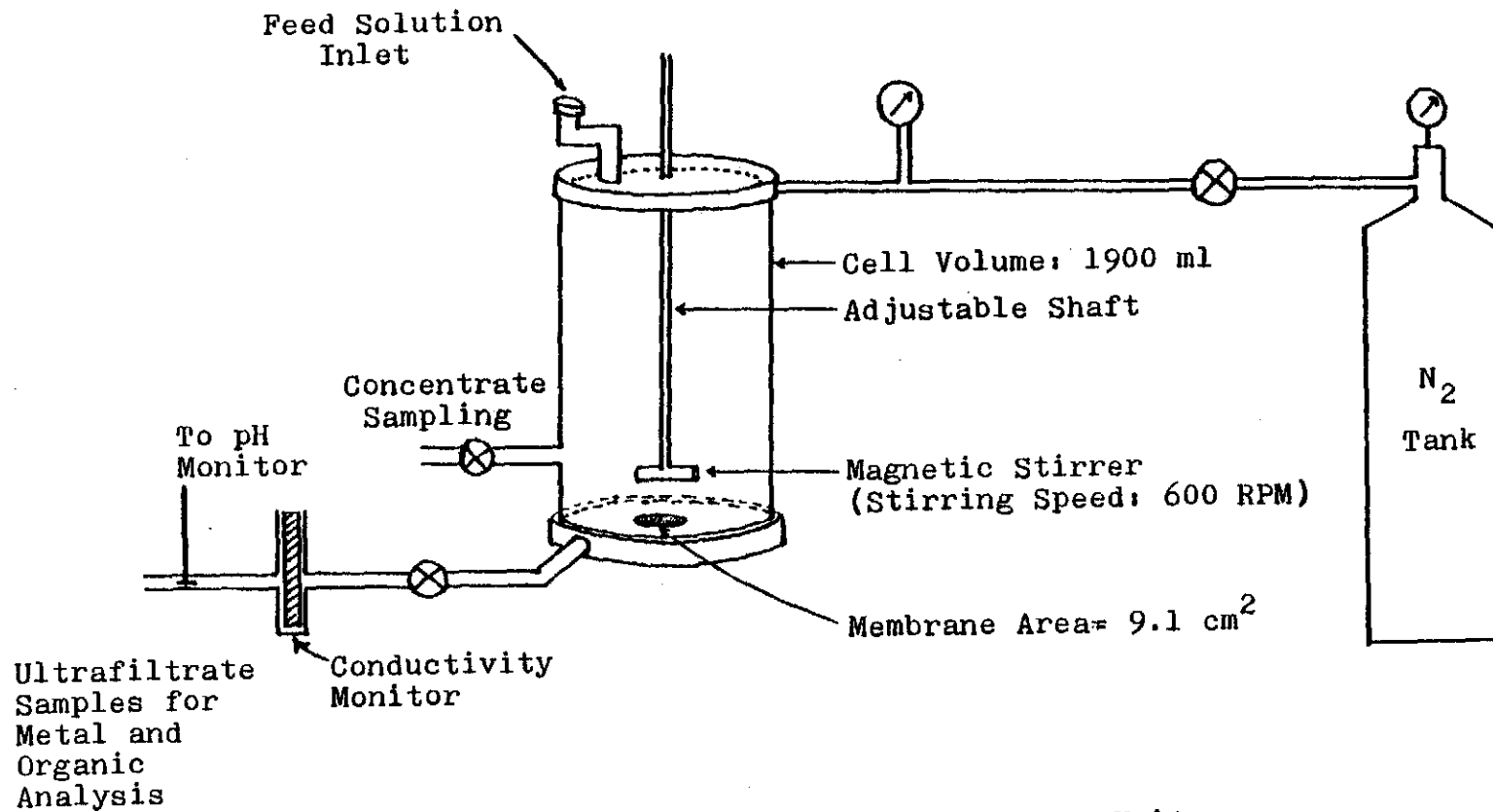
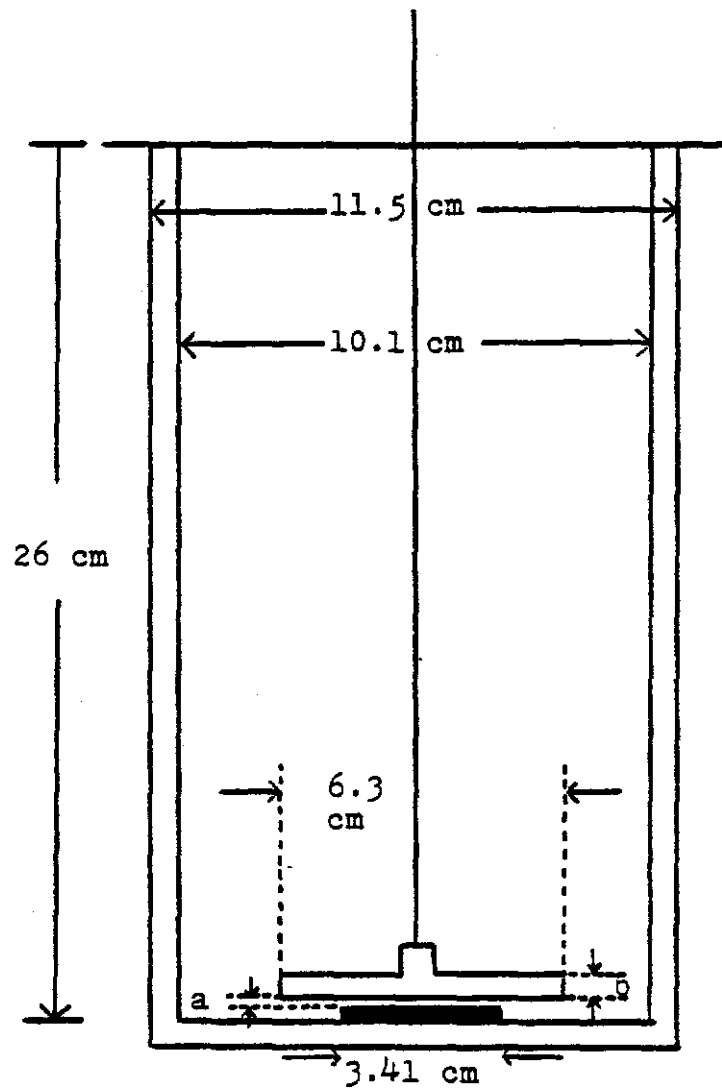


Figure 14. Schematic Diagram of Membrane Unit



a: 0.4 cm

b: 1.0 cm

Figure 15. Specifications of the Ultrafiltration Cell

study, which is more than the Reynolds number required for turbulent flow for such system ($Re = 10000$).

Millipore PTAL negatively-charged noncellulosic ultrafiltration membranes were used in this study. The membranes used for this study were cut from dry membrane sheet and then soaked for fifteen minutes in distilled water before being cut to the exact size and installed in the unit. Some properties of these membranes are shown in Table 7.

B. Chemicals Used

The following analytical reagent grade chemicals were used in this study:

ammonium chloride	NH_4Cl
ammonium hydroxide	NH_4OH
cadmium chloride	$CdCl_2 \cdot 2(1/2)H_2O$
cadmium nitrate	$Cd(NO_3)_2 \cdot 4H_2O$
copper(II) chloride	$CuCl_2 \cdot 2H_2O$
copper(II) sulfate	$CuSO_4 \cdot 5H_2O$
copper(I) cyanide	$CuCN$
copper(II) nitrate	$Cu(NO_3)_2 \cdot 3H_2O$
EDTA disodium salt	$C_{10}H_{14}O_8N_2Na_2 \cdot 2H_2O$
hydrochloric acid	HCl

TABLE 7

Properties of PTAL membranes

Composition	noncellulosic skin on noncellulosic backing
Membrane thickness	240 μm
Skin thickness	$\approx 500 \text{ \AA}$
Membrane pores	$\approx 15 \text{ to } 20 \text{ \AA}$
Operating pH	1-12.5
Temperature limit	70°C
Pressure limit	$9 \times 10^5 \text{ N/M}^2$
Fixed charge	negative sulfonate group
Charge capacity	$\approx 350 \text{ mM}$
Normal operating pressure	$5.5 \times 10^5 \text{ N/M}^2$
Typical water flux at normal operating pressure	$1.3 \times 10^{-3} \text{ cm/sec}$

oxalic acid	$\text{H}_2\text{C}_2\text{O}_4 \cdot 2\text{H}_2\text{O}$
sodium cyanide	NaCN
sodium hydroxide	NaOH
sodium nitrate	NaNO_3
zinc chloride	ZnCl_2
zinc cyanide	$\text{Zn}(\text{CN})_2$
zinc nitrate	$\text{Zn}(\text{NO}_3)_2 \cdot 6\text{H}_2\text{O}$

C. Procedure

Preparation of Solutions

a. Metal-cyanide Solutions

A known amount of $\text{Zn}(\text{CN})_2$, CuCN , or CdNO_3 was dissolved in a solution which contained a predetermined quantity of NaCN . The pH was adjusted to 10 by adding known concentrations of NaOH and HCl stock solutions under vigorous stirring. The total metal concentration was varied in the range of 0.31 mM to 15.5 mM, and the total cyanide to total metal molar ratio was varied in the range of 4.0 to 40.0.

b. Metal-EDTA Solutions

A known amount of ZnCl_2 , CuCl_2 , or CdCl_2 was weighed

out before adding to the solution containing EDTA (disodium salt). The pH of the solution was then adjusted by adding known concentrations of NaOH and HCl stock solution under vigorous stirring. The metal concentration of 1.55 mM was used, and the total EDTA to total metal ratio was varied in the range of 0.5 to 2.0.

c. Metal-oxalate Solutions

Only the Cu^{2+} -OX system was studied here because of the occurrence of precipitate in Zn-OX and Cd-OX over the pH range (pH 4-6), concentration range (0.155-15.5 mM) and oxalate to metal molar ratio range (0-20).

A known amount of CuNO_3 salt was weighed out and added to the solution containing oxalic acid. The pH was then adjusted by using known concentrations of NaOH and HCl stock solutions under vigorous stirring. The metal concentration was varied in the range of 0.775 to 7.75 mM. The pH was varied from 4 to 6, and the total oxalate to total metal ratio was varied from 0.5 to 12.

Distilled water of 4 $\mu\text{mole/cm}$ was used to prepare all of the above solutions.

Experimental Procedure

1. Runs at Negligible Water Recovery

The cell was filled with distilled water and run for 30 minutes. After the distilled water flux data were taken, the cell was emptied and filled with the feed solution. At the same time, two 50 ml feed solutions were collected as an additional check of the prepared solution. One of them was filtered through a 0.45 um Millipore membrane filter. The cell was run for three hours at 600 RPM. Frequent checks were made by using a simple salt such as CuCl_2 to insure the membrane had not deteriorated from previous runs. The ultrafiltrate samples were collected each hour. Typical runs were 2-3 hours long. At the end, a portion of the feed solution was collected as the end feed solution for further analysis of metal ions and complexing agents. The cell was washed, rinsed and filled with distilled water and run for another 30 minutes. The distilled water flux data were then taken as a reference.

2. Runs at High Water Recovery

The Zn-CN, Cu^{2+} -EDTA, and Cu^{2+} -OX systems were also studied under various recovery conditions. A total complexing agent to total metal molar ratio of 4 was used for Zn-CN and Cu^{2+} -OX systems and the ratios of 2 and 4 were used for Cu^{2+} -EDTA systems. The pH of the Cu^{2+} -EDTA ($\text{EDTA}_T/\text{Cu}_T = 4$) and Cu^{2+} -OX systems were kept at 4 while

the pH of Zn-CN system was kept at 10 because of the formation of HCN at lower pH. The pH of 10 was also used for the Cu^{2+} -EDTA ($\text{EDTA}_T/\text{Cu}_T = 2$) system in order to compare with another Cu^{2+} -EDTA system. The same operating procedures were used as that of the negligible water recovery runs. Three days were employed for each of these high recovery runs with frequent sampling of feed and ultrafiltrate and the subsequent analysis of these samples. The temperature was kept constant at $25 \pm 1^\circ\text{C}$.

D. Analytical Procedures

Metal analysis of ultrafiltrate, feed, and concentrate samples were done by atomic absorption. A Varian AA 375 Atomic Absorption Spectrophotometer was used for such purposes. The analytical accuracy was $\pm 2\%$, and Table 8 lists the principal absorption wavelength, flame type, and sensitivity for the three metals in this study.

The analysis of total complexing agents was done by TOC (total organic carbon) measurements. The Beckman Model 915 Total Organic Carbon Analyzer was used for such purpose. The analytical accuracy was $\pm 4\%$.

Conductivity measurements were taken from samples by using a Leeds and Northrup Conductivity Monitor.

The pH of the sample solutions were monitored by a

TABLE 8

Atomic Absorption Characteristics

<u>Metal</u>	<u>Wavelength (nm)</u>	<u>Flame type</u>	<u>Sensitivity(mg/l)</u>
Zn ²⁺	213.86	air-C ₂ H ₂	0.009
Cd ²⁺	228.80	air-C ₂ H ₂	0.011
Cu ²⁺	324.80	air-C ₂ H ₂	0.003

Corning Model 12 Research pH meter.

All the filtrations of feed and concentrate solutions were done by using Millipore 0.45 μm pore size filters. This step was used to check the possible precipitate formation in the sample or feed solutions.

VII. RESULTS AND DISCUSSIONS

A. Membrane Characterization

Previous studies (9-11) on charged membrane ultrafiltration were conducted under continuous flow, steady state operation which required a large volume of feed solution. The steady state operating condition of continuous cell could also be effectively simulated with the semi-batch cell utilizing small membrane area. In order to keep the feed volume and feed concentration changes negligible (less than 5 %) over a two to three hours operating period, selection of membrane area of about 9 cm^2 and a feed volume of 2 liters was utilized. This mode of operation provided water flux and ultrafiltrate concentration characteristics similar to that obtained with continuous cells. This type of cell has also been used by other investigators in their reverse osmosis and ultrafiltration studies (21).

Membrane performance is found to be greatly influenced by the concentration polarization and fouling effects (35). In order to reduce and/or eliminate these undesirable effects, high speed magnetic stirring was used. The flux data of all low recovery runs were compared with the distilled water flux before and after the run. The results of this comparison is shown in Figure 16. No significant

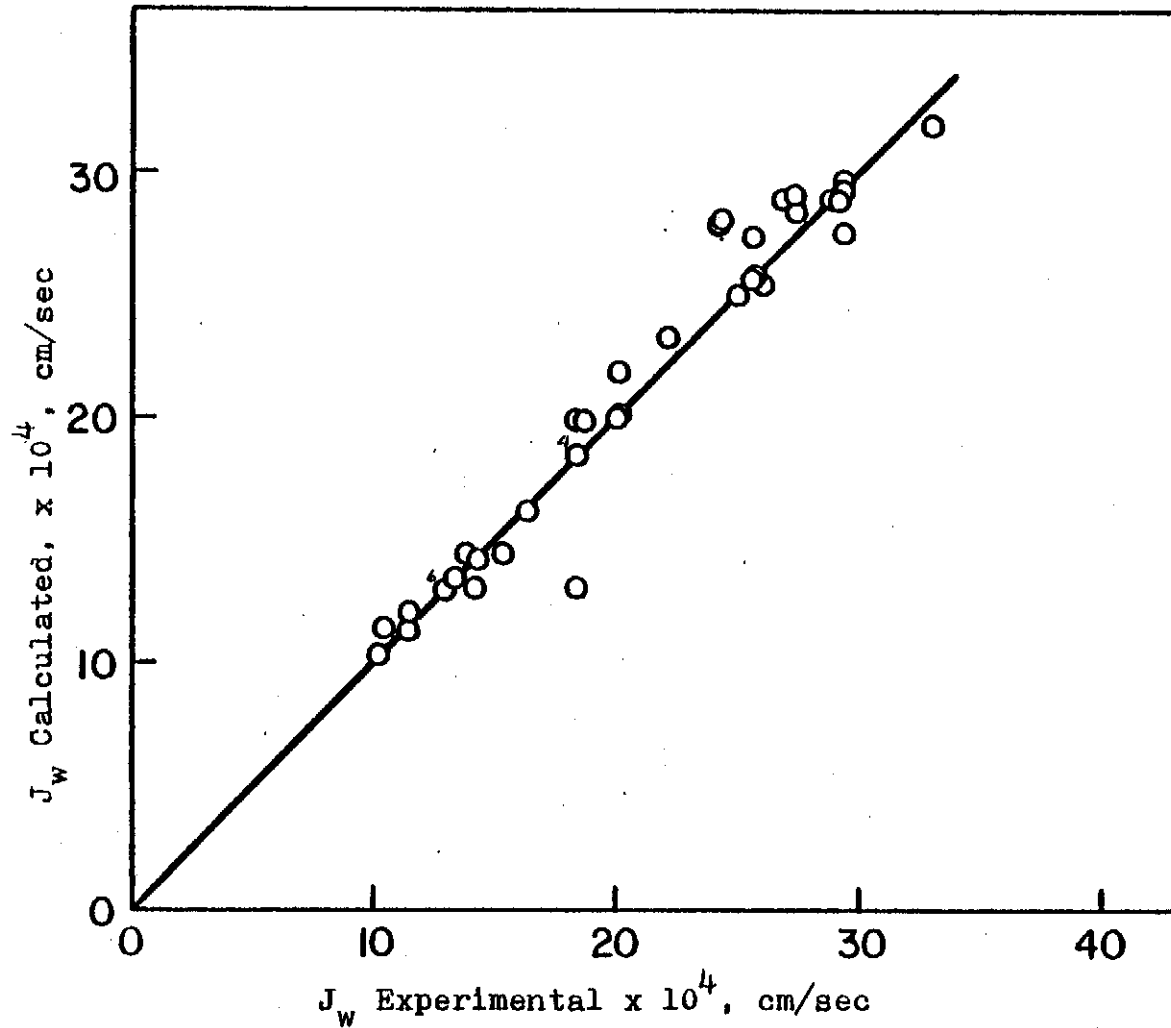


Figure 16. Comparison of Calculated and Experimental Water Fluxes for PTAL Membranes

concentration polarization or fouling problem was found throughout the studies.

In order to test the effect of pressure on the water flux through the membrane, several distilled water flux data were obtained under different pressures, as shown in Figure 17. Flux reproducibility is extremely good below $8.0 \times 10^5 \text{ N/m}^2$ for negatively charged ultrafiltration membrane. The nonlinearity and the nonreproducibility of flux over the high pressure (above $10 \times 10^5 \text{ N/m}^2$) was due to irreversible change in membrane pore structure.

Membrane variation of different batch products is shown in Table 9. The results could be used to correct all the experimental data throughout the study whenever comparison among different membranes was necessary.

B. Rejection of Individual Complexing Agents

Cyanide rejection as a function of pH was not performed in the laboratory because of possible formation of hydrogen cyanide gas. However, the concentration effect was studied for sodium cyanide and the result is shown in Table 10. Very low rejection was found at all concentration levels. This is due to the fact that CN^- has relatively small ionic radius with single charge on it. The rejection dropped significantly as the feed concentration

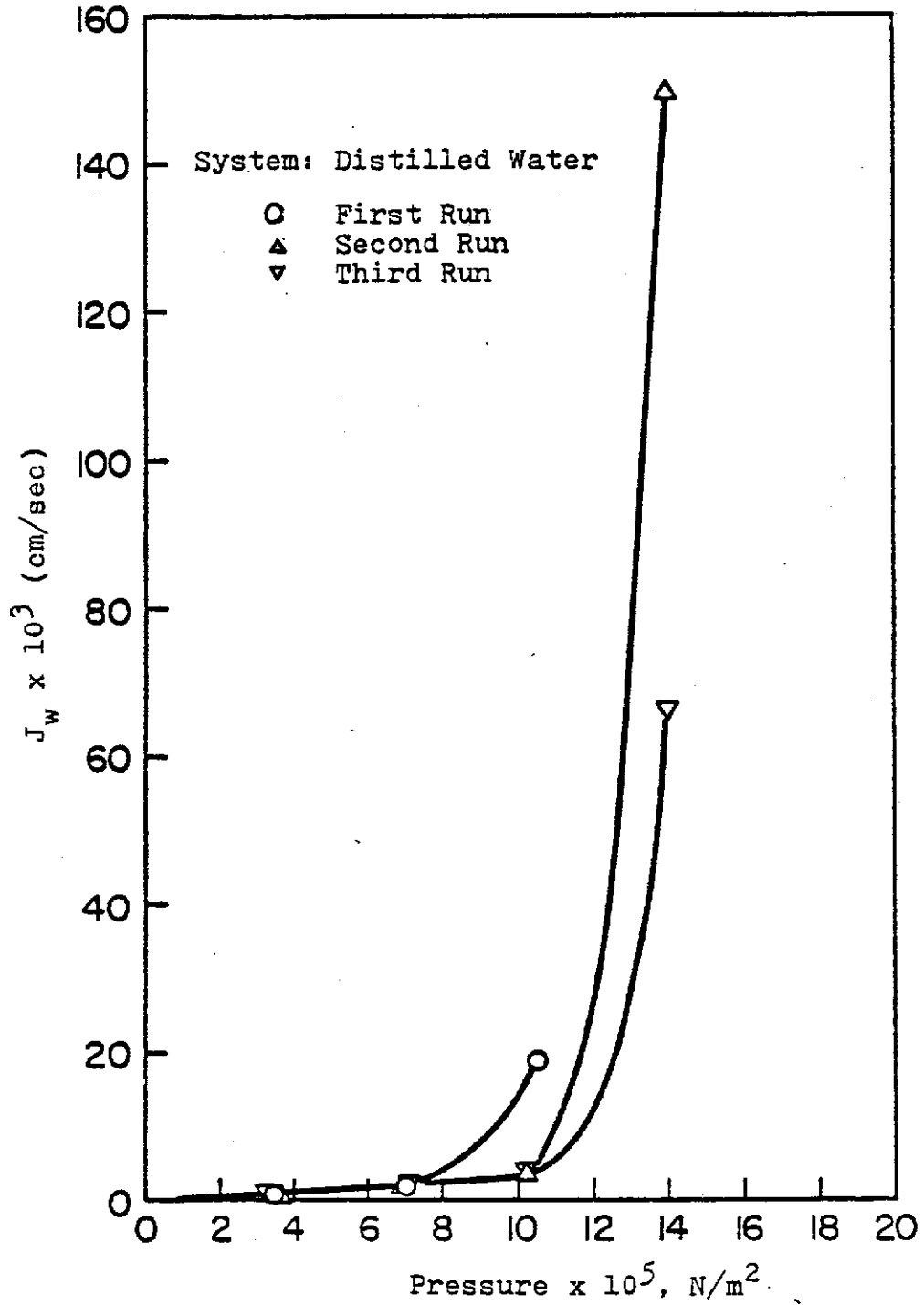


Figure 17. Distilled Water Flux (Solute Free) at Various Applied Pressure for PTAL Membranes

TABLE 9

Characteristics of New Membranes

Membrane Batch No.	R_m	J_w^* , (cm/sec)	$R_{CuCl_2}^{**}$
1	2.35×10^8	23.8×10^{-4}	0.33
2	2.37×10^8	23.6×10^{-4}	0.34
3	3.0×10^8	18.6×10^{-4}	0.64
4	3.57×10^8	15.7×10^{-4}	0.57
5	3.33×10^8	16.8×10^{-4}	0.61

* at $\Delta P = 5.6 \times 10^5 \text{ N/m}^2$

** $CuCl_2$ concentration = 1.55 mM, pH = 4

TABLE 10

Rejection of NaCN at pH 10

<u>Concentration (mM)</u>	<u>Rejection</u>
3.1	0.28
8	0.17
560	0

of CN_T increased. This conforms to the Donnan equilibrium model and Nernst-Planck model stated before.

The rejection of $EDTA_T$ at various pH values is shown in Figure 18. The plot shows that the rejection of $EDTA_T$ is relatively high at pH 4 or higher. Moreover, the rejection increases as pH increases. These observations can be rationalized by looking back to Figure 2 where it shows that higher charge species such as $H(EDTA)^{3-}$ or $EDTA^{4-}$ are predominant in the solution as pH increases. The relatively large size of the EDTA molecules contributes to high rejection behavior even at low pH where the lower charge species such as $H_3(EDTA)^{1-}$ or $H_2(EDTA)^{2-}$ predominate.

The rejection of oxalic acid at various pH values is shown in Figure 19. This figure shows that the rejection of oxalic acid is greatly enhanced as the pH value increases from 4 to 7. This behavior can be explained on the basis of ionization (Figure 3). As pH increases, the higher rejection is definitely due to the conversion of the low charge species $H(OX)^{1-}$ into the higher charge species OX^{2-} . The Nernst-Planck model can be used to explain the difference in the rejection behavior of EDTA or oxalate when the charge on predominant species being equal in both cases. It should also be noted that the rejection of mono-

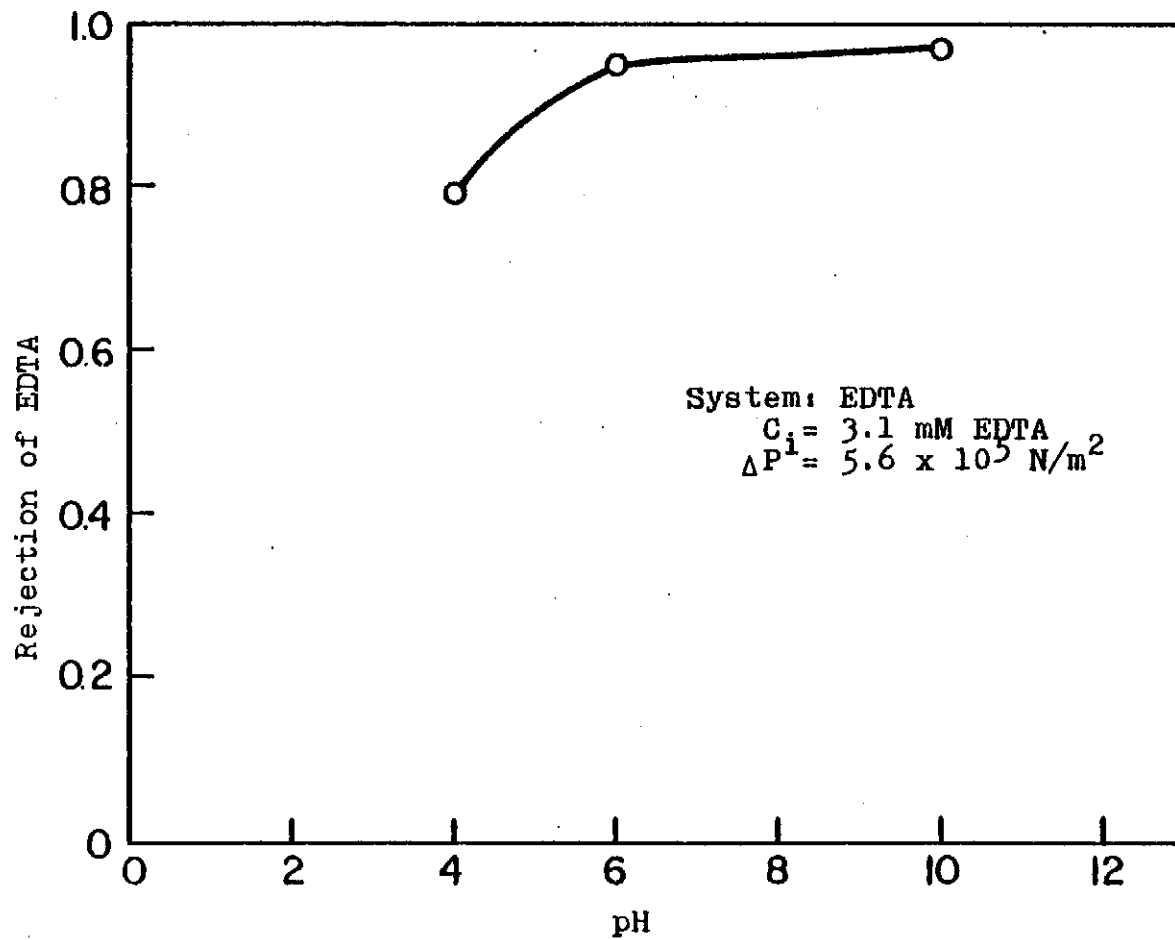


Figure 18. Effect of pH on EDTA Rejection

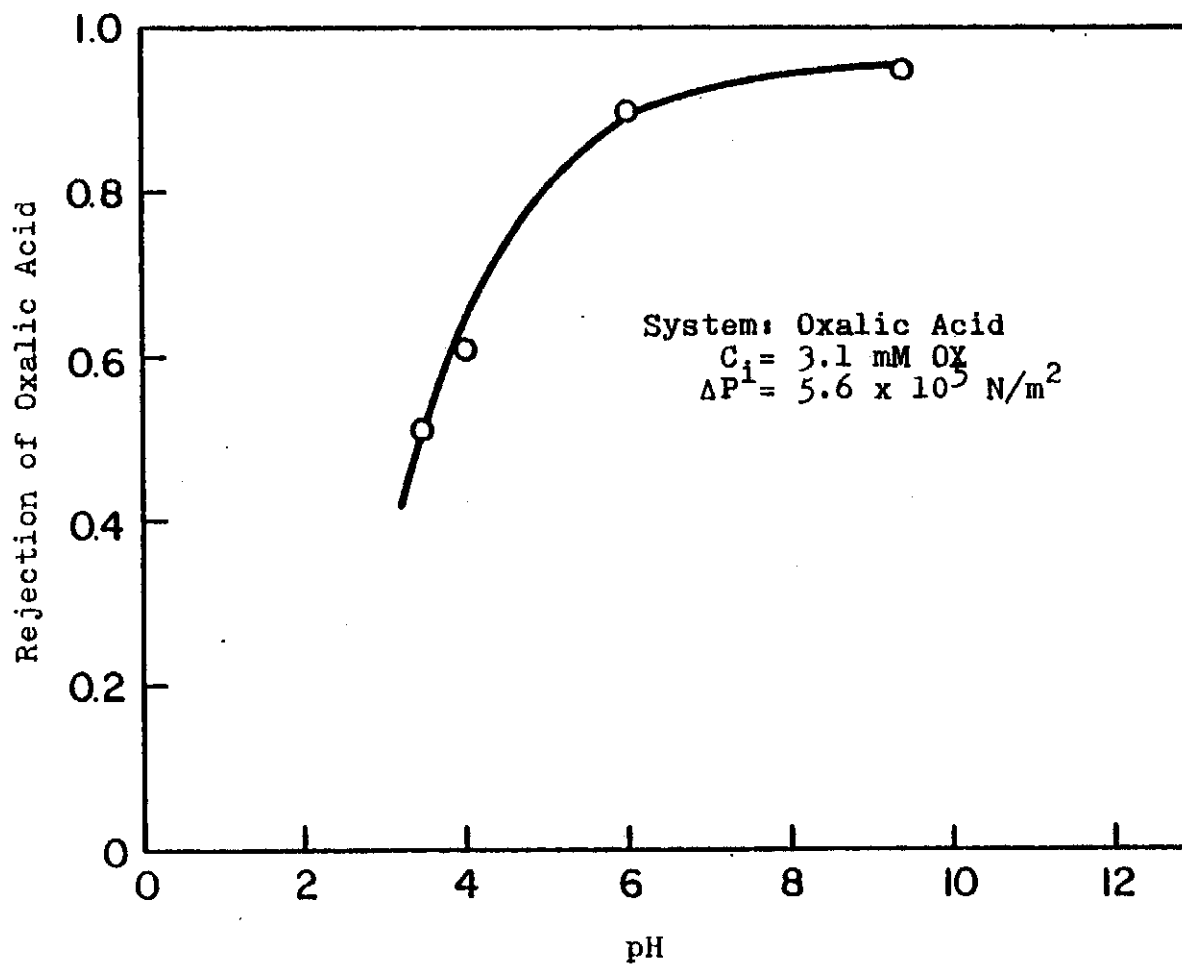


Figure 19. Effect of pH on Oxalic Acid Rejection

valent species may be lower in the presence of di- or tri-valent species, and hence the prediction of overall rejection may not conform to the additive rule (15).

C. Metal-Cyanide Rejection Studies

Rejections of total zinc (Zn_T) and total (CN_T) at various total cyanide to total metal ratios (CN_T/Zn_T) were studied quite extensively here; similar experiment runs were carried out for Cd and Cu for comparison. In order to explain the results of the above studies, an ionic strength effect was investigated for the Zn-CN system. The concentration effect was also investigated in order to provide valuable information on water recovery.

A pressure of $5.6 \times 10^5 \text{ N/m}^2$ was used for most runs to obtain maximum (asymptotic) rejection. As shown in Figure 20, the system is essentially free of solute diffusion effects above a ΔP of $5 \times 10^5 \text{ N/m}^2$.

1. Effect of CN_T/Zn_T on the Total Metal and Total Cyanide Rejection

Rejections of M_T ($M = \text{Zn, Cd, or Cu}$) and CN_T at various CN_T/M_T ratios and at pH 10 are shown in Figures 21, 22 and 23. The rejections of Zn_T , Cd_T , and Cu_T were found to be increased considerably in the presence of complexing agent. This is due to the fact that the complexed metal

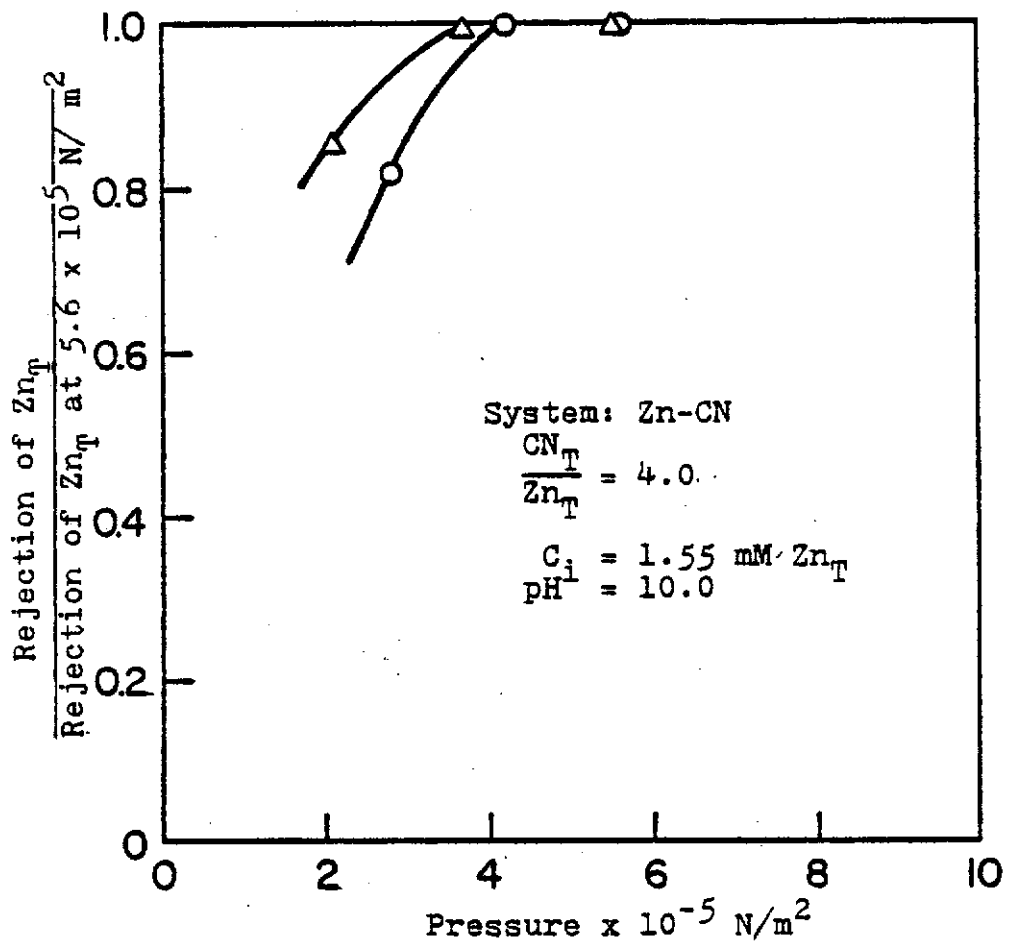


Figure 20. Effect of Pressure on the Rejection of Zn_T in Zn-CN System

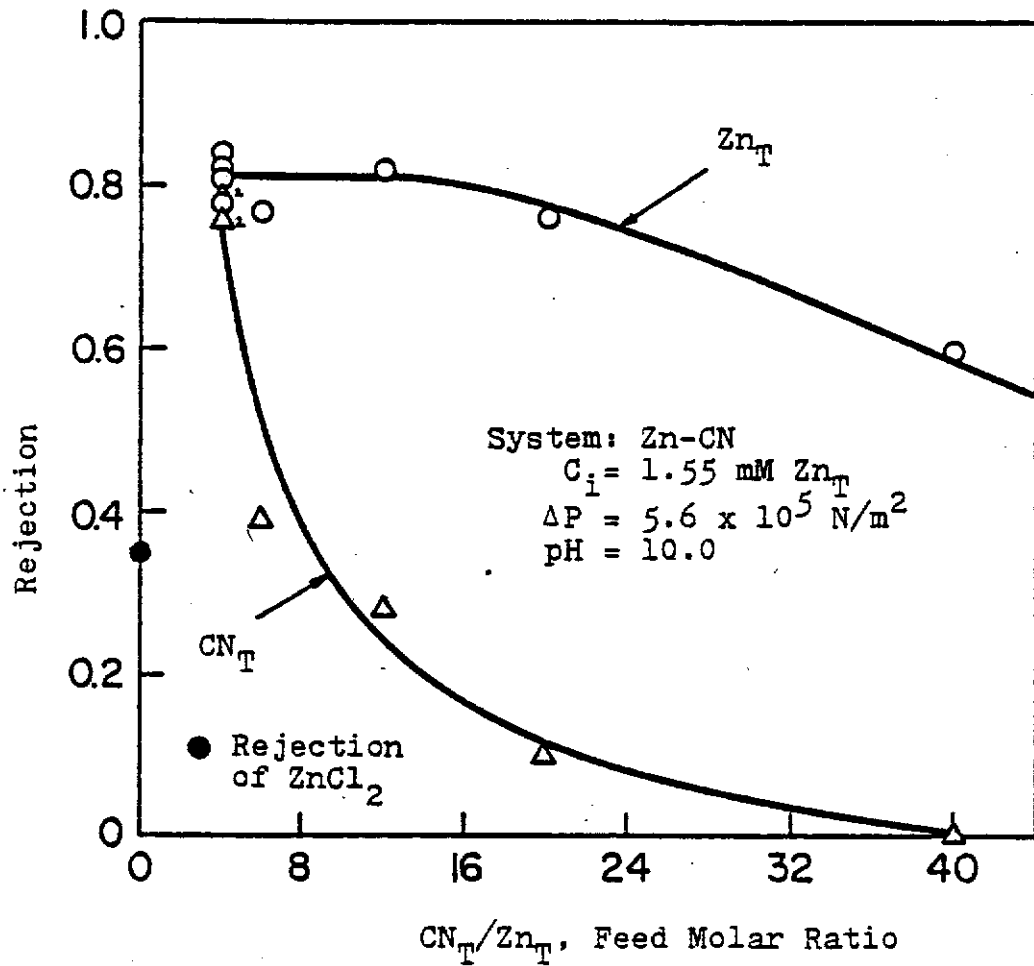


Figure 21. Rejection Behavior of Zn_T and CN_T as a Function of Feed Molar Ratio (CN_T/Zn_T) for Zn-CN System

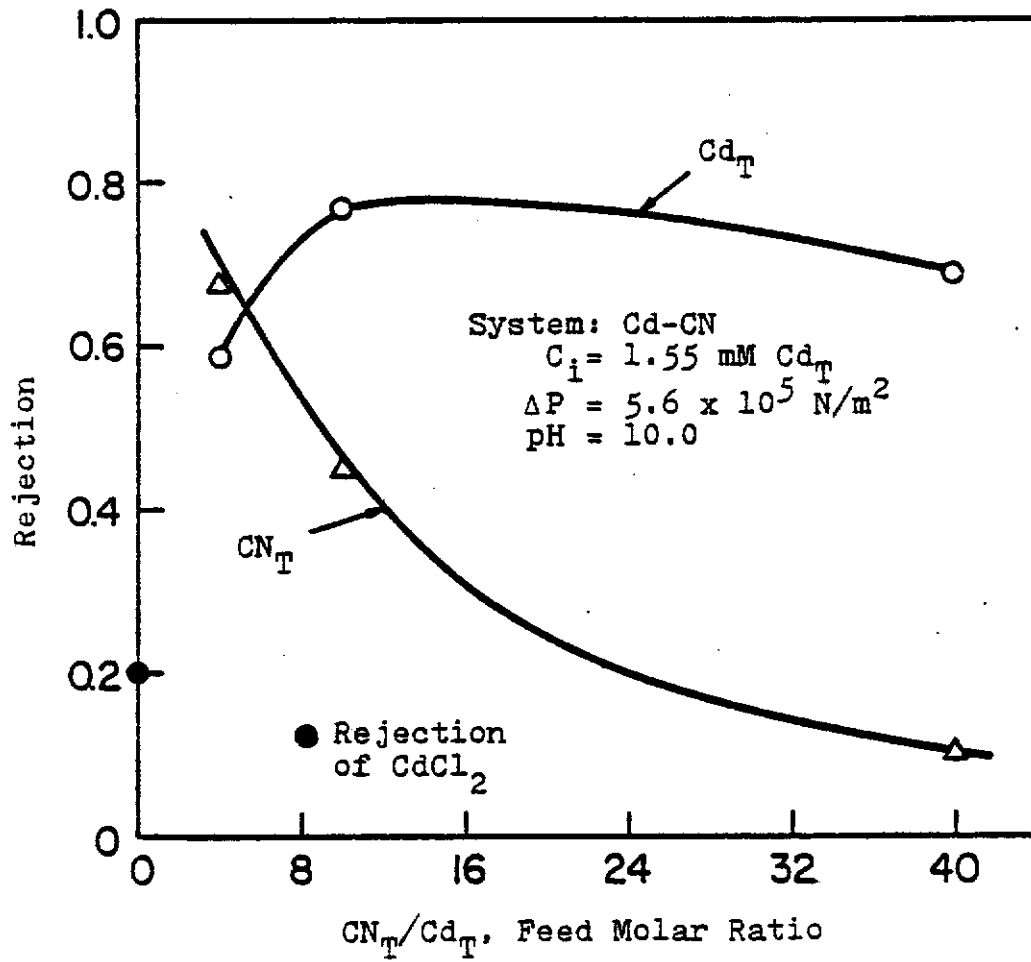


Figure 22. Rejection Behavior of Cd_T and CN_T as a Function of Feed Molar Ratio (CN_T/Cd_T) for Cd-CN System

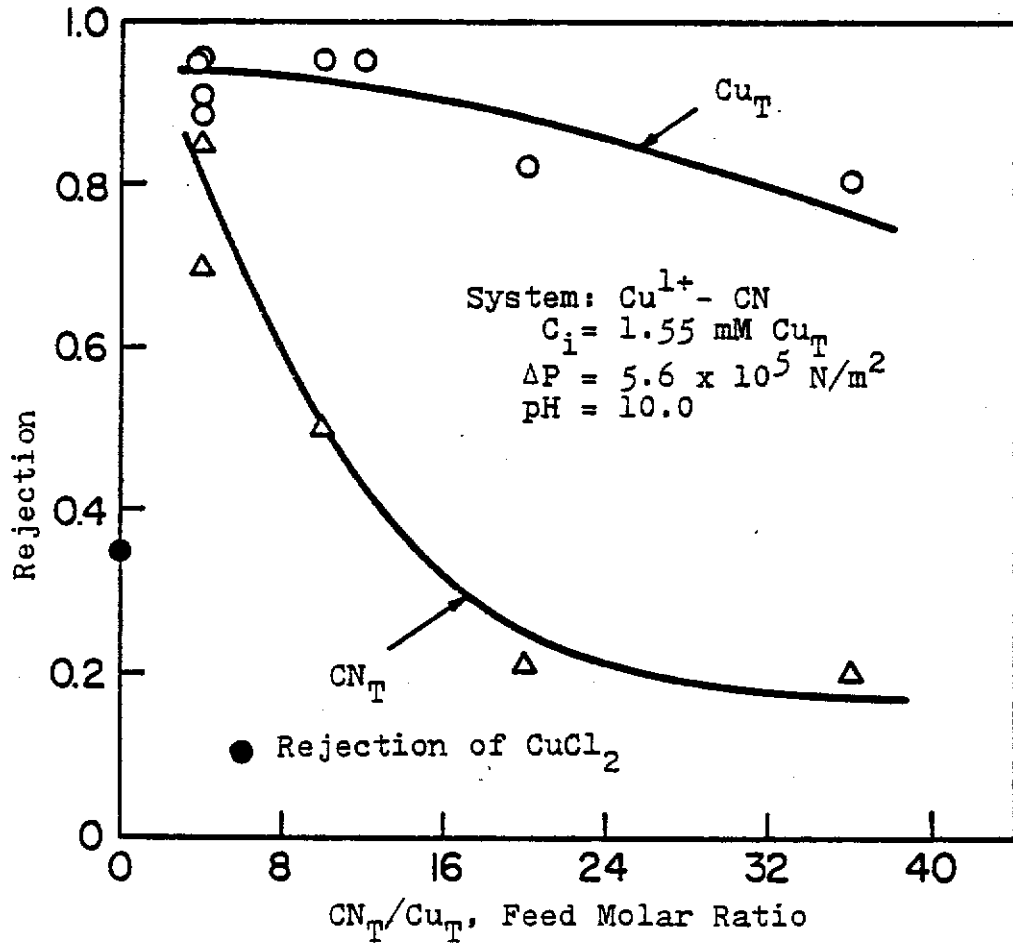


Figure 23. Rejection Behavior of Cu_T and CN_T as a Function of Feed Molar Ratio (CN_T/Cu_T) for Cu^{1+} -CN System

cyanide anions are rejected better than M^{2+} ions. The rejections of Cu_T and CN_T were found to be highest for the copper(I)-cyanide solution at pH 10 under various CN_T/M_T ratios. This phenomenon could be explained by Figure 12. The average charge n for the Cu^{1+} -CN system clearly exceeds that of the Zn-CN and Cd-CN systems at all CN_T/M_T ratios. The Cd_T rejection is significantly lower than that of the Cu_T and Zn_T at $CN_T/M_T = 4$. This is probably due to the formation of poorly rejected uncharged species $Cd(CN)_2$ in the solution (Figure 6).

If the metal containing complex is treated as a coion $[M^{Z_m+}(CN)_Y]^{-(Y-Z_m)}$, the Nernst-Planck equation (Equation 19) predicts higher metal and cyanide rejection for the Cu^{1+} -CN system. The rejection of total cyanide is shown to be approximately equal to the rejection of metal ion at low ratio because of low free cyanide in water. As CN_T/M_T increases, the metal rejection should have increased. However, the rejection dropped as CN_T/M_T increased. The rejection drop was particularly substantial for Zn. This is due to the fact that rejection is a function of both n (average charge) and ionic strength. Ionic strength increases as free cyanide increases. Total cyanide rejection drops drastically as CN_T/M_T increases because of the large increase in poorly rejecting free cyanide ions.

The free cyanide concentrations in the case of $CN_T/Zn_T = 4$ and 40 could be calculated (using Figures 5 and 12), and shown in Table 11.

2. Effect of Ionic Strength on Zn-CN System

In order to prove the effect of excess free CN^- , studies of the effect of ionic strength (using $NaNO_3$) on total zinc rejection in the Zn-CN system were carried out. $NaNO_3$ was selected for the adjustment of ionic strength because $NaNO_3$ does not form any metal complexes and that the rejection of $NaNO_3$ is similar to NaCN.

The rejection of zinc is also shown (Figure 24, top) at various CN_T/Zn_T ratios and constant ionic strength. The result clearly indicates that the rejection of Zn_T increases at constant ionic strength as the CN_T/Zn_T ratio increases; the increase is due to an increase in average negative charge as indicated in Figure 10 by n values.

Figure 24 (bottom) shows that as ionic strength (i.e. added $NaNO_3$) increases rejection tends to drop in value.

3. Effect of Feed Concentration on Zinc Cyanide Rejection

As stated in the Donnan equilibrium model and Nernst Planck model, the rejection of simple salts decreases with

TABLE 11

Calculated Concentrations of Various Species in Zn-CN
Systems (pH = 10, $C_i = 1.55 \text{ mM Zn}_T$)

<u>CN_T/Zn_T ratio</u>	<u>species</u>	<u>Feed Concentration (mM)</u>
4	Zn(CN) ₃ ⁻	1.41
4	Zn(CN) ₄ ²⁻	0.14
4	Free CN ⁻	1.41
4	Complexed cyanide (as CN)	4.80
40	Zn(CN) ₃ ⁻	0.30
40	Zn(CN) ₄ ²⁻	1.25
40	Free CN ⁻	56.0
40	Complexed cyanide (as CN)	5.90

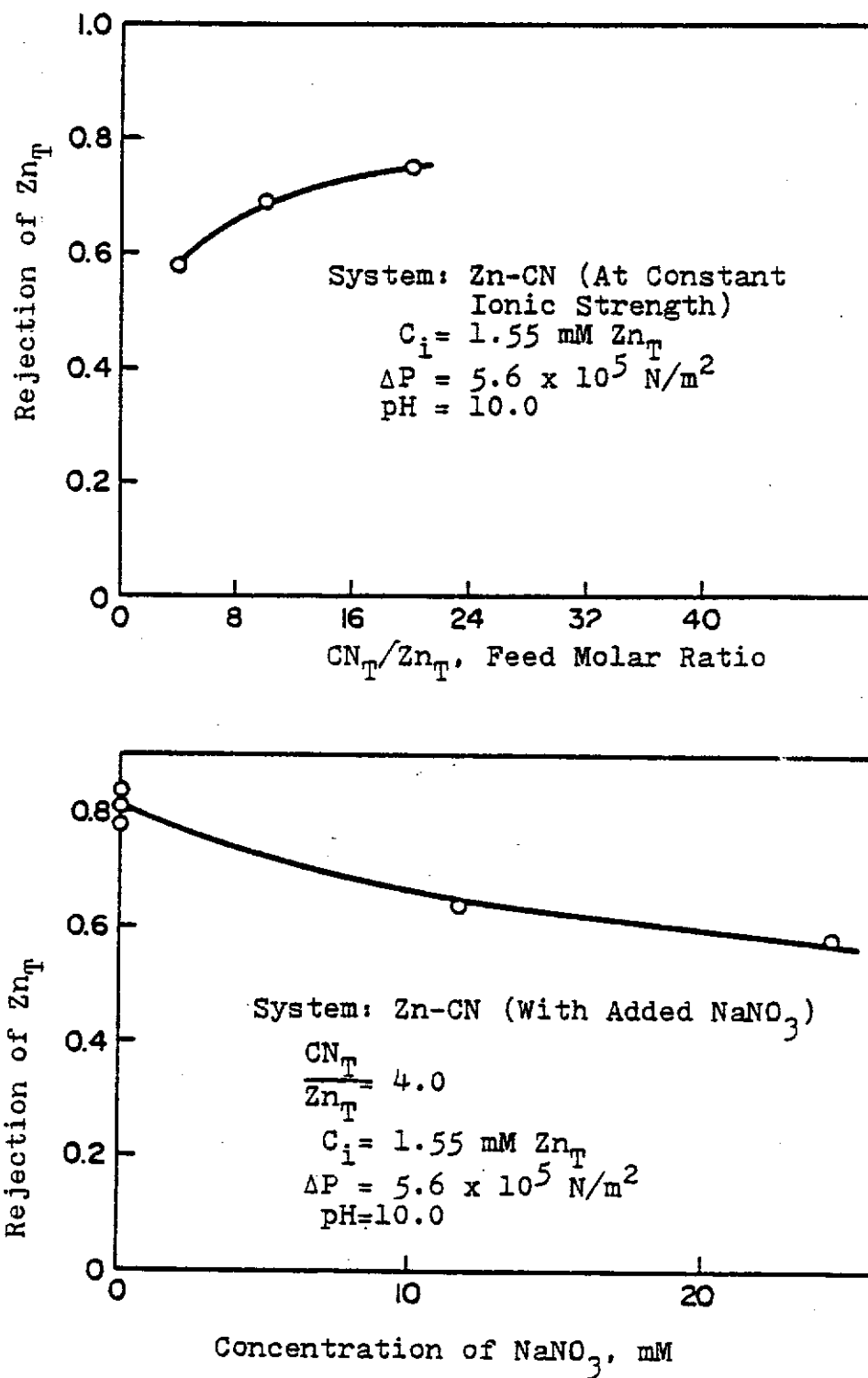


Figure 24. Effect of Ionic Strength (NaNO₃) on Zn_T Rejection for Zn-CN System

an increase in concentration of the feed solution. This is again verified to be the same for zinc cyanide complex solution. The results are shown in Figure 25. Note also from this figure that the rejection of zinc at $CN_T/Zn_T=40$ is significantly lower at the high Zn_T concentration level. This is due to the ionic effect as discussed in the previous section.

For design purposes a plot of $\log C_f$ versus $\log C_i$ should give useful information. According to Donnan equilibrium, the slope should be between 1 and 2. As shown in Figures 26 and 27, least square lines are drawn for the case of $CN_T/Zn_T = 4$ to correlate the C_f and C_i values obtained from the experiments. The corresponding parameters, n and k , are shown in Table 12 with excellent correlation. The higher k value for metal rejection is seen in the case of $CN_T/Zn_T = 40$, which is again due to much higher ionic strength even in the presence of higher average charge in the solution.

Table 12 also shows negligible CN_T rejection in the case of $CN_T/Zn_T = 40$. This is because of the much higher percentage of the poorly rejected free cyanide (Table 11) in the solution.

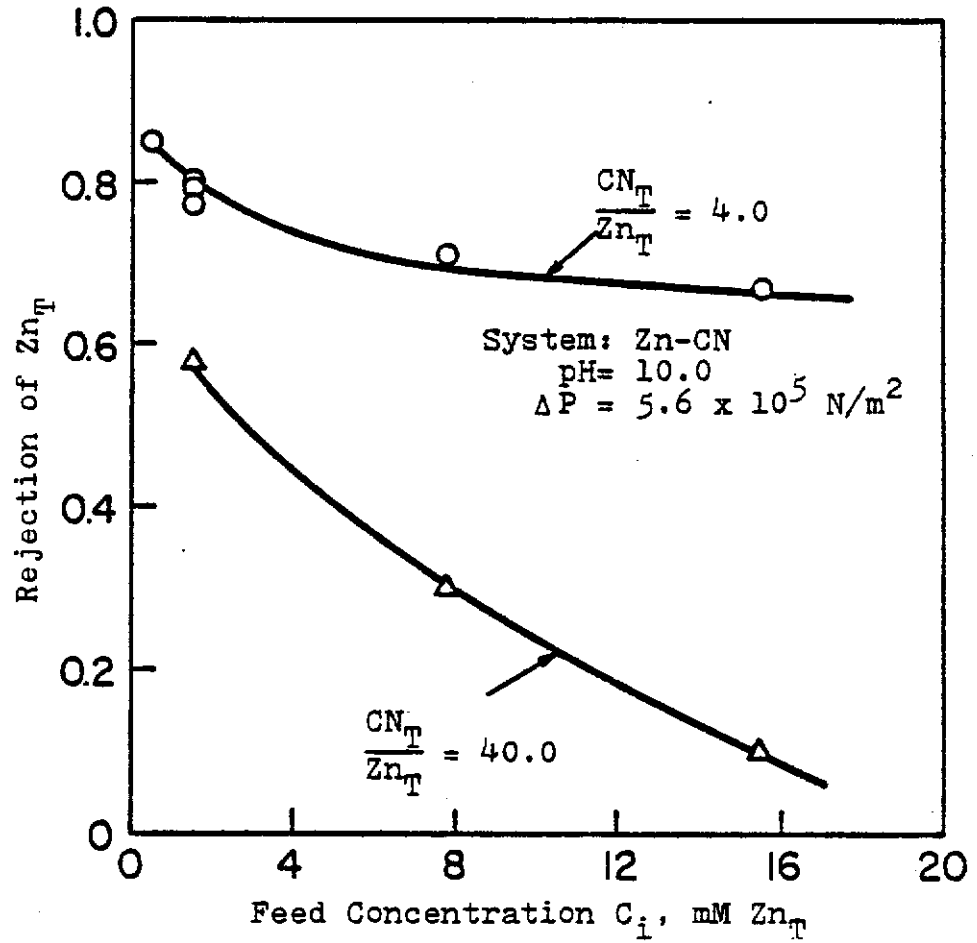


Figure 25. Effect of Feed Zn_T Concentration on Zinc Rejection

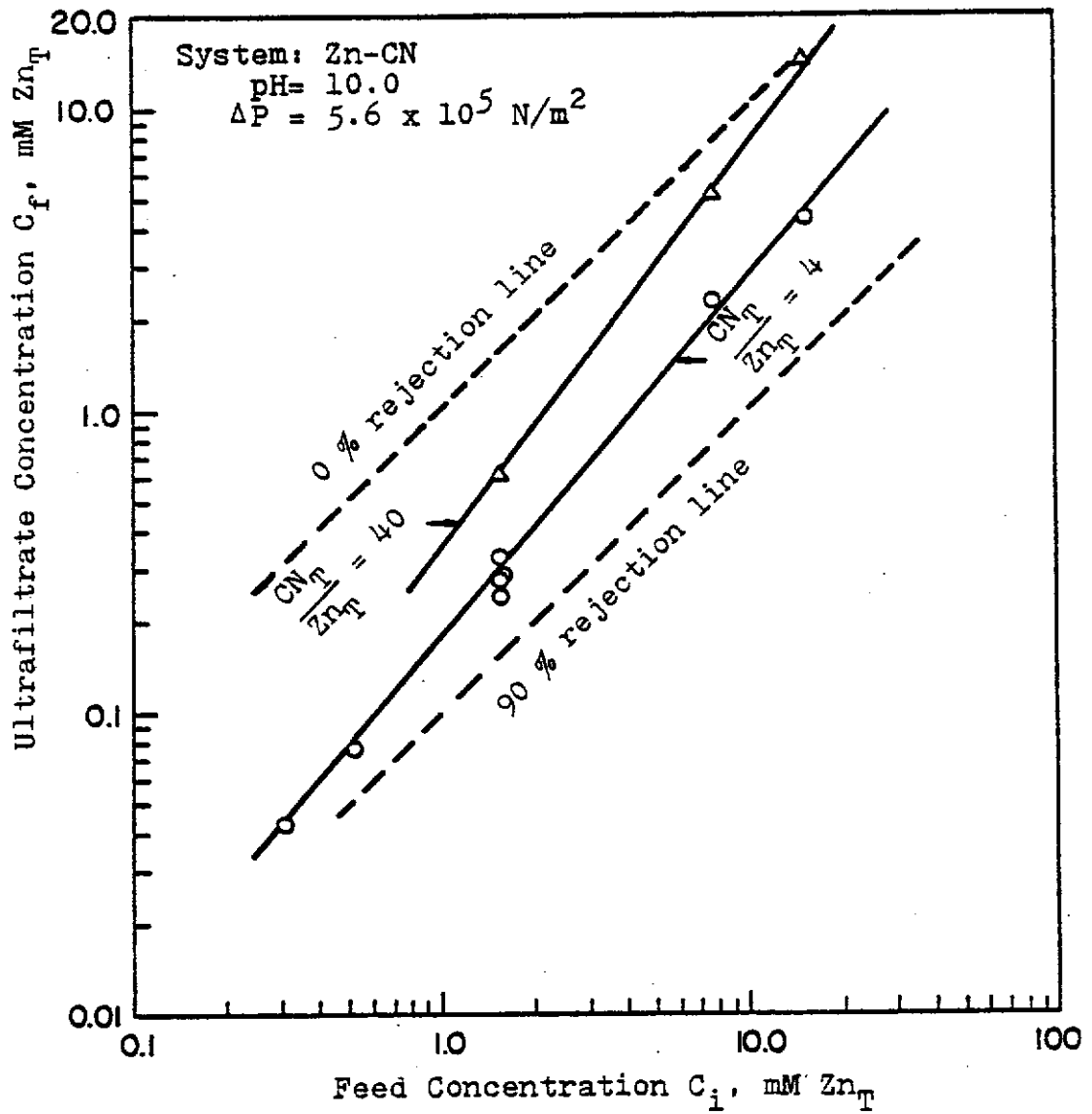


Figure 26. Effect of Feed Zn_T Concentration on Ultrafiltrate Zinc Concentration for Zn-CN System

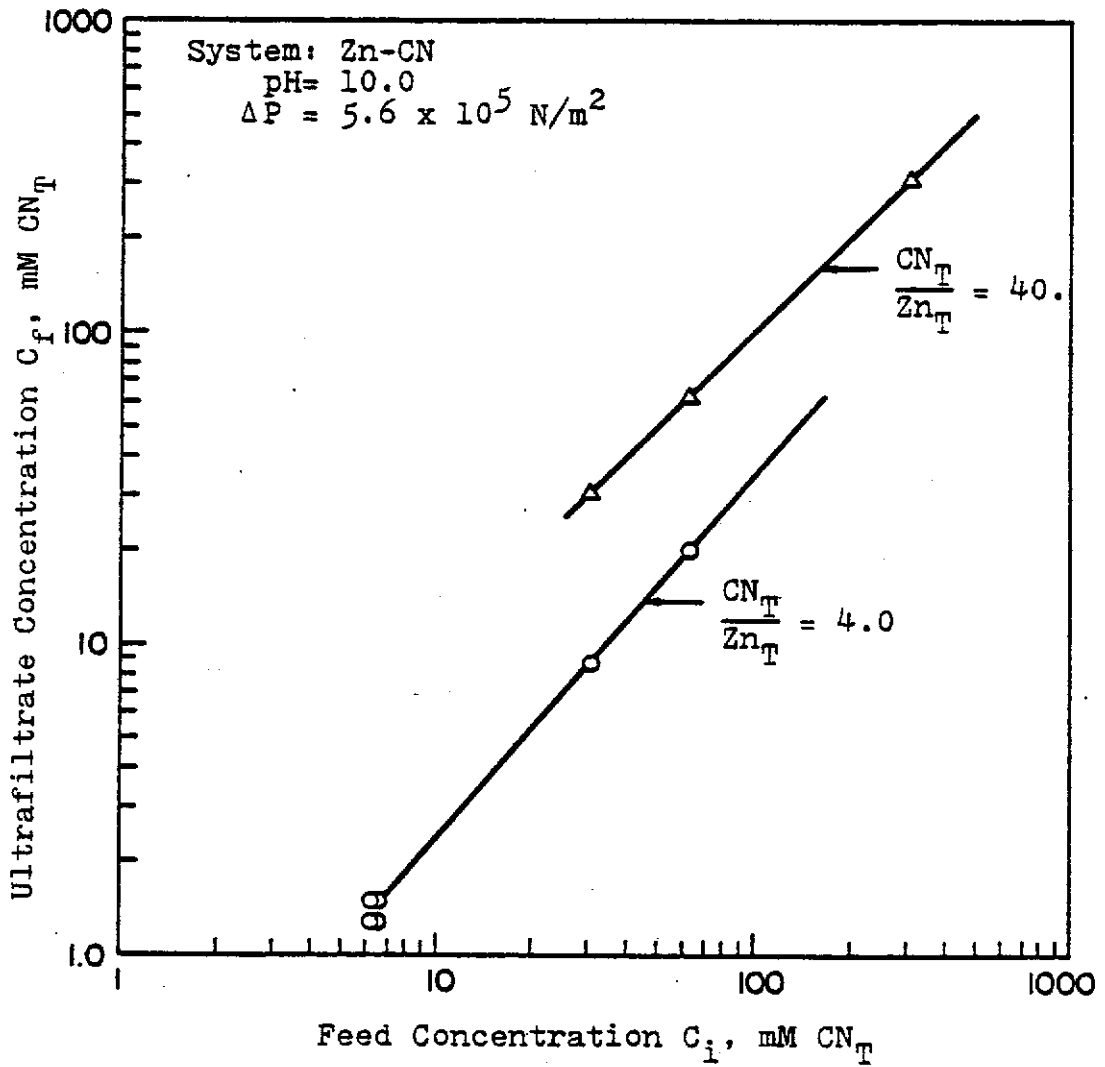


Figure 27. Effect of Feed CN_T Concentration on Ultrafiltrate Cyanide Concentration for Zn-CN System

TABLE 12

Parameters to fit $C_f = kC_i^n$ for Zn-CN system

<u>CN_T/Zn_T</u>	<u>Rejection</u>	<u>k</u>	<u>n</u>	<u>correlation coefficient</u>
4	Zn _T	0.17	1.20	0.9994
4	CN _T	0.16	1.17	0.9999
40	Zn _T	0.34	1.34	0.9998
40	CN _T [*]	-	-	-

* Total cyanide rejection is negligible because of high free cyanide (90 % of total cyanide).

4. Calculation of Free Cyanide (CN^-) Rejection in the Metal-complex Systems

The relationship between C_f and C_i for the Zn-CN system (for $\text{CN}_T/\text{Zn}_T = 4$) could be expressed as:

$$\text{Zn}_T \text{ rejection: } C_f = 0.17 C_i^{1.20} \quad (54)$$

$$\text{CN}_T \text{ rejection: } C_f = 0.16 C_i^{1.17} \quad (55)$$

For the Zn-CN system where $C_i = 1.55$ mM Zn and $\text{CN}_T/\text{Zn}_T = 4.0$, the rejection of total Zn and total cyanide could be found to be 0.81 and 0.78, respectively, from Equations 54 and 55. The complex cyanide and the free cyanide (CN^-) concentrations are 4.80 mM and 1.41 mM, respectively (Table 11).

If the assumption is made that the rejection of free cyanide is zero, the total cyanide rejection could be calculated in the following way:

$$R_{\text{CN}_T} = 1 - [(1-0.81)(4.8)+1.4]/6.2 = 0.63$$

The rejection of total cyanide was found to be 0.78 experimentally. Thus, the assumption of zero free cyanide rejection is not true.

In order to obtain the rejection of 0.78 for total cyanide, free cyanide in the ultrafiltrate could be cal-

culated as follows:

$$0.78 = 1 - [(1-0.81)(4.8) + C_{F_{CN^-}}] / 6.2$$

$$\text{where } C_{F_{CN^-}} = 0.452 \text{ mM.}$$

Thus, the free cyanide rejection is found to be 0.68. This rejection is considerably higher than that found with pure NaCN solution at $CN^- = 1.41 \text{ mM}$.

The same procedures could be employed to calculate free complexing agent rejection for other cases as long as the distribution of various complexes in the solution is known and the experimental results for both metal and total complexing agent rejections are available.

D. Metal-EDTA Rejection Studies

1. Effect of $EDTA_T/M_T$ on Rejection

The rejections of Zn_T , Cd_T , Cu_T and $EDTA_T$ at various L_T/M_T ratios and at pH 4 are shown in Figures 28, 29 and 30. At $EDTA_T/M_T = 1$, M_T rejection = $EDTA_T$ rejection since the metal containing species is primarily $M(EDTA)^{2-}$, which is a complex of 1:1 type. It should also be noted that the Cd-EDTA complexes showed lower rejection. This could be due to the orientation of the complexes inside the membrane

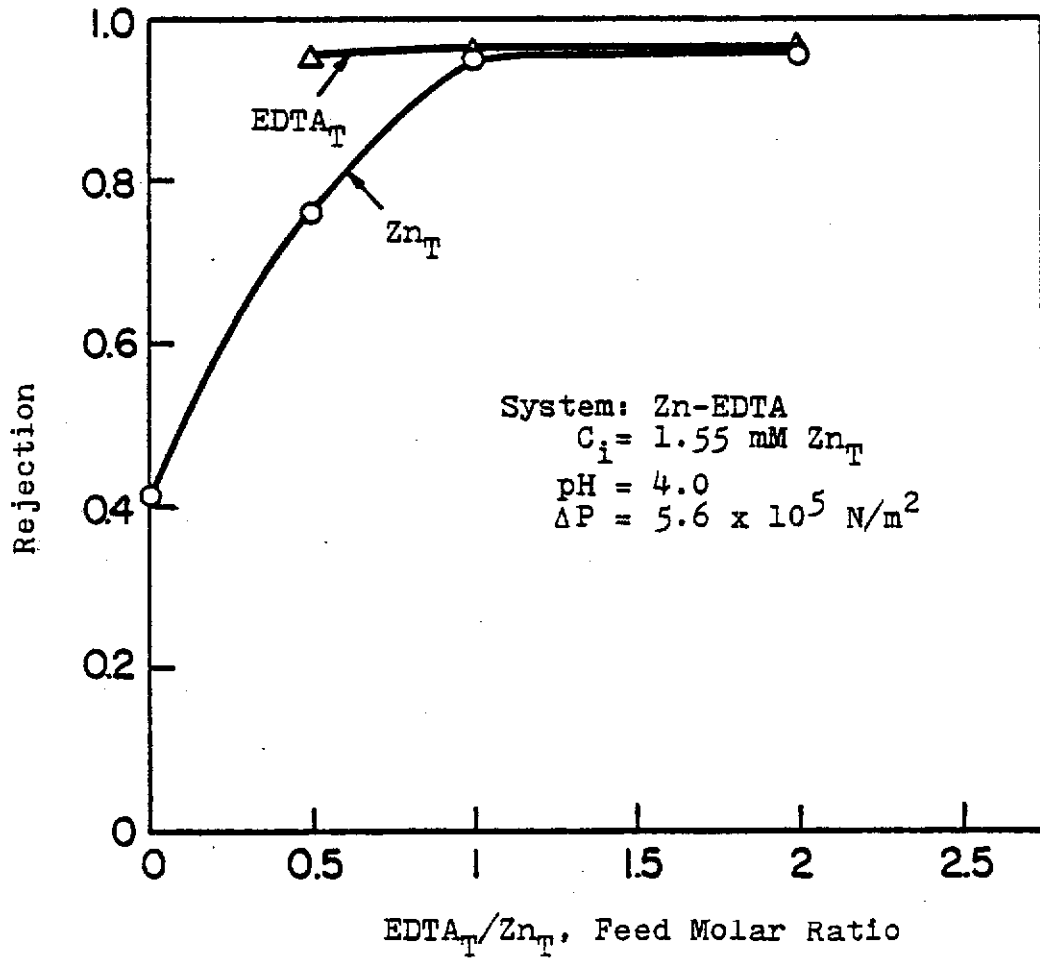


Figure 28. Rejection Behavior of Zn_T and EDTA_T as a Function of Feed Molar Ratio (EDTA_T/Zn_T) for Zn-EDTA System

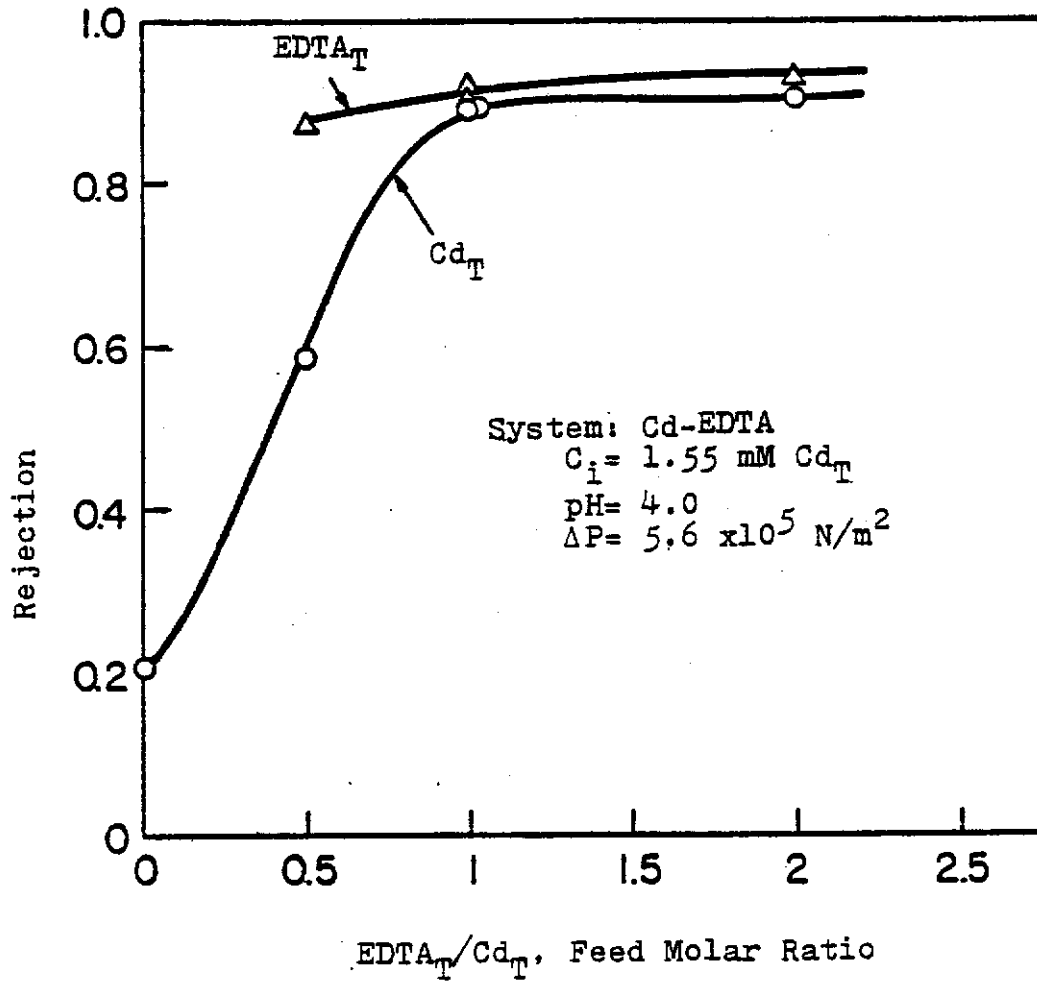


Figure 29. Rejection Behavior of Cd_T and EDTA_T as a Function of Feed Molar Ratio ($\text{EDTA}_T/\text{Cd}_T$) for Cd-EDTA System

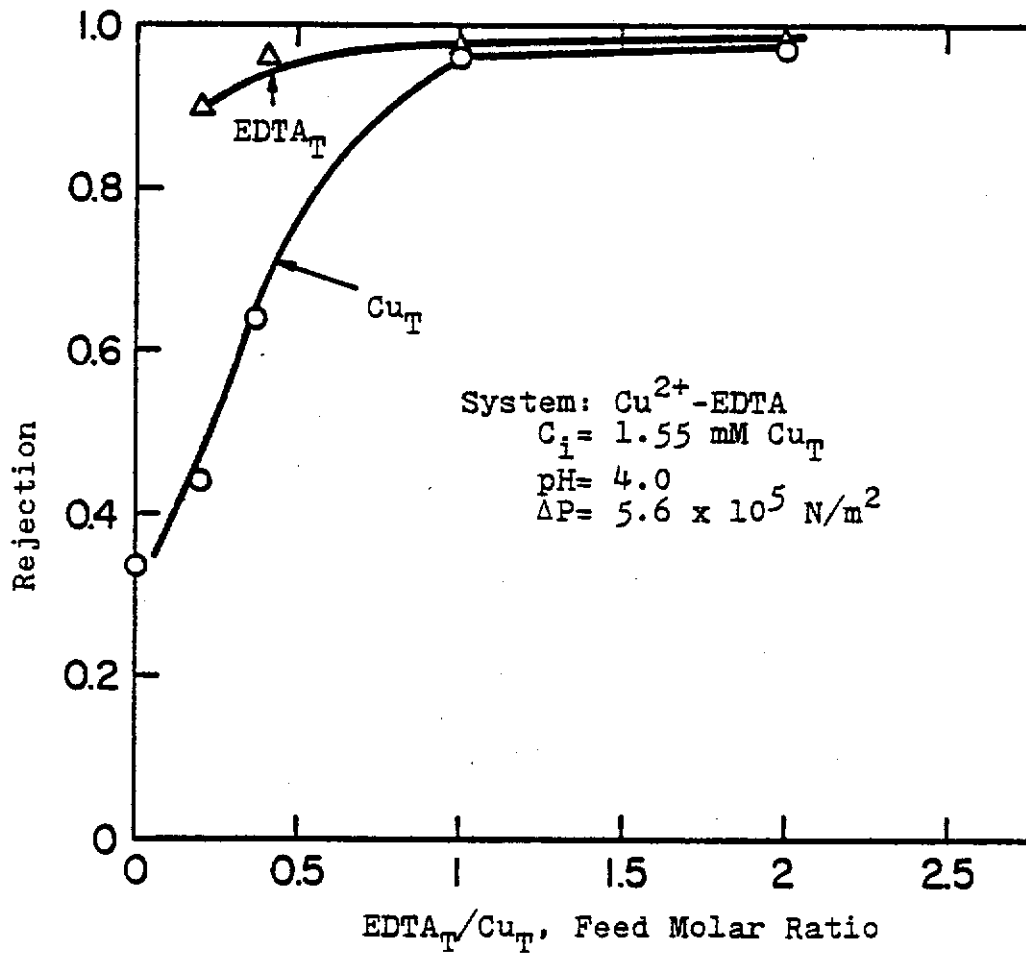


Figure 30. Rejection Behavior of Cu_T and EDTA_T as a Function of Feed Molar Ratio ($\text{EDTA}_T/\text{Cu}_T$) for Cu^{2+} -EDTA System

pores. The metal rejection remains high at EDTA_T/M_T of between 1 and 2 because all the metals in the solution are in the highly rejected $\text{M}(\text{EDTA})^{2-}$ complex form.

The rejections of total metal and $\text{M}(\text{EDTA})^{2-}$ are different at $\text{EDTA}_T/M_T < 1$ (metal species: $\text{M}(\text{EDTA})^{2-}$ and M^{2+}) because of the presence of poorly rejecting free M^{2+} in the solution. Thus, the total metal rejection is less than that of the $\text{M}(\text{EDTA})^{2-}$ complexes. The rejection of EDTA_T is lower at a $\text{EDTA}_T/M_T < 0.5$. This is probably due to the fact that $\text{M}(\text{EDTA})^{2-}$ complexes show lower rejection in the presence of significant free metal ions. The rejection of free EDTA (primarily $\text{H}_2(\text{EDTA})^{2-}$) was shown to be 0.8 at pH 4.0 (Figure 18). However, total EDTA rejection remains approximately constant at $1 < \text{EDTA}_T \leq 2$ in all three cases. Thus, the presence of $\text{M}(\text{EDTA})^{2-}$ complexes may enhance the rejection of free EDTA ($\text{H}_2(\text{EDTA})^{2-}$).

2. Calculation of Total Metal Rejection Based on Rejections of Individual Components

Total metal rejection at $\text{EDTA}_T/M_T < 1$ could be calculated if the rejection of free metal (M^{2+}) and the $\text{M}(\text{EDTA})^{2-}$ complex is known and in the absence of synergistic effects. For example, at a ratio of 0.4, the concentration of $\text{Cu}(\text{EDTA})^{2-}$, and Cu^{2+} are 0.62 and 0.93 mM, respectively. Hence, if the rejection of $\text{Cu}(\text{EDTA})^{2-}$ stays

constant ($R = 0.96$, obtained from Figure 30) at a ratio of 1, Cu^{2+} rejection is 0.34, the calculated Cu_T concentration in ultrafiltrate at $\text{EDTA}_T/\text{Cu}_T = 0.4$ would be $0.93(1-0.34) + 0.62(1-0.96)$ or 0.64 mM. Thus, Cu_T rejection at 0.4 ratio is $1-0.65/1.55 = 0.59$.

The calculated results of the three metals are shown in Table 13. Of course, as $\text{EDTA}_T/M_T \rightarrow 0$, calculated and experimental rejections must be equal. At higher ratios, the experimental values are higher than the calculated values, possibly due to enhanced rejection of M^{2+} in the presence of $M(\text{EDTA})^{2-}$.

E. Metal-oxalate Rejection Studies

The effects of pH, OX_T/M_T ratio, feed concentration variation, and ionic strength were studied for the copper-oxalate system. For Cd and Zn, metal oxalate precipitate (at the pH range of interest) was formed and hence the ultrafiltration behavior was not studied. Table 14 shows that the solute diffusion effect (which lowers rejection) is negligible at a pressure of $3.7 \times 10^5 \text{ N/m}^2$ and above, and hence all other runs were made at $5.6 \times 10^5 \text{ N/m}^2$. Solution pH was controlled in pH 4 to 6 range so that $\text{Cu}(\text{OH})_2$ precipitate formation could be avoided.

TABLE 13

Calculated Total Metal Rejection Values Based on
Experimental Rejections of M^{2+} and $M(EDTA)^{2-}$

<u>Metal</u>	<u>EDTA_T/M_T</u>	<u>Rejection of M_T</u>	
		<u>Calculated</u>	<u>Experimental</u>
Zn	0.5	0.65	0.76
Cd	0.5	0.55	0.58
Cu	0.4	0.59	0.64
Cu	0.2	0.46	0.44

TABLE 14

Effect of Pressure on Cu_T Rejection in Cu^{2+} -OX System
($\text{OX}_T/\text{Cu}_T = 4$)

<u>Pressure, N/m^2</u>	<u>R_{Cu}^* / (R_{Cu} at $5.6 \times 10^5 \text{ N/m}^2$)</u>
2.1×10^5	0.78
3.5×10^5	0.995
5.6×10^5	1.0

* Rejection of total copper

1. Effect of pH on the Rejection of Total Copper and Total Oxalate in Cu^{2+} -OX System

Rejections of total copper (Cu_T) in the presence of oxalate at three pH values are shown in Figure 31. The rejection of Cu_T shows significant increase as the pH of the solution increases. This is due to the fact that more and more charged species $\text{Cu}(\text{OX})_2^{2-}$ is converted from uncharged $\text{Cu}(\text{OX})$ in the solution as indicated in Table 14. In the presence of uncharged $\text{Cu}(\text{OX})$, it appears that $\text{Cu}(\text{OX})_2^{2-}$ rejection is considerably lower. Total oxalate (OX_T) rejection is also shown in the same figure. The sharp increase in OX_T rejection is due to the dissociation of the $\text{H}(\text{OX})^-$ at pH 3.5 to higher rejecting species OX^{2-} at pH 6. The OX_T rejection behavior is similar to that observed in Figure 19.

2. Effect of OX_T/Cu_T Molar Ratio on the Total Copper and Total Oxalate Rejection

Rejection of copper and oxalate at various OX_T/Cu_T molar ratios at pH 4 is shown in Figure 32. The rejection of copper does not drop at high ratio indicating that the charge effect (see Figure 13) is predominant over the presence of the ionic strength effect. The rejection of copper goes through a minimum at OX_T/Cu_T of about 1 because of the presence of significant amount of uncharged $\text{Cu}(\text{OX})$

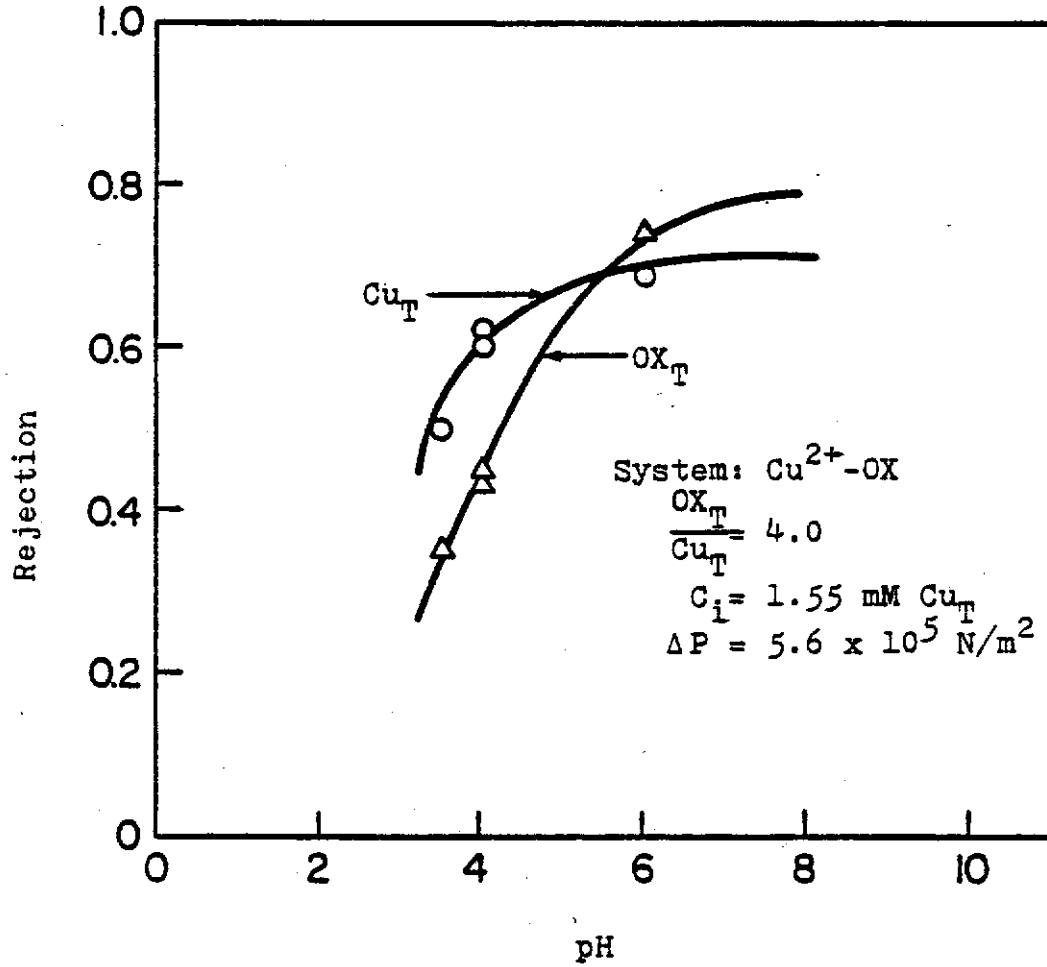


Figure 31. Rejection Behavior of Cu_T and OX_T as a Function of pH for Cu-OX_T System

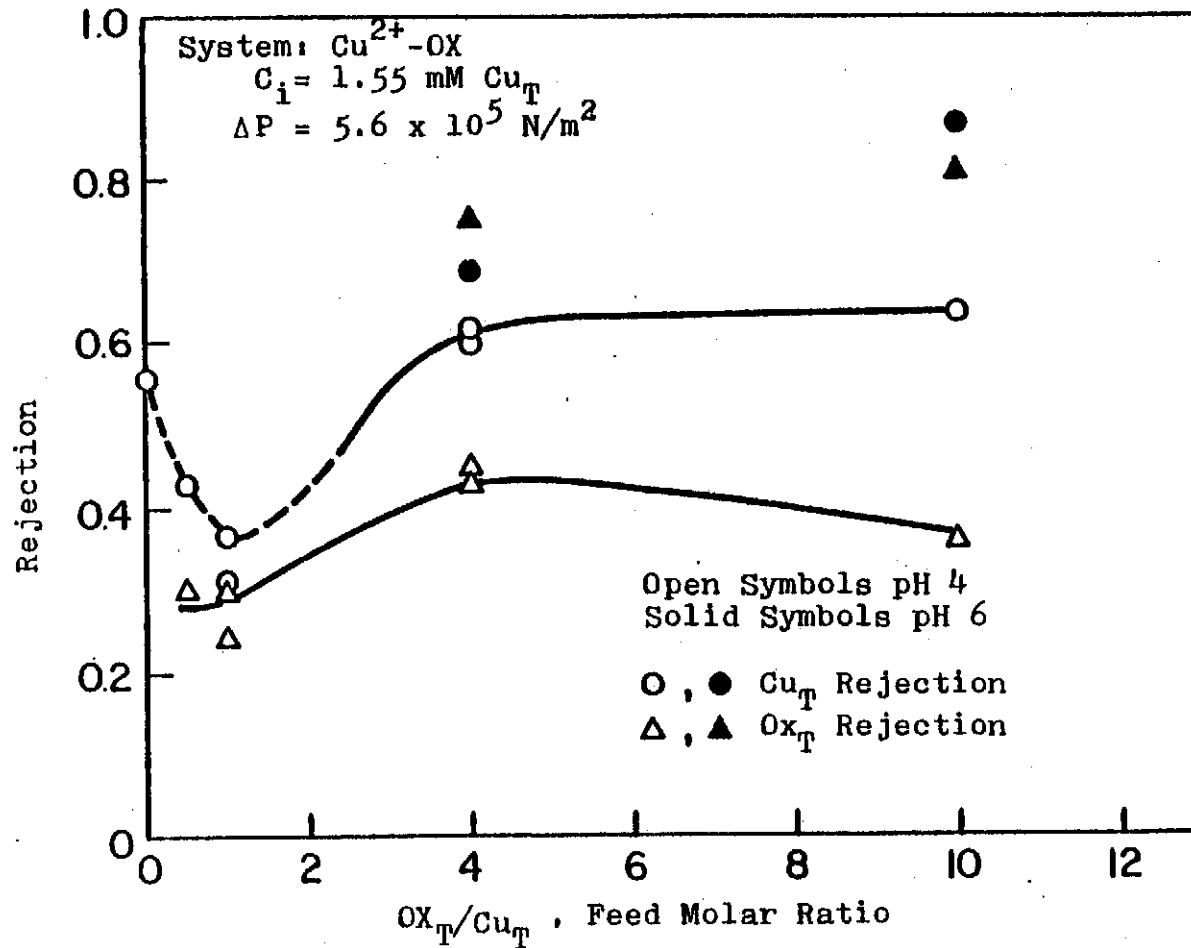


Figure 32. Rejection Behavior of Cu_T and OX_T as a Function of Feed Molar Ratio (OX_T/Cu_T) for Cu^{2+} -OX System at pH 4.0 and 6.0

(zero rejection) in the solution (see Figure 9). At $OX_T/Cu_T < 1$, Cu_T rejection increases because of an increase in Cu^{2+} concentration. It should also be noted that the rejection of Cu_T is much higher at pH 6, particularly at ratio 10. This is because of the fact that Cu_T is present primarily as $Cu(OX)_2^{2-}$ (see Table 15).

The rejection of total oxalate is also shown in Figure 32. The total oxalate rejection is the sum of rejection of complexed metal oxalate and free oxalate. The lower rejection of OX_T at pH 4 for $OX_T/Cu_T > 4$ is principally due to the poor rejection of monovalent $H(OX)^{1-}$. At pH 6, since the predominant free oxalate species is divalent OX^{2-} , the total oxalate rejection is higher.

3. Effect of Ionic Strength on the Rejection of Total Copper in the Presence of Oxalate

The ionic strength (addition of $NaNO_3$ which does not form metal complexes) effect on the rejection of Cu_T at $OX_T/Cu_T = 4$ is shown in Figure 33. Results show that the rejection of Cu_T decreases with the addition of sodium nitrate. This behavior is similar to that observed with the Zn-CN system.

TABLE 15

Concentration of Uncharged Cu(OX) species

<u>OX_T/Cu_T</u>	<u>% Cu(OX) species</u>	
	<u>pH 4</u>	<u>pH 6</u>
1.0	36	-
2.0	19	-
4.0	3	1
10.0	1	0.3

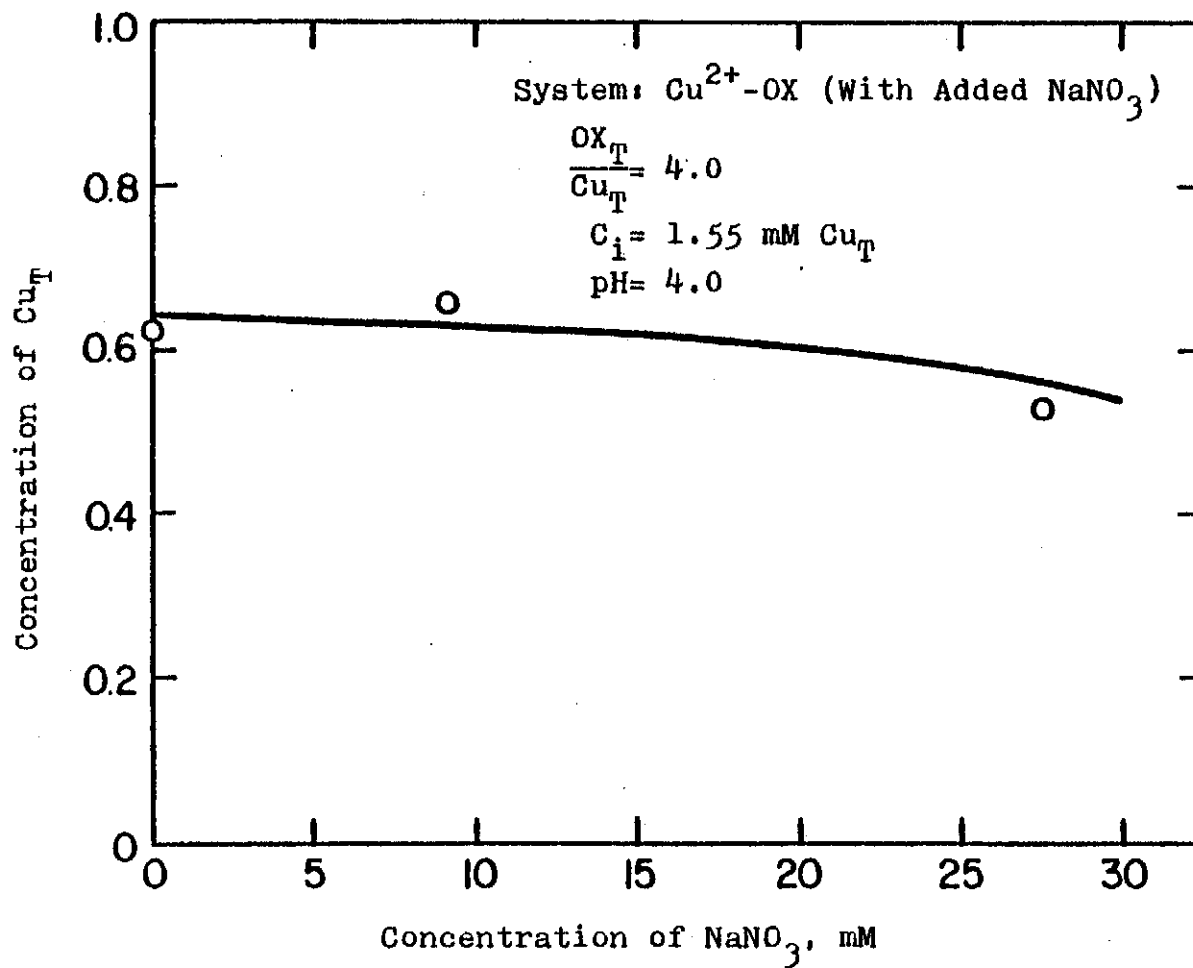


Figure 33. Effect of Ionic Strength (NaNO_3) Rejection for Cu^{2+} -OX System

4. Effect of Feed Concentration on Total Copper and Total Oxalate Rejection

The effect of feed copper concentration on ultrafiltrate concentration of Cu_T and OX_T was investigated for $OX_T/Cu_T = 4$ at pH 4. The following correlations were obtained from Figures 34 and 35.

$$Cu_T \text{ rejection: } C_f = 0.42 C_i^{0.90} \quad (56)$$

$$OX_T \text{ rejection: } C_f = 0.56 C_i^{1.03} \quad (57)$$

The power on C_i of approximately unity indicates constant rejection over the entire concentration range. In contrast to total cyanide rejection (Equation 55), OX_T rejection is considerably lower as shown by high a "k" ($k = 0.56$) value. At $C_i = 1.55$ mM the concentrations (in mM) of individual species (calculated from Figure 3 and 9) are : $Cu(OX)_2^{2-} = 1.50$, $Cu(OX) = 0.05$, and free oxalate = 3.15 ($H(OX)^- = 1.96$, $OX^{2-} = 1.19$). The presence of a significant concentration of $H(OX)^-$ may be responsible for lower OX_T rejection. For example, the calculated (using Equations 56 and 57, and species distribution information) rejection of free oxalate is found to be only 0.22, which is considerably lower than that observed with pure oxalic acid (see Figure 19) rejection at pH 4.

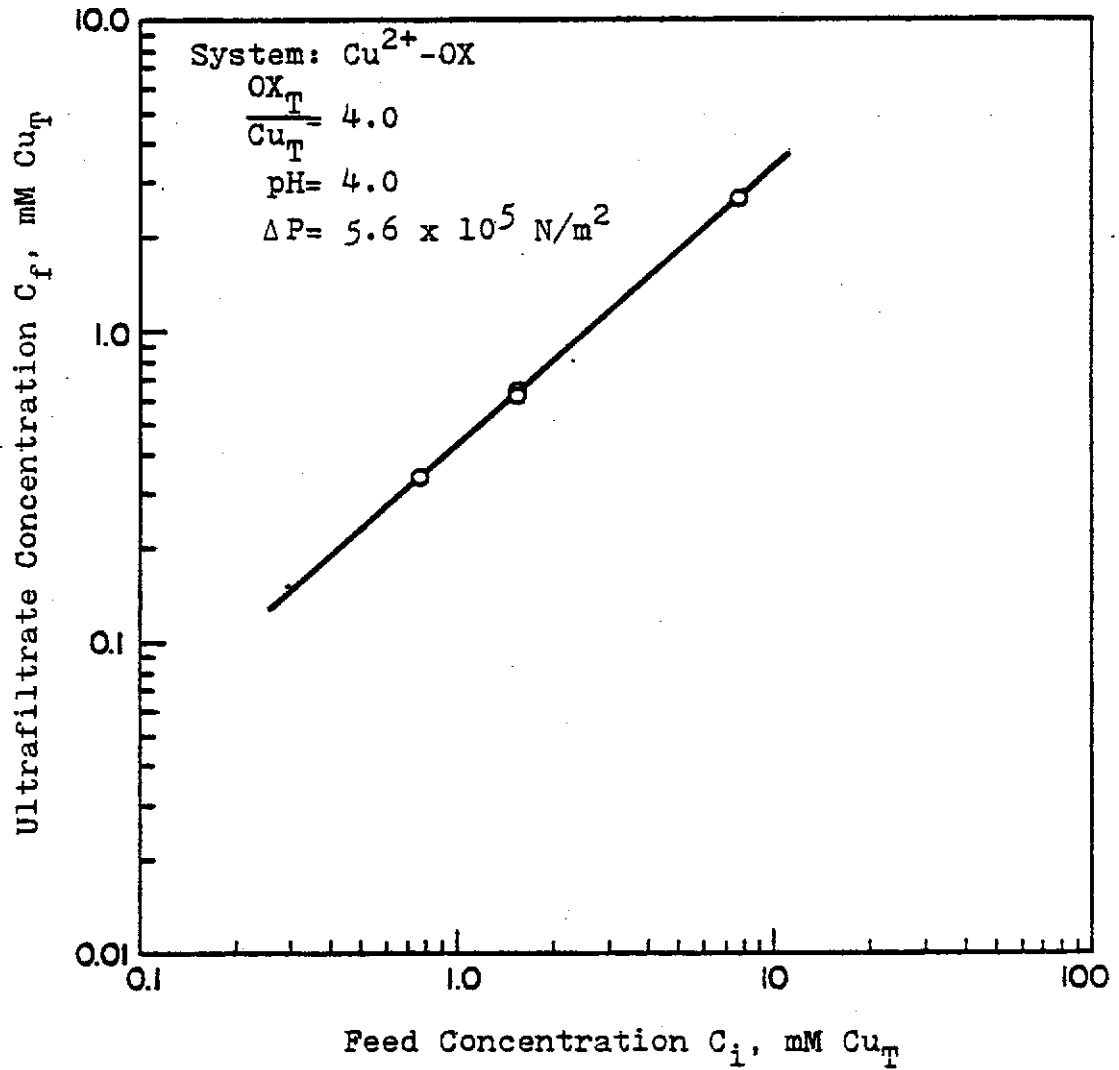


Figure 34. Effect of Feed Cu_T Concentration on Ultrafiltrate Copper Concentration for Cu^{2+} -OX System

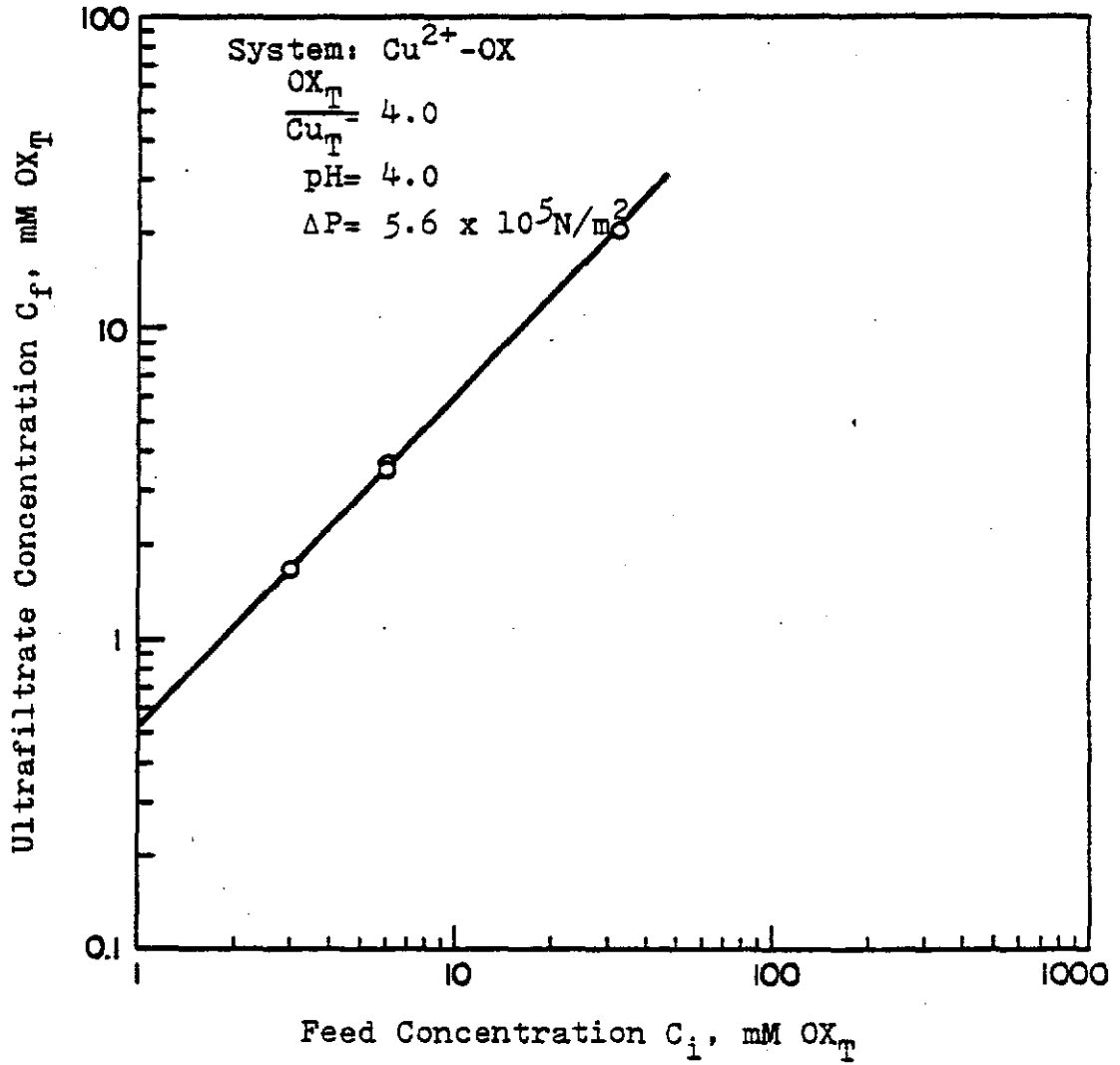


Figure 35. Effect of Feed OX_T Concentration on Ultrafiltrate Oxalate Concentration for Cu^{2+} -OX System

F. Ultrafiltration Experiments at High Water Recovery

Since the rejection behavior of metals and complexing agents is a function of initial feed concentration (Equations 54-57), the overall solute removal would be dependent on the extent of water recovery. The fractional water recovery, r , is defined as the total volume of ultrafiltrate collected divided by the initial feed solution volume. The overall solute removal is defined as:

$$\text{Removal at any } r = 1 - C_{f,av}/C_i \quad (58)$$

where $C_{f,av}$ = the average ultrafiltrate concentration

$C_{f,av}$ can easily be computed from the knowledge of the instantaneous C_f vs. time and water flux vs. time data.

Equations 54-55 have been used to correlate the experimental data in the case of negligible water recovery runs. The parameter "n" characterizes the system, and "k" is smaller for membranes with higher salt rejection. Thus, by knowing "n", one could predict the rejection behavior of other membranes simply by obtaining one C_f value experimentally at a chosen C_i from the negligible water recovery run on this new membrane.

The results obtained from negligible water recovery runs could also be used to predict the rejection behavior of another membrane under high water recovery conditions. A membrane with higher rejection was deliberately selected for the high water recovery experiments. The fractional metal removal obtained from experiment were compared with the calculated values obtained from known "n" (from negligible water recovery run) and the adjusted "k". Zn-CN and Cu-OX systems show excellent fit between the experimental values and calculated values (Figures 36-38 , see Appendix 3 for calculations). The dependence of metal removal at different initial metal concentrations are also calculated, and the results are shown in Figure 39 for Zn-CN system. The value of "n" for EDTA has not been found experimentally because of the concentration polarization problem with EDTA. Thus, the comparison of metal removal between the experimental values and the calculated values is not possible here. However, metal removal in the Cu-EDTA system stays high compared with that of the two other systems even under the severe concentration polarization condition. The metal removal behavior at all values of r was:

Removal of M-EDTA > Removal of M-CN > Removal of M-OX

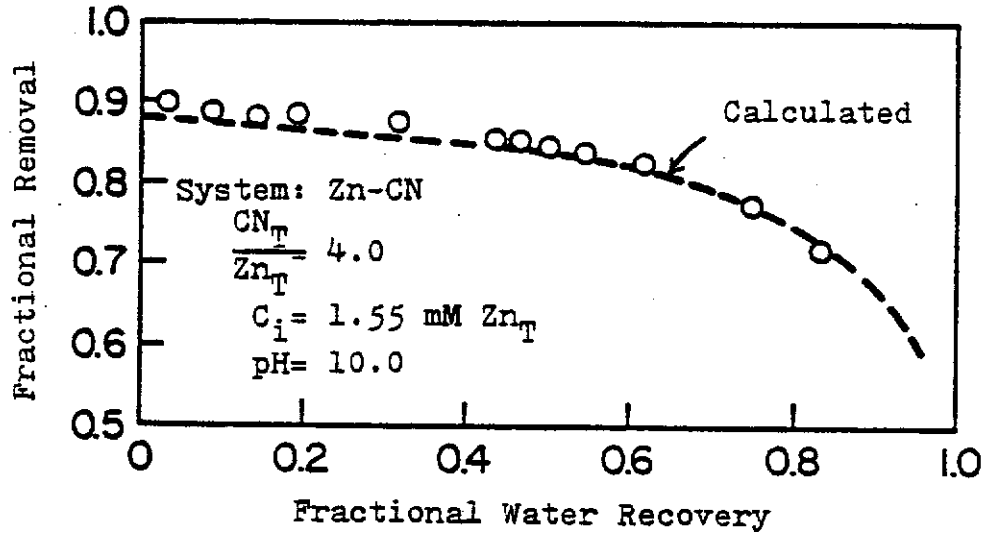


Figure 36. Fractional Removal of Zn_T as a Function of Water Recovery for Zn-CN System at $CN_T/Zn_T = 4.0$

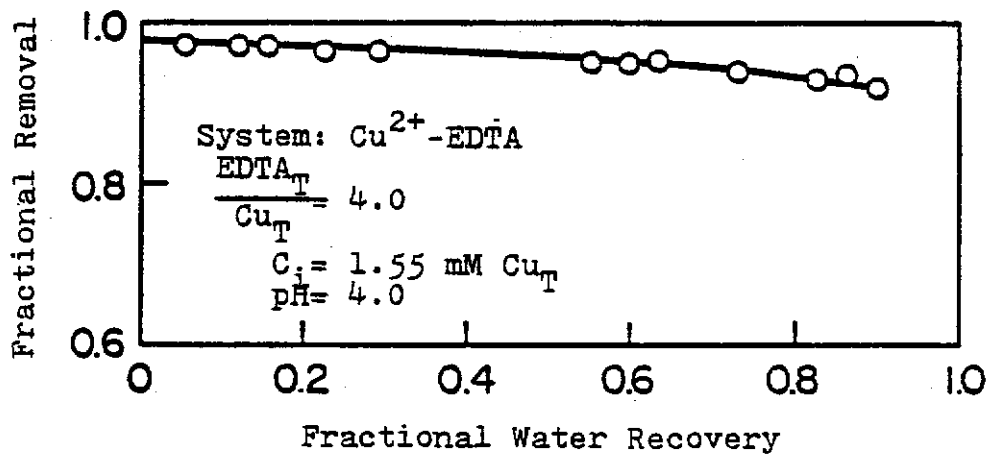


Figure 37. Fractional Removal of Cu_T as a Function of Water Recovery for Cu^{2+} -EDTA System at $EDTA_T/Cu_T = 4.0$

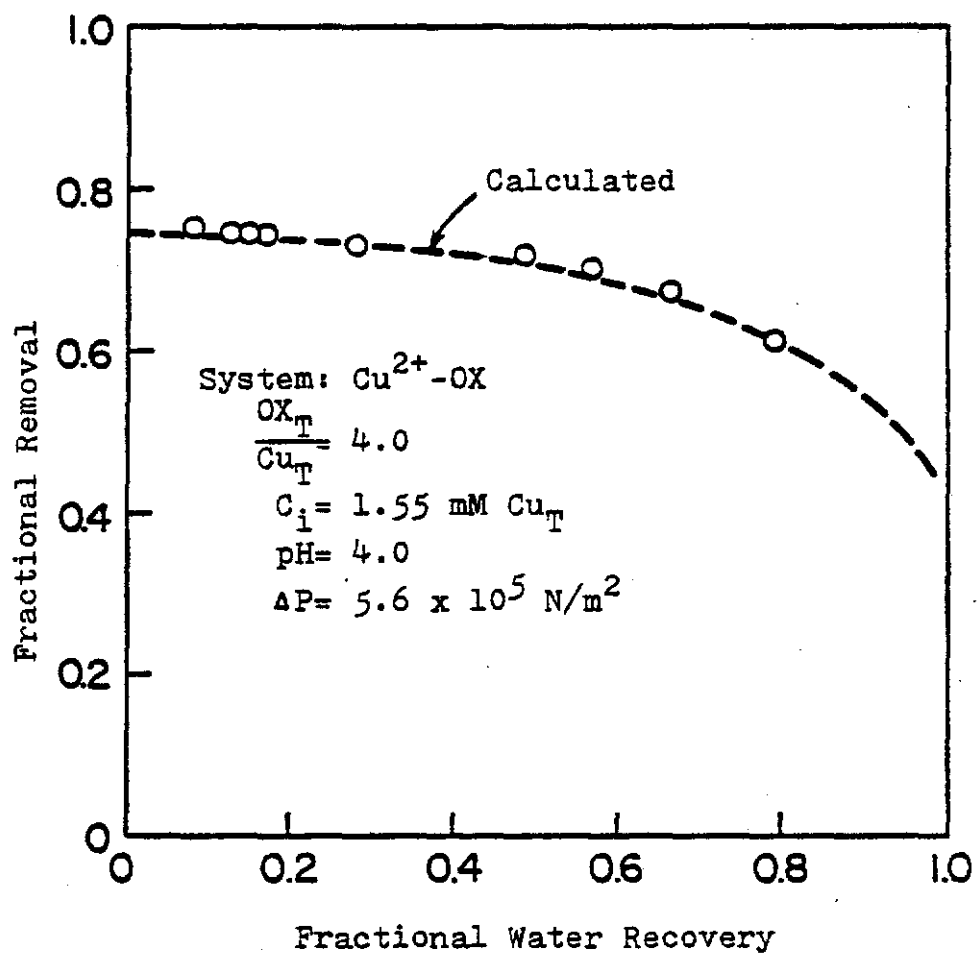


Figure 38. Fractional Removal of Cu_T as a Function of Water Recovery for Cu^{2+} -OX System at $\text{OX}_T/\text{Cu}_T = 4.0$

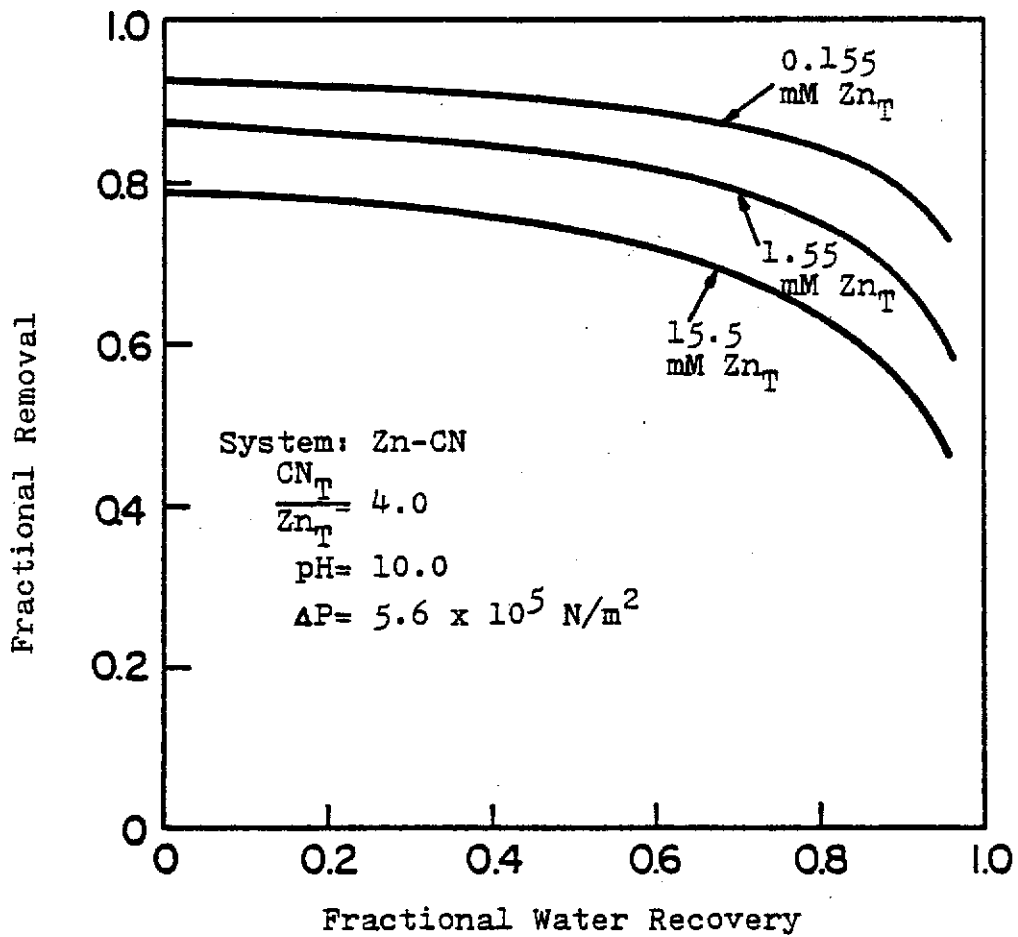


Figure 39. Calculated Fractional Removals of Zn_T as a Function of Water Recovery for Zn-CN System at $CN_T/Zn_T = 4.0$

VIII. SUMMARY AND CONCLUSIONS

An extensive investigation was conducted with negatively-charged, noncellulosic ultrafiltration membranes to establish relative rejection behaviors of complexed heavy metals under insignificant concentration polarization condition. A transmembrane pressure of $5.6 \times 10^5 \text{ N/m}^2$ provided maximum rejection. The negatively charged membranes used have a typical water flux of $13 \times 10^{-4} \text{ cm/sec}$ at $5.6 \times 10^5 \text{ N/m}^2$. The charge capacity (sulfonic acid groups) is between 300-400 millimolar.

The rejection dependence of the heavy metals (Zn^{2+} , Cd^{2+} , Cu^{1+} and Cu^{2+}) and free complexing agents (CN^- , EDTA and oxalate) was found to be a function of feed metal concentrations, types of metals, complexing agent to metal feed molar ratio (L_T/M_T), pH, ionic strength, and transmembrane pressure difference (below $5.6 \times 10^5 \text{ N/m}^2$). The effect of pH and feed L_T/M_T ratio on rejection could be explained in terms of metal complex species distribution and the Nernst-Planck model. Extensive computer calculations were made to establish the distribution of various species in the solution. The effect of feed concentration on ultrafiltrate concentration was fit by power function. At fixed L_T/M_T ratio, the total metal and total

complexing agent drop with feed concentration for the case of the metal-cyanide system while for the EDTA and oxalate systems, the rejection is approximately constant ($n \approx 1$), and the concentration effect is further verified by the high water recovery experiments.

In addition to feed concentration dependence, metal rejection is also dependent upon the type of metal in the solution. For example, Figure 40 (top) shows the relative rejection behavior of all three metals in M-CN systems. The average charge ($n = Y - Z_m$) of species $(M^{Z_m^+} (CN)_Y)^{-(Y-Z_m)}$ is shown in Figure 40 (bottom). Copper rejects much better than cadmium or zinc in M-CN systems. This is because of the higher average charge in the Cu^{2+} -CN system at fixed CN_T/M_T molar ratio. Cadmium rejects better than zinc above $CN_T/M_T = 20$ because of the higher average charge in the Cd-CN system. Cadmium shows lower rejection at lower ratios because of the presence of uncharged $Cd(CN)_2$ in the solution.

The rejection of metals is reduced in the presence of high free cyanide concentration in the solution ($CN_T/Zn_T > 12$). This is due to the ionic effect created in the solution at high ratios. In order to verify this postulate, constant ionic strength runs were performed with the Zn-CN system. Results clearly indicates that the Zn_T

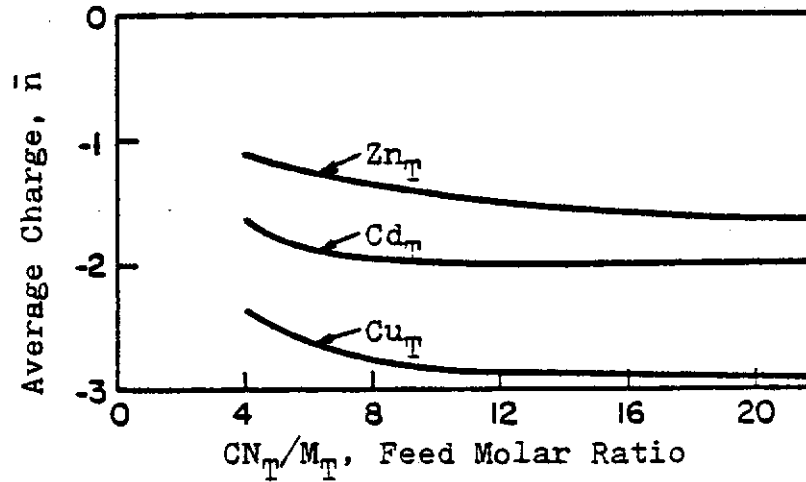
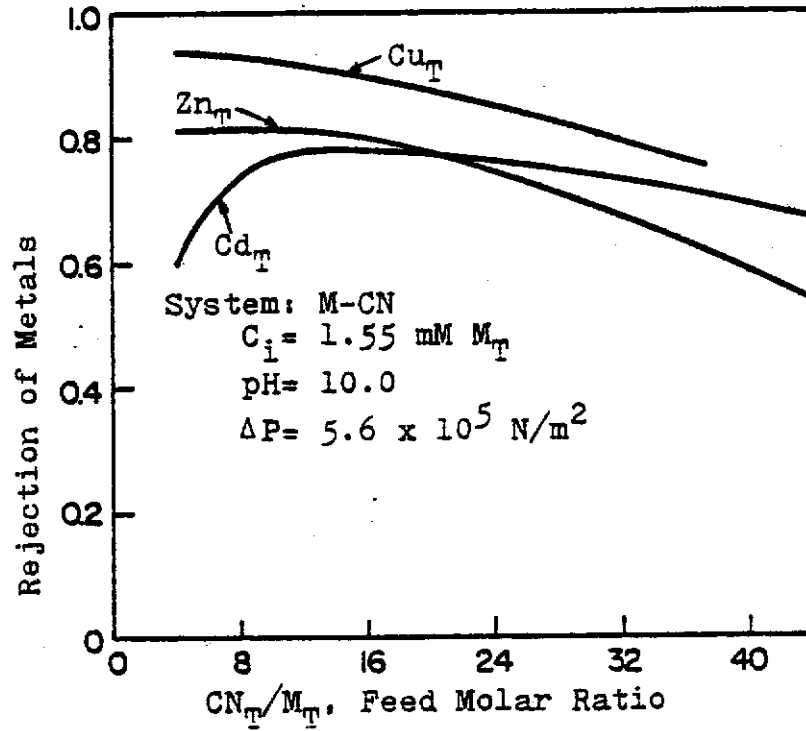


Figure 40. Comparisons of Metal Rejection Behavior with average charge \bar{n}

rejection actually increases as CN_T/Zn_T molar ratio increases at the absence of ionic strength effect (as shown in Figure 41). Figure 41 also shows a calculated species distribution curve in Zn-CN systems. The formation of higher negatively-charged species increases rejection.

The relative metal rejection behavior in the presence of complexing agent is compared in Figure 42. The ordinate indicates the relative change in ultrafiltrate metal concentration in the presence of complexing agents. Knowing the metal rejection in the absence of complexing agent, one could use Figure 42 to predict the metal rejection that could be achieved at various L_T/M_T ratios. The Cu^{2+} salts were used for comparison in the M-EDTA and M-OX systems. The Zn^{2+} salts were used for M-CN system because of the nonavailability of $Cu(CN)_2$ salt. The Zn^{2+} -CN system would be expected to be similar to the Cu^{2+} -CN system. For all cases, the metal rejections show the following trend:

$$R_{M-EDTA} > R_{M-CN} > R_{M-OX}$$

Figure 42 also indicates that high metal rejections could be obtained at $L_T/M_T = 1.0$, pH 4-10 with EDTA; at $L_T/M_T = 4-6$, pH 9-10 with cyanide; and at $L_T/M_T = 10-12$, pH 6-7 with oxalate. With EDTA even at $L_T/M_T = 1$, the

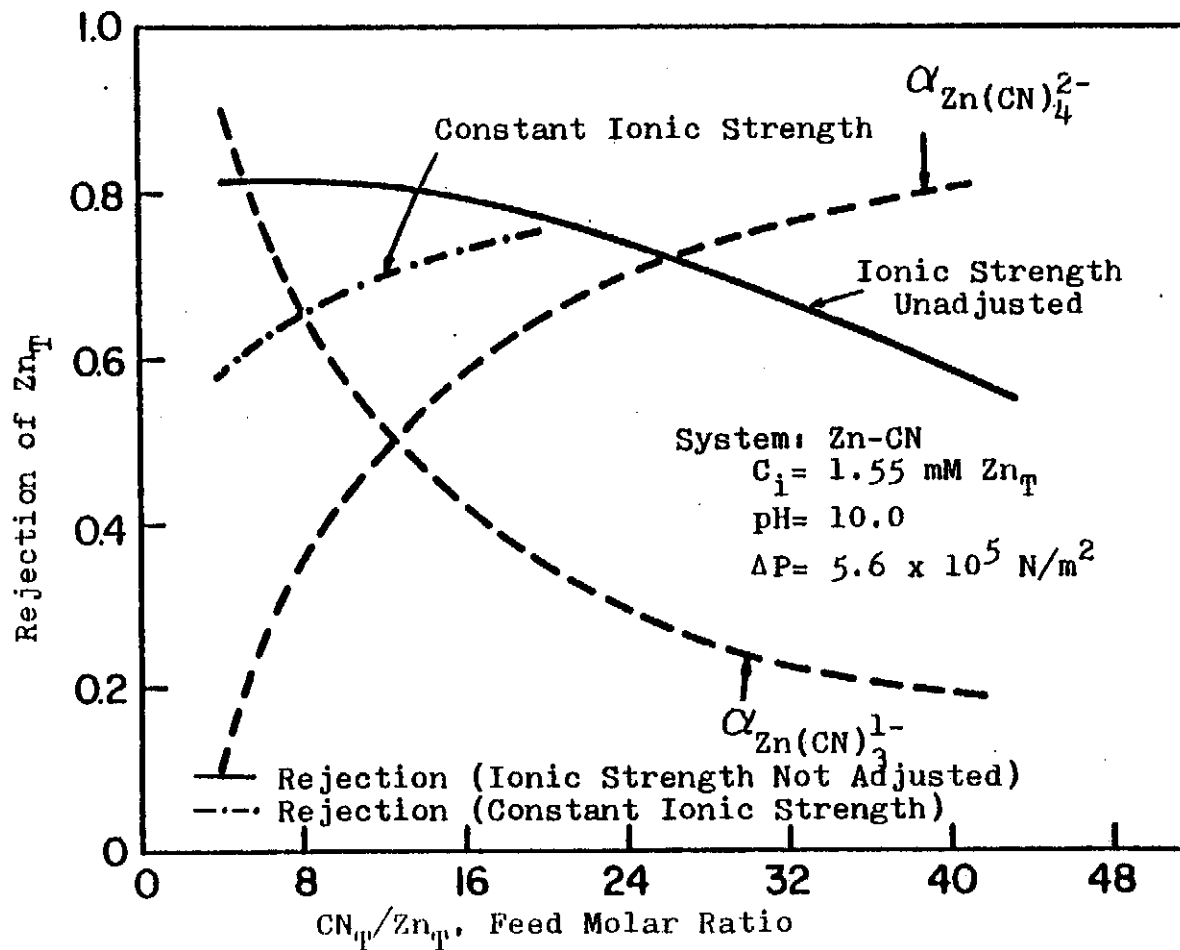
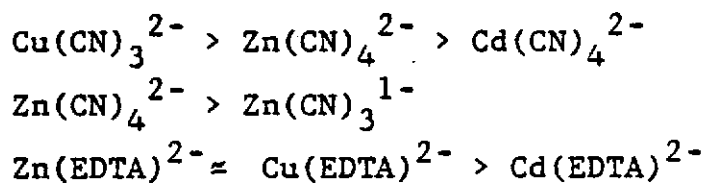


Figure 41. Dependence of Zn_T Rejection on Feed Solution Species Distribution for Zn-CN System

metal concentration in the ultrafiltrate would be 1/20 th of the concentration that can be obtained without complexing agents. With oxalate the metal rejection is poor at $L_T/M_T < 2$ because of uncharged $Cu(OX)$ formation (as shown in Figure 42).

Free complexing agent rejection is found to be different in the presence of metal complexes. Higher rejections are found for free cyanide and free EDTA in the presence of metal ions in the solution at $L_T/M_T < 4$. Free oxalate rejection is poorer at pH 4, but higher free oxalate rejection is found at high pH compared to the case where no metals are present in the solution. For M-CN systems, the free CN^- rejection is negligible at $L_T/M_T > 10$. This could be advantageous for the selective concentration of metal cyanide complexes.

The approximate rejection values of various anions could be calculated from the experimental data, as shown in Table 16 (see Appendix 2). The primary counterion is Na^+ in all cases. The following conclusions could be drawn from this table for the rejection of various species:



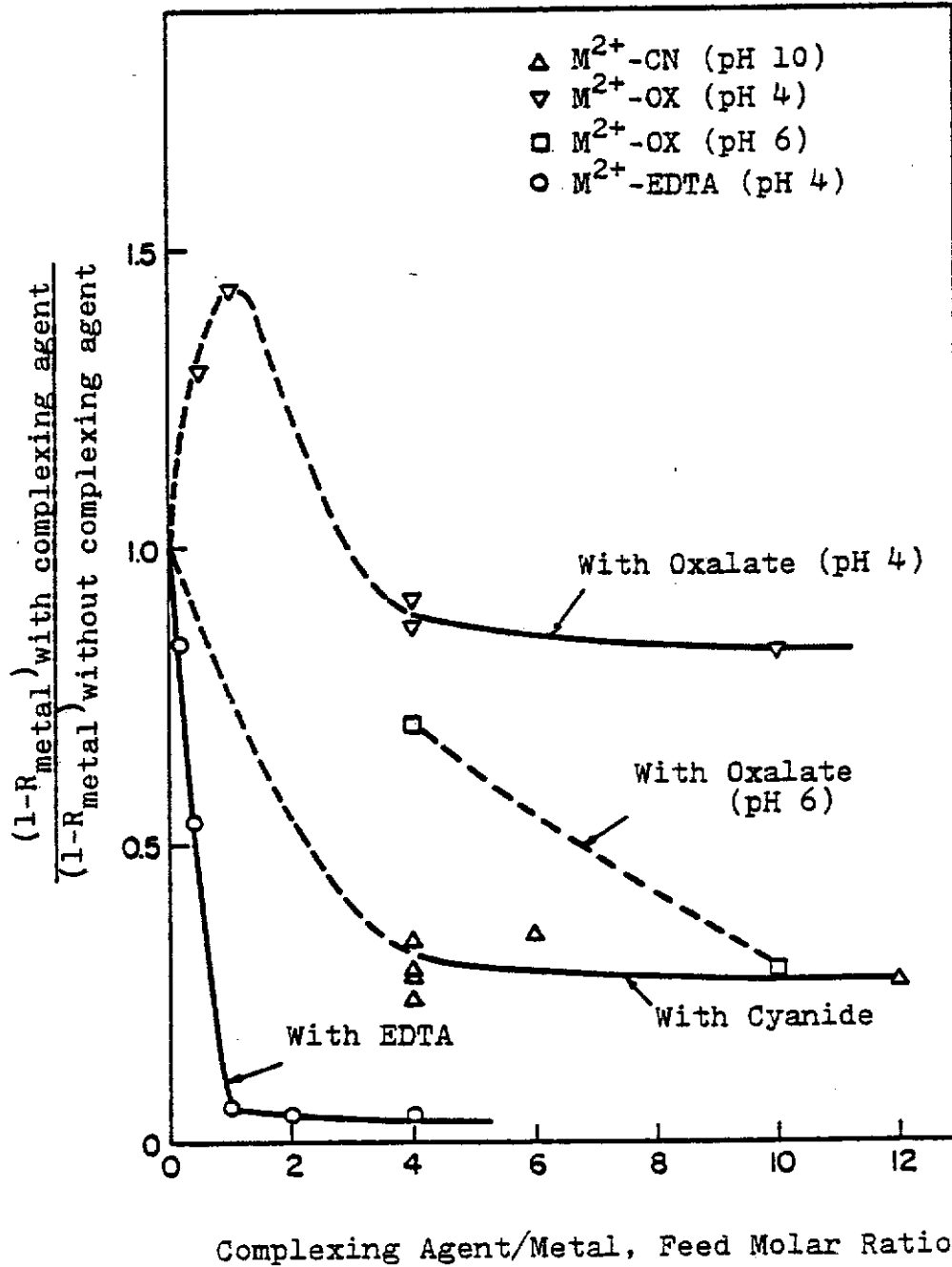


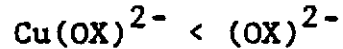
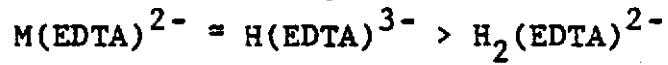
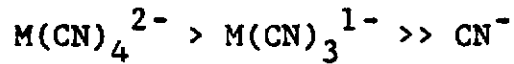
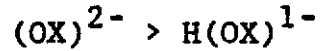
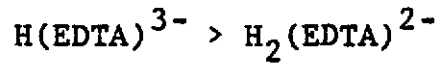
Figure 42. Effect of Three Different Complexing Agents on Relative Metal Rejection Behavior

TABLE 16

Approximate Rejection Values of Various Anions Based on

$$R_{\text{CuCl}_2} = 0.34 \text{ at } 1.55 \text{ mM, } \Delta P = 5.6 \times 10^5 \text{ N/m}^2$$

<u>Species</u>	<u>Rejection</u>
Zn(CN) ₃ ¹⁻	0.81
Zn(CN) ₄ ²⁻	0.90
Cu(CN) ₃ ²⁻	0.94
Cu(CN) ₄ ³⁻	0.95 ⁺
Cu(CN) ₄ ²⁻	0.77
Zn(EDTA) ²⁻	0.95
Cu(EDTA) ²⁻	0.96
Cd(EDTA) ²⁻	0.89
Cu(OX) ²⁻	0.80
CN ⁻	0.30
SO ₄ ²⁻	0.81
H ₂ (EDTA) ²⁻	0.80
H(EDTA) ³⁻	0.96
OX ²⁻	0.93
H(OX) ¹⁻	0.51



Obviously, the species with higher charge density will be rejected better if similar species are compared. Also, higher species rejection is observed for larger species (low diffusion coefficient) provided that the charge densities are comparable. Effective selective separation could be done by adjusting the pH, complexing agent to metal molar ratio, ionic strength, transmembrane pressure, and feed metal or complexing agent concentration in order to maximize or minimize one or more of the complexing species involved. Ultrafiltration of mixed metal systems in the presence of complexing agents should provide precise information on selective metal recovery and ultrafiltrate quality.

NOMENCLATURE

- C_F = Ultrafiltrate concentration, mM metal or complexing agents
- $C_{F,av}$ = Average ultrafiltrate concentration, mM
- C_i = Feed concentration, mM metal or complexing agents
- C_j = Concentration of jth ion, mM
- $C_{j(m)}$ = Concentration of jth ion in membrane phase, mM
- C_m^* = Membrane charge capacity, mM
- C_o = Concentrate concentration, mM
- C_s = Solute concentration, mM
- C_y = Coion concentration in the feed, mM
- $C_{y(m)}$ = Coion concentration in the membrane phase, mM
- Cd_T = Total cadmium molar concentration, mM
- CN_T = Total cyanide molar concentration, mM
- Cu_T = Total copper molar concentration, mM
- D = Diameter of impeller or length normal to axis of rotation, cm
- $D_{j(m)}$ = Diffusivity of jth ion in the membrane phase, cm^2/sec
- D_m = Diffusivity of counterion, cm^2/sec
- D_s = Diffusivity of solute, cm^2/sec
- D_y = Diffusivity of anion, cm^2/sec
- E = Equilibrium Donnan potential, volts
- $EDTA_T$ = Total EDTA molar concentration, mM
- F = Faraday constant

- J_j = Flux of jth ion, (mmole)/(cm².sec)
 J_s = Salt flux, (mmole)/(cm².sec)
 J_w = Water flux (in the presence of salt), cm/sec
 J_w^D = Distilled water flux (in the absence of salt), cm/sec
 J_y = Coion (anion) flux, (mmole)/(cm².sec)
 k = Membrane parameter
 K = Stepwise dissociation constant
 K_{ML} = Conditional stability constant
 K^* = salt distribution coefficient
 L_T = Total complexing agent concentration, mM
 M_T = Total metal concentration, mM
mM = Millimolar
 n = Membrane parameter (Equation 20)
 n' = See Equation 5 in Appendix 3
 \bar{n} = Average charge
 N = Angular velocity of agitator, revolution per second or RPS
 N' = Number of pores per unit area
 OX_T = Total oxalate molar concentration, mM
 ΔP = Transmembrane pressure difference, N/m²
 r = Fractional water recovery
 r' = Pore radius, cm
 R = Rejection parameter
 R' = Universal gas constant

- R_m = Resistance of ultrafiltration membrane to water flux, $(N/m^2)/(cm/sec)$
 T = Absolute temperature
 V_j = Partial molar volume of jth component, $cm^3/mole$
 V' = Volume of the solution
 x = Distance coordinate in the membrane, cm
 Z_j = Charge on the jth ion
 Z_m = Charge on the metal cation
 Z_y = Charge on the anion
 Zn_T = Total zinc molar concentration, mM
 α_i = Fraction of metal containing species in the solution
 β_j = Coupling coefficient of jth ion
 β = Overall stability constant
 γ = Activity coefficient of the salt in solution
 γ_j = Activity coefficient of the jth ion in solution
 $\gamma_{j(m)}$ = Activity coefficient of the jth ion in the membrane phase
 γ_m = Activity coefficient of the salt in the membrane phase
 μ = Viscosity of water, g/cm.sec
 ϵ = Porosity of the membrane
 λ = Membrane thickness, cm
 μ_j = Chemical potential of the jth ion
 $\Delta\pi$ = Transmembrane osmotic pressure difference, N/m^2
 ρ = Density of the fluid

APPENDIX

APPENDIX 1

Program for Calculating Species Distribution in Metal Complex (Zn-CN) System

```

DOUBLE PRECISION P1,P2,P3,P4,P5,P6,P7,P8,X7,DEX,PAST,S1,S2
DOUBLE PRECISION F,CHECK,ZNT,CNT,CN,CN3,CN4,CONC,POH,RATIO
DOUBLE PRECISION A,B,C,E,ANS,P9
DIMENSION A(7,7),B(7,1),C(7,7),E(7,1),ANS(7)
WRITE(5,999)
999  FORMAT(/// ' PLEASE ENTER CONCENTRATION OF METAL AND POH')
READ(5,*)CONC,POH
WRITE(5,997)
997  FORMAT(/// ' PLEASE ENTER X7 AND DEX')
READ(5,*)X7,DEX
WRITE(5,98)X7,DEX
S1=X7
S2=DEX
98   FORMAT(2E20.7)
WRITE(5,996)
996  FORMAT(///1X,'METAL = ZN',/1X,'LIGNAND = CN')
WRITE(5,995)POH,CONC
995  FORMAT(1X,'POH = ',F4.1,/1X,'CONC. OF METAL = ',E15.5)
WRITE(5,901)
901  FORMAT(/36X,'% OF SPECIES AS TOTAL ZN',42X,
1     '% OF SPECIES AS TOTAL CN')
WRITE(5,900)
900  FORMAT(1X,'RATIO',8X,'ZNCN3',9X,'ZNCN4',10X,'ZNOH',
1     9X,'ZNOH2',9X,'ZNOH3',10X,'ZN',8X,5X,'CN',11X,
1     'ZNCN3',9X,'ZNCN4')
100  READ(5,*)RATIO
IF(RATIO.LE.0.)GO TO I11
P1=10.**17.312
P2=10.**19.176
P3=10.**4.4
P4=10.**11.1
P5=10.**14.4
P6=CONC
P7=P6*RATIO
P8=10.**(-POH)
P9=10.**(-9.2)
X7=S1
DEX=S2
II=0
PAST=0.
13   DO 10 I=1,7
DO 10 J=1,7
10   A(I,J)=0.
A(1,2)=1.
A(1,6)=-P2*X7**4
A(2,3)=1.
A(2,6)=-P3*P8
A(3,4)=1.
A(3,6)=-P4*P8**2
A(4,5)=1.
A(4,6)=-P5*P8**3
A(5,1)=1.
A(5,2)=1.
A(5,3)=1.
A(5,4)=1.
A(5,5)=1.
A(5,6)=1.
A(6,1)=3.

```

```

A(6,2)=4.
A(6,7)=1.
A(7,7)=1.
B(1,1)=0.
B(2,1)=0.
B(3,1)=0.
B(4,1)=0.
B(5,1)=P6
B(6,1)=P7-X7
B(7,1)=10.**(-14.)/P8*X7/P9
II=II+1
CALL INVERT(A,C,7)
CALL MULT(C,B,7,7,1,E)
F=E(1,1)-P1*E(6,1)*X7**3
IF(DABS(F).LE.0.00000001)GO TO 11
GO TO 12
11 IF(E(1,1).LE.0.)GO TO 12
   IF(E(2,1).LE.0.)GO TO 12
   IF(E(3,1).LE.0.)GO TO 12
   IF(E(4,1).LE.0.)GO TO 12
   IF(E(5,1).LE.0.)GO TO 12
   IF(E(6,1).LE.0.)GO TO 12
   IF(E(7,1).LE.0.)GO TO 12
   GO TO 14
12 CHECK=F*PAST
   IF(CHECK.GE.0..OR.PAST.GT.0.)GO TO 13
   F=0.
   X7=X7-DEX
   DEX=0.1*DEX
   GO TO 20
13 X7=X7+DEX
20 PAST=F
   GO TO 15
14 ZNT=E(1,1)+E(2,1)+E(3,1)+E(4,1)+E(5,1)+E(6,1)
   DO 30 I=1,6
   DO 30 J=1,1
   ANS(I)=E(I,J)/ZNT*100.
30 CONTINUE
   CNT=X7+3*E(1,1)+4*E(2,1)+E(7,1)
   CN=X7/CNT*100.
   CN3=3*E(1,1)/CNT*100.
   CN4=4*E(2,1)/CNT*100.
   WRITE(5,994)RATIO,(ANS(I),I=1,6),CN,CN3,CN4
994 FORMAT(/,1X,F4.0,6(7X,F7.4),1X,3(7X,F7.4))
   WRITE(5,988)(E(I,1),I=1,6),X7,E(1,1),E(2,1)
988 FORMAT(6X,6(2X,E12.6),1X,3(2X,E12.6))
   WRITE(5,222)E(7,1)
222 FORMAT(9X,'HCN = ',E12.6)
   GO TO 100
111 STOP
   END
SUBROUTINE INVERT(B,A,N)
C
C B : INPUT MATRICES, KEEP IT AFTER INVERSE
C A : OUT MATRIX, INVERSE B
C N : DIMENSION OF A
C
DOUBLE PRECISION A,B,C,AMAX,TEMP,PIVOT
DIMENSION INDEX(7,2),A(7,7),B(7,7),C(7,7)
DO 107 I=1,N
DO 107 J=1,N
107 A(I,J)=B(I,J)
DO 108 I=1,N
108 INDEX(I,1) = 0
   II = 0
109 AMAX = -1.

```

```

DO 110 I=1,N
  IF (INDEX(I,1)) 110,111,110
111 DO 112 J=1,N
  IF (INDEX(J,1)) 112,113,112
113 TEMP =DABS(A(I,J))
  IF (TEMP-AMAX) 112,112,114
114 IROW = I
  ICOL = J
  AMAX = TEMP
112 CONTINUE
110 CONTINUE
  IF(AMAX) 225,115,116
116 INDEX (ICOL,1) = IROW
  IF (IROW-ICOL) 119,118,119
119 DO 120 J = 1,N
  TEMP = A(IROW,J)
  A(IROW,J) = A(ICOL,J)
120 A(ICOL,J) = TEMP
  II = II + 1
  INDEX (II,2) = ICOL
118 PIVOT = A(ICOL,ICOL)
  A(ICOL,ICOL) = 1.0
  PIVOT = 1./PIVOT
  DO 121 J = 1,N
121 A(ICOL,J)=A(ICOL,J)*PIVOT
  DO 122 I = 1,N
  IF (I-ICOL) 123,122,123
123 TEMP = A(I,ICOL)
  A(I,ICOL) = 0.0
  DO 124 J = 1,N
124 A(I,J) = A(I,J) - A(ICOL,J) * TEMP
122 CONTINUE
  GO TO 109
125 ICOL = INDEX(II,2)
  IROW = INDEX(ICOL,1)
  DO 126 I= 1,N
  TEMP = A(I,IROW)
  A(I,IROW) = A(I,ICOL)
126 A(I,ICOL) = TEMP
  II = II - 1
225 IF (II) 125,127,125
127 CONTINUE
  DO 130 I = 1,N
  DO 130 J = 1,N
  C(I,J) = 0.
  DO 130 K = 1,N
130 C(I,J) = C(I,J) + B(I,K)*A(K,J)
  GO TO 134
115 WRITE(5,133)
133 FORMAT(11X,'ZERO PIVOT')
134 RETURN
END
SUBROUTINE MULT(X,Y,L,M,N,Z)
  DOUBLE PRECISION X,Y,Z
  DIMENSION X(L ,M ),Y(M ,N ),Z(L ,N )
  DO 109 I=1,L
  DO 109 J=1,N
  Z(I,J)=0.
  DO 110 K=1,M
110 Z(I,J)=Z(I,J)+X(I,K)*Y(K,J)
109 CONTINUE
  RETURN
END

```

METAL = ZN
 LIGAND = CN
 POH = 4.0
 CONC. OF METAL = 0.15500E-02

RATIO	% OF SPECIES AS TOTAL ZN					% OF SPECIES AS TOTAL CN			
	ZNCN3	ZNCN4	ZNOH	ZNOH2	ZNOH3	ZN	CN	ZNCN3	ZNCN4
4.	91.7625 .142232E-02 HCN = .194586E-03	8.2372 .127676E-03	0.0000 .941157E-11	0.0003 .471696E-08	0.0001 .941157E-09	0.0000 .374681E-11	19.8025 .122776E-02	68.8219 .142232E-02	8.2372 .127676E-03
6.	78.5842 .121806E-02 HCN = .590740E-03	21.4158 .331945E-03	0.0000 .288058E-12	0.0000 .144371E-09	0.0000 .288058E-10	0.0000 .114678E-12	40.0787 .372732E-02	39.2921 .121806E-02	14.2772 .331945E-03
8.	68.5696 .106283E-02 HCN = .993605E-03	31.4304 .487171E-03	0.0000 .528233E-13	0.0000 .264744E-10	0.0000 .528233E-11	0.0000 .210294E-13	50.5583 .624922E-02	25.7136 .106283E-02	15.7152 .487171E-03
10.	60.7403 .941474E-03 HCN = .140110E-02	39.2597 .608526E-03	0.0000 .166877E-13	0.0000 .836367E-11	0.0000 .166877E-11	0.0000 .664350E-14	57.0346 .884037E-02	18.2221 .941474E-03	15.7039 .608526E-03
20.	38.4208 .595523E-03 HCN = .347428E-02	61.5792 .954477E-03	0.0000 .692317E-15	0.0000 .346980E-12	0.0000 .692316E-13	0.0000 .275616E-15	70.7137 .219212E-01	5.7431 .595523E-03	12.3158 .954477E-03
30.	28.0047 .434073E-03 HCN = .957270E-02	71.9953 .111593E-02	0.0000 .122285E-15	0.0000 .412876E-13	0.0000 .122285E-13	0.0000 .486825E-16	75.6158 .351614E-01	2.8005 .434073E-03	9.5994 .111593E-02
40.	22.0110 .341170E-03 HCN = .768050E-02	77.9890 .120883E-02	0.0000 .367119E-16	0.0000 .183996E-13	0.0000 .367119E-14	0.0000 .146153E-16	78.1624 .484607E-01	1.6508 .341170E-03	7.7989 .120883E-02

APPENDIX 2

Calculation of Approximate Rejections of Various Coions

At pH 10 and $CN_T/Zn_T = 4$, the predominant species in the solution is $Zn(CN)_3^{1-}$ (see Figure 5). A rejection value of 0.81 could be assigned to represent the rejection of such species. At very high CN_T/Zn_T ratio, the predominant species becomes $Zn(CN)_4^{2-}$. Figure 24 (top) could be used to calculate the rejection of $Zn(CN)_4^{2-}$ (in addition to Figure 21) as follows:

$$(1-0.58)/(1-0.77) = (1-0.81)/(1-R_{Zn(CN)_4^{2-}})$$

Thus, $R_{Zn(CN)_4^{2-}} = 0.90$ could be assigned at the ratio of 4. The predominant species in the solution is $Cu(CN)_3^{2-}$. A rejection value of 0.94 could be assigned for $Cu(CN)_3^{2-}$ as shown in Figure 23.

The rejection of $Cu(EDTA)$ could easily be assumed to be 0.96 (Figure 30) since it is the only species in the solution at $EDTA_T/Cu_T = 1$.

A value of 0.80 could be assigned as the rejection of $Cu(OX)^{2-}$ since the $Cu(OX)^{2-}$ is the predominant species in the solution at pH 6 and at $OX_T/Cu_T = 10$.

The rejection of H(EDTA)^{3-} could be assigned as 0.96 since it is the only species in the pure EDTA solution at pH 8.3 (see Figures 2 and 18). Similarly, $\text{H}_2(\text{EDTA})^{2-}$ rejection could be assigned as 0.80 due to the same reason (see Figures 2 and 18).

A rejection of 0.9 could be assigned for $(\text{OX})^{2-}$ since it is the only species in pure oxalic acid solution at a pH of 6 (see Figures 3 and 19). Similarly, a value of 0.51 is assigned for the rejection of H(OX)^{1-} at pH 3.5.

CN^- rejection is assigned to be 0.30 since it is the predominant species in the pH value we are interested in.

APPENDIX 3

Calculation of Solute Removal at Significant Water Recovery Condition

For semi-batch ultrafiltration operation, the mass balance can be written as:

$$d(V'C) = C_f dV' \quad (1)$$

Since $C_f = kC^n$ (Equation 20),

$$-V'dC = C dV' - kC^n dV' = C(1-kC^{n-1})dV' \quad (2)$$

On integration,

$$\int_{C_i}^{C_o} \frac{dC}{C(1-kC^{n-1})} = - \int_{V_i'}^{V_o'} \frac{dV'}{V'} \quad (3)$$

$$\text{Since } r = (V_i' - V_o')/V_i', \quad (4)$$

the following equation can be easily derived:

$$C_o^{n'}(1-kC_i^{n'})/[C_i^{n'}(1-kC_o^{n'})] = [1/(1-r)]^{n'} \quad (5)$$

where $n' = n-1$ for $n \neq 0$, $r \neq 1$.

Knowing n' and k from experimental value, the concentrate composition can be calculated from Equation 5 for various water recovery, r . Knowing C_o , $C_{f,av}$ can be computed from mass balance:

$$C_{f,av} = [(1-r)C_o - C_i]/r \quad (6)$$

Thus, removal (as defined in Equation 58) can be calculated at any value of r .

REFERENCES

1. Mattson, M. E., "Significant Developments in Membrane Desalination," Desalination, 28, 207 (1979).
2. Nomura, H., Seno, M., Takahashi, H., and Yamabe, T., "Reverse Osmosis by Composite Charged Membranes," Desalination, 29, 239 (1979).
3. Bhattacharyya, D., Schaaf, D. P. and Grieves R. B., "Charged Membrane Ultrafiltration of Heavy Metal Salts: Application to Metal Recovery and Water Reuse," Can. J. Chem. Eng., 54, 185 (1976).
4. Bhattacharyya, D., Garrison, K. A., Jumawan, A. B., and Grieves, R. B., "Membrane Ultrafiltration of a Non-ionic Surfactant and Inorganic Salts from Complex Aqueous Suspensions: Design for Water Reuse," AICHE Journal, 21, 1057 (1975).
5. Bhattacharyya, D., Jumawan, A. B., and Grieves, R. B., "Charged Membrane Ultrafiltration of Heavy Metals from Nonferrous Metal Industry," Journal WPCF, 51, 176 (1979).
6. Bhattacharyya, D., Garrison, K. A., and Grieves, R. B., "Membrane Ultrafiltration for Treatment and Water Reuse of TNT-manufacturing Waters," Journal WPCF, 51, 176 (1979).
7. Gregor, H. P., "Membranes in Separation Processes - a Workshop Symposium," Sponsored by the National Science Foundation, Case Western Reserve University, Cleveland, Ohio (1973).
8. Gyte, C. C. and Gregor, H. P., "Poly (Styrene Sulfonic Acid) - Poly (Vinylidene Fluoride) Interpolymer Ion - Exchange Membranes, Ultrafiltration Properties," J. Polymer Sci., 14, 1855 (1976).

9. Bhattacharyya, D., McCarthy, J. M., and Grieves, R. B., "Charged Membrane Ultrafiltration of Inorganic Ions in Single and Multi-salt Systems," AICHE Journal, 20, 1206 (1974).
10. Bhattacharyya, D., Moffitt, M. and Grieves, R. B., "Charged Membrane Ultrafiltration of Toxic Metal Oxyanions and Cations from Single- and Multi-salt Aqueous Solutions," Separation Science and Technology, 13, 449 (1978).
11. Bhattacharyya, D., Bewley, J. L., and Grieves, R. B., "Ultrafiltration of Laundry Waste Constituents," Journal WPCF, 46, 2372 (1974).
12. Kamizawa, Chiyosi, "The Permeation Behavior of Metal Complex Solutions through Cellulose Acetate Membranes," Journal of Applied Polymer Science, 22, 2867 (1978).
13. Hopfenberg, H. B., Lee, K. L., and Wen, C. P., "Improved Membrane Separations by Selective Chelation of Metal Ions in Aqueous Feeds," Desalination, 24, 175 (1978).
14. Sachs, S. B., Zisner, E., and Herscovici, G., "Hybrid Reverse Osmosis - Ultrafiltration Membranes," Desalination, 18, 99 (1976).
15. Lonsdale, H. K., Pusch, W., and Walch, A., "Donnan-membrane Effects in Hyperfiltration of Ternary Systems," Journal of the Chemical Society, Faraday Transactions I, 71, 501 (1975).
16. Bhattacharyya, D., and Grieves, R. B., "Charged Membrane Ultrafiltration," in Recent Developments in Separation Science, N. N. Li. (ed.), Vol. III, p. 261, Chem. Rubber Co. Press, Cleveland, Ohio (1977).

17. Sourirajan, S., "Research Osmosis and Synthetic Membranes," National Research Council of Canada, Ottawa, Canada (1977).
18. Bjerrum, N., and Manegold, E., Kolloid-Z., 43, 5 (1967).
19. Ferry, J. D., "Ultrafilter Membranes and Ultrafiltration," Chemical Reviews, 18, 373 (1936).
20. Lonsdale, H. K., "Industrial Processing with Membranes," R. E. Lacey and S. Loeb, eds., Ch. 8, John Wiley & Sons, New York (1972).
21. Johnson, J. S., "Polyelectrolytes in Aqueous Solutions - Filtration, Hyperfiltration, and Dynamic Membranes," in Reverse Osmosis Membrane research, H. K. Lonsdale, and H. E. Podall, (eds.), p379, Plenum Press, New York (1972).
22. Shor, A. J., Kraus, K. A., Smith, W. T., and Johnson, J. S., "Salt Rejection Properties of Dynamically Formed Hydrous Zirconium (IV) Oxide Membranes," J. Phys. Chem., 72, 2200 (1968).
23. Dresner, L., "Some Remarks on the Integration of the Extended Nernst-Planck Equations in the Hyperfiltration of Multicomponent Systems," Desalination, 10, 27 (1972).
24. Laksharinarayanaiah, N., Transport Phenomena in Membranes, Academic Press, New York (1969).
25. Werner, Neuere Anschauungen auf dem Gebiete der anorganischen Chemie, Fourth Edition, p44, Friedrich Vieweg & Sohn, Brunswick (1920).

26. Pauling, L., The Nature of the Chemical Bond, 3rd edition, Cornell, Ithaca, New York (1960).
27. Ballhausen, C. J., Introduction to Ligand Field Theory, McGraw-Hill, New York (1962).
28. Gray, H. B., "Molecular Orbital Theory for Transition Metal Complexes," J. Chem. Educ., 41, 2 (1964).
29. Mohlex, J. B., Electroplating and Related Processes, Chemical Publishing Co., New York (1969).
30. Torpy, M. F., "Electroplating and Cyanide Wastes: Literature Review," Journal WPRF, 49, 1182 (1977).
31. McNulty, K. J., Goldsmith, R. L., Gollan, A., and Grant, D., "Reverse Osmosis Field Test: Treatment of Copper Cyanide Rinse Waters," EPA-600/2-77-170 (1977).
32. Skoog, D. A. and West, D. M., Fundamentals of Analytical Chemistry, 2nd edition (1970).
33. Ringborn, A. J., Complexation in Analytical Chemistry, Interscience Publishers (1963).
34. Perry, R. H. and Chilton, C. H., Chemical Engineers' [Handbook], 5th edition, McGraw Hill (1973).
35. Bhattacharyya, D., Jumawan, A. B., Grieves, R. B. and Harris, L. R., "Ultrafiltration Characteristics of Oil-Detergent-Water Systems: Membrane Fouling Mechanisms," Separation Science and Technology, 14, 529 (1979).